

UNIVERSITÉ PIERRE & MARIE CURIE

INSTITUT DES SYSTÈMES INTELLIGENTS ET DE ROBOTIQUE

École Doctorale Sciences Mécanique, Acoustique, Électronique et Robotique de Paris

Spécialité: Robotique

THÈSE DE DOCTORAT

présentée par

Tommaso Proietti

Characterizing the reciprocal adaptation in physical
Human-Robot interaction to address the inter-joint
coordination in neurorehabilitation

Paris, Mars 2017

JURY

Rapporteur	BURDET Etienne	Imperial College London
Rapporteur	SOUÈRES Philippe	LAAS-CNRS
Examinateur	REDARCE Tanneguy	INSA-LYON CNRS
Examinateur	SIGAUD Olivier	ISIR-CNRS, Université Pierre & Marie Curie
Directeur de thèse	ROBY-BRAMI Agnès	ISIR-CNRS, Université Pierre & Marie Curie
Encadrant	JARRASSÉ Nathanaël	ISIR-CNRS, Université Pierre & Marie Curie



A dissertation submitted in fulfilment
of the requirements for the degree of
Doctor of Philosophy
(Robotics Engineering)

in Université Pierre et Marie Curie - Sorbonne Universités
ISIR - Institut des Systèmes Intelligents et de Robotique
École doctorale Sciences Mécaniques, Acoustique, Électronique & Robotique

tommaso.proietti.88@gmail.com

Résumé

L'accident vasculaire cérébral est la première cause mondial de handicap neurologique acquis chez l'adulte. Alors que de nombreux exosquelettes destinés à la rééducation neuromotrice ont été développés ces dernières années, ces dispositifs n'ont pas encore permis de vrai progrès dans la prise en charge de ces patients cérébrolésés par rapport aux thérapies conventionnelles avec un kinésithérapeute, ou même à la thérapie robotisée exploitant de simples robots manipulandums planaires qui n'interagissent qu'avec la main.

Parmi les perspectives d'amélioration de la thérapie robotisée, l'une des pistes de recherche les plus prometteuses est celle de l'adaptation. En effet, durant une rééducation neuromotrice, les kinésithérapeutes adaptent naturellement et constamment leur actions aux capacités du patient en faisant varier le niveau des forces appliquées sur le membre de ce dernier et en adaptant la difficulté des exercices. Une des clés pour améliorer les faibles résultats thérapeutiques obtenus serait donc de reproduire un tel comportement et de constamment adapter la thérapie robotisée en fonction de l'évolution du patient et de sa récupération, en adaptant l'assistance fournie par le robot pour maximiser l'engagement du patient. L'objectif de cette thèse est donc de mieux comprendre les processus d'adaptations réciproques dans un contexte d'interaction physique Homme-Exosquelette; afin de développer des stratégies de contrôle innovante pour la rééducation robotisée. Concrètement, nous souhaitons développer des solutions plus efficaces d'adaptation de l'assistance fournie par le robot, modulées par les variations de performance du patient, mais aussi et surtout, étudier et comprendre comment le comportement moteur de sujets peut être contraint à l'aide d'un dispositif exosquelettique appliquant des champs de force, et comment il serait possible de favoriser la rétention d'un comportement moteur modifié ou appris et son transfert à d'autres contextes que celui de la séance de rééducation avec le robot.

Dans cette optique, nous avons donc, dans un premier temps, développé un nouveau type de contrôleur adaptatif qui assiste le sujet "au besoin", en modulant l'assistance fournie; et évalué différents signaux pour piloter cette adaptation afin de suivre au mieux la récupération du patient. La simplicité de mise en œuvre de la solution développée permet de l'implémenter sur la plupart des architectures de contrôle pour exosquelette existantes. Afin de suivre le plus finement possible différents aspects de la récupération motrice des patients (trajectoires de la main ou des articulations intermédiaires par exemple), nous avons aussi étudié la possibilité d'utiliser différentes variables pour piloter cette adaptation.

Dans un deuxième temps, comme lors d'une interaction physique homme-robot le sujet adapte aussi son comportement, nous avons cherché à étudier l'adaptation de sujets à l'application de champs de forces distribués par un exosquelette sur leur bras durant la réalisation de mouvements dans l'espace. En effet, bien que l'adaptation motrice humaine ait été étudiée de manière intensive ces dernières années en perturbant l'organe terminal de sujet (c.a.d. la main) à l'aide de champs de forces appliqués par des robots planaires, très peu d'études ont été conduites sur l'adaptation à la perturbation sur des mouvements dans l'espace 3D et sur l'impact de perturbations appliquées au niveau articulaire, que seul un exosquelette peut générer. Pourtant l'étude de ce problème est fondamentale pour l'application de rééducation neuromotrice en raison de l'atteinte importante des synergies (coordinations inter-articulaires) du membre supérieur des patients cérébrolésés. Nous avons donc appliqué des champs de forces résistifs (visqueux) distribués (à l'aide d'un exosquelette) sur le bras de sujets sains afin de modifier volontairement leur coordinations inter-articulaires et d'étudier l'effet de l'exposition à cette contrainte. D'importantes différences inter-individuelles ont été observées, avec une adaptation à la contrainte imposée pour seulement 21% des sujets, mais avec des effets à-posteriori persistants

mesurés chez 85% d'entre eux; ainsi qu'une généralisation dans l'espace de ces effets et un transfert à des contextes différents (hors du robot).

Ce premier travail de compréhension de l'interaction homme-exosquelette au un niveau articulaire lors de la réalisation de gestes conjoints pourrait permettre à terme de développer de nouvelles approches de rééducation neuromotrice robotisée qui pourrait permettre d'obtenir, enfin avec des exosquelettes, de vraies améliorations dans la récupération.

Mots clés: Robotique de rééducation, Exosquelettes de membre supérieur, Contrôle adaptatif, Apprentissage de coordinations motrices.

Abstract

Stroke is one of the main causes of acquired neurological impairments in adults worldwide. While numerous robotic exoskeletons have been developed for neurorehabilitation in recent years, the few clinical results obtained so far do not exhibit better performance than training with human physiotherapists or with planar robots controlling the hand movement.

One important feature which could unleash the potentiality of rehabilitation robotics is adaptation. During physical rehabilitation, human physiotherapists naturally adapt to the patient capabilities by varying the interaction forces with the patients limb and the rehabilitation exercises. A key to improve the efficacy of the therapy is to adapt the assistance provided by the robot in order to maximize the subject engagement and physical effort, by having the robotic therapy evolving with the patient recovery. This is why we aim at better understanding the process of reciprocal adaptation in a context of physical human-robot interaction, in order to develop innovative control strategies for rehabilitation robotics. This may help developing efficient solutions to guide the adaptation of the robot with respect to the human performance, and to study the way the motor behaviour is constrained and adapted when the robot control action is performed and the transfer of adapted behaviours beyond the robot training.

In this context, we first developed and tested a new adaptive controller, which assists the subject “as-needed”, by regulating its interaction to maximize the human involvement. The simplicity of this solution permits to implement this strategy with most of the existing controllers for exoskeleton. We further compared different signals driving this adaptation, to better following the functional recovery level of the patients.

While the control action is performed by the exoskeleton, the subject is also adapting his movements. Although human adaptation has been extensively studied when perturbing the end-effector through a planar robot, there is still a need to understand this adaptation when dealing with 3D movements, joint coordination, and exoskeletons. Indeed the analysis of the upper-limb synergies is critical with stroke patients, due to the presence of pathological patterns of movements. Therefore, we exposed human free motions to distributed resistive viscous force fields, generated by the exoskeleton at the joint level, to produce specific inter-joint coordination and to analyse the effects of this exposition. With healthy participants, we observed important inter-individual difference, with adaptation to the fields in 21% of the participants, but post-effects and persisting retention of these in time in 85% of the subjects, together with spatial generalization, and, preliminarily, transfer of the effects outside of the exoskeleton context.

This initial work towards understanding the human-robot interaction in multijoint arm movements could provide insights on innovative ways to develop novel rehabilitation controllers for improving stroke motor recovery with robotic exoskeletons.

Keywords: Rehabilitation Robotics, Upper-limb Robotic Exoskeletons, Adaptive Control, Motor Coordination Learning.

List of publications

Journals

- Jarrassé N., Proietti T., Crocher V., Robertson J., Sahbani A., Morel G. and Roby-Brami A. (2014) *Robotic exoskeletons: a perspective for the rehabilitation of arm coordination in stroke patients*. Frontiers in Human Neuroscience, 8:947
- Proietti T., Crocher V., Roby-Brami A., and Jarrassé N. (2016) *Upper-limb robotic exoskeletons for neurorehabilitation: a review on control strategies*. IEEE Reviews in Biomedical Engineering, vol. 9, pp. 4-14
- (*Under review*) Proietti T., Guigon E., Roby-Brami A., and Jarrassé N. (2017) *Modifying upper-limb inter-joint coordination in healthy subjects by training with a robotic exoskeleton*. Submitted to Journal of NeuroEngineering and Rehabilitation (JNER).

Conferences

- Proietti T., Jarrassé N., Roby-Brami A., and Morel G. (2015) *Adaptive control of a robotic exoskeleton for neurorehabilitation*. 7th International IEEE/EMBS Conference on Neural Engineering (NER15, Montpellier), pp. 803-806
- Proietti T., Roby-Brami A., and Jarrassé N. (2016) *Learning motor coordination under resistive viscous force fields at the joint level with an upper-limb robotic exoskeleton*. Converging Clinical and Engineering Research on Neurorehabilitation II, Springer International Publishing, proceedings of 3rd International Conference on NeuroRehabilitation (ICNR16, Segovia), pp. 1175-1179
- Proietti T., Morel G., Roby-Brami A., and Jarrassé N. (2017) *Comparison of different error signals driving the adaptation in assist-as-needed controllers for neurorehabilitation with an upper-limb robotic exoskeleton*. Accepted to IEEE International Conference on Robotics and Automation (ICRA17, Singapore)
- (*Under review*) Proietti T., Roby-Brami A., and Jarrassé N. (2017) *A preliminary investigation on the transfer of a motor adaptation learnt by training with an exoskeleton*. Submitted to IEEE International Conference on Rehabilitation Robotics (ICORR15, London).

Contents

List of publications	6
1 Introduction and context	10
1.1 Human upper-limb motor control	10
1.1.1 Redundancy and synergies	10
1.1.2 End-effector kinematics	11
1.1.3 Learning and adaptation	12
1.2 Stroke and Rehabilitation	12
1.2.1 Stroke: a neurological disease	12
1.2.2 Stroke effects: hemiparesis and hemiplegia	13
1.2.3 Post-stroke care: neurorehabilitation	15
1.2.4 Key factors for efficacious rehabilitation	15
1.3 Rehabilitation robotics	17
1.3.1 What is an exoskeleton?	18
1.3.2 Robotic exoskeletons for rehabilitation	19
1.3.3 The ABLE exoskeleton	20
1.4 Thesis objectives	21
1.4.1 Structure of the thesis	22
2 Control strategies for robotic exoskeletons: a state of the art	23
2.1 Review methodology	23
2.2 Available devices	24
2.3 Control strategies for stroke rehabilitation	25
2.3.1 Assistive modes	27
2.3.2 Corrective modes	32
2.4 Discussion	33
2.4.1 Hardware limiting control possibilities	33
2.4.2 The problem of reference definition	34
2.4.3 Addressing coordination control	35
2.4.4 Clinical testing issues	35
2.4.5 Lack of adaptation	36
3 Robot adaptation to the human action	38
3.1 Introduction	38
3.2 Adaptive control	39
3.2.1 Working principle	39
3.2.2 Control algorithm	40
3.2.3 Performance metrics	41
3.3 Proof-of-concept	42

3.3.1 Preliminary test: mimicking relearning	42
3.3.2 Advanced test: more dynamical behaviour and different adaptation rates	44
3.4 Comparison of different error signals driving the adaptation	47
3.5 Conclusions and perspectives	53
4 Human adaptation to the robot action	55
4.1 Introduction	55
4.1.1 Results on motor adaptation with planar robots	56
4.1.2 Exoskeletons potentialities	57
4.2 Modifying the inter-joint coordination: the experimental setup	58
4.2.1 The exoskeleton controllers	58
4.2.2 Experimental protocol	59
4.2.3 Quantification of the human spontaneous variability within the exoskeleton	62
4.3 Data processing	62
4.3.1 Data gathering	62
4.3.2 Joint kinematics	62
4.3.3 End-effector kinematics	63
4.3.4 Principal Component Analysis	63
4.3.5 Statistics	63
4.4 Results	64
4.4.1 Individual results	64
4.4.2 Movements towards ET: adaptation to KSC	67
4.4.3 Movements towards GT: catch-trials unexposed to KSC	71
4.5 Discussion	74
4.5.1 Adapting to new upper-limb synergies	74
4.5.2 Application to rehabilitation / Limits	75
4.5.3 Assessing learning effects with an exoskeleton	76
4.6 Transferring of post-effects outside the robot	76
4.7 Conclusions and perspectives	81
5 Conclusions and perspectives	83
A Elements of Anatomy	85
B The Kinematic Synergy Control	88
C Upper-limb rehabilitation assessment methods	90
D Additional Material: CERES certificate	93
Bibliography	94
List of figures	109
List of tables	110

Nomenclature

AAN Assist-As-Needed

ADL Activity of Daily Living

BCI/BMI Brain Computer/Machine Interface

CNS Central Nervous System

DOF Degrees Of Freedom

EEG Electroencephalography

EMG Electromyography

ET Experimental Target

EXP Experimental phase

FOL Follow up phase

GDM Goal-Directed Mode

GT Generalization Target

KSC Kinematic Synergy Control

PCA Principal Component Analysis

PCs Principal Components

PCT Path-Constrained Tracking Mode

pHRI physical Human-Robot Interaction

PID Proportional-Integral-Derivative Control

PRE Preliminary phase

WAS Wash-out phase

Chapter 1

Introduction and context

Contents

1.1	Human upper-limb motor control	10
1.1.1	Redundancy and synergies	10
1.1.2	End-effector kinematics	11
1.1.3	Learning and adaptation	12
1.2	Stroke and Rehabilitation	12
1.2.1	Stroke: a neurological disease	12
1.2.2	Stroke effects: hemiparesis and hemiplegia	13
1.2.3	Post-stroke care: neurorehabilitation	15
1.2.4	Key factors for efficacious rehabilitation	15
1.3	Rehabilitation robotics	17
1.3.1	What is an exoskeleton?	18
1.3.2	Robotic exoskeletons for rehabilitation	19
1.3.3	The ABLE exoskeleton	20
1.4	Thesis objectives	21
1.4.1	Structure of the thesis	22

1.1 Human upper-limb motor control

The human *upper-limb* or *upper extremity* is the part of the human body extending from the deltoid region to the hand. It includes the shoulder (girdle and joint), the arm, the forearm, the wrist, and the hand. A detailed description of these components is presented in Appendix A. This complex musculoskeletal system provides 10 Degrees Of Freedom (DOF) to the human body, without considering the hand and fingers mobility: these are usually divided into the 3-DOF of the scapula and the 7-DOF of the arm (respectively, 3-DOF at the shoulder joint, 1-DOF at the elbow, and 3-DOF at the wrist).

1.1.1 Redundancy and synergies

The presence of a large number of DOF allows the human upper-limb to potentially perform any movement in an infinite variety of joint configurations: therefore, the human arm is redundant to the so-called Activities of Daily Living (ADL), meaning that the number of DOF required to achieve any common task (such as, for example, pointing in the space, drinking and eating a meal, dressing, opening or moving boxes, etc.) is less than the number of DOF available. For example, when considering grasping any object in the space, only 6-DOF

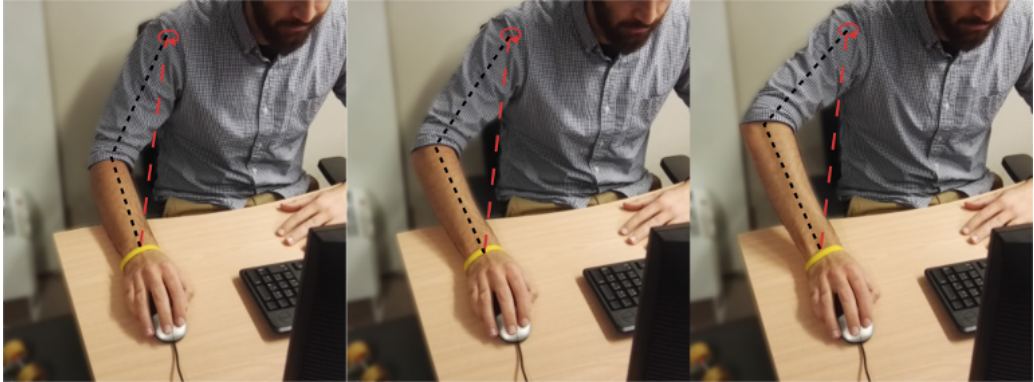


Figure 1.1: An example of upper-limb redundancy, *i.e.* a self-motion, while grasping an object. The elbow can turn around a virtual axis (in dashed red in the picture) connecting the shoulder to the hand, without affecting the object position and orientation.

are required to describe the position and the orientation of the hand. Thus, we still have at least one additional degree of freedom to those necessary to grasp (not considering the scapula). In this case, the redundancy can be illustrated by considering the possible movement of the arm when grasping the object in a fixed position, around a virtual axis connecting the shoulder to the hand, as shown in figure 1.1. The upper-limb redundancy is even larger when considering the arm muscles. In fact, for each DOF of the arm, there exist a muscle pair, agonist/antagonist. The exact number of muscles in the human arm is difficult to determine, however there exist about 23 teamed muscle groups controlling the whole upper-limb, excluding the hand.

This redundancy provides human beings a dexterous and highly manoeuvrable tool. However, the control of such a redundant system implies a complex set of control laws for the Central Nervous System (CNS). A classical hypothesis is that “synergies” [14], fundamental building blocks of motor control, are used by the CNS to decrease the redundancy of the system. According to this concept, synergies (i) combine several elements, which share the same spatio-temporal properties and work together, and (ii) may be combined in a task specific way so that a limited number of synergies can give rise to a continuum of responses. However, there is still no agreement on the space (muscle or joints) in which synergies are encoded. Some authors study synergies at muscle level [15]. Mathematical techniques such as linear decomposition have been used to identify muscle synergies in healthy subjects in a variety of tasks such as posture [172] or reaching [33, 32]. Other authors have considered synergies at joint kinematics level, endowed with properties of flexibility and automatic compensation between elements in order to stabilize the important task related variable [99] (as, for example, the gun orientation in a pistol shooting task [159]). Despite the large redundancy of the upper-limbs, the final posture, reaching a given position in the space, is usually reproducible for each individual subject [37]. However the factors that determine these final postures remain disputed, in particular the relative importance of static versus dynamic constraints ([47], [49], [126], see [66] for a review).

1.1.2 End-effector kinematics

Healthy upper-limb movements are further characterised by invariants of the end-effector kinematics. The trajectory of the end-point in 3D space, in most of the case the hand or the grasped object, follows either straight path or curves, defined by smooth velocity profiles [4]. When a subject is told simply to move his hand from one visual target to another, the path of the hand is generally straight, and the hand speed profile is bell-shaped. When the subject is required to produce curved hand trajectories, the path usually approximates a curve with low curvature elements. Hand speed profiles associated with curved trajectories contains speed inflections which are temporally associated with the local maxima in the trajectory curvature. Interestingly, when people are asked to move their arm in space, every person uses a very specific configuration of their upper-limb, which is different among subjects, but which is highly reproducible among movements [37, 36].

1.1.3 Learning and adaptation

The CNS, consisting of the brain and the spinal cord, is the structure pursuing the motor control in vertebrates. The above-mentioned properties – smoothness, speed profiles, reproducible synergies – are typical of healthy people. However, they are not immutable properties, but rather the results of learning, adaptation, and experience. Everyday life shows that the CNS can learn new motor strategies through practice, at least in healthy people [164]. There are still numerous controversies and unknown mechanisms behind the CNS and the way it reacts and adapts to external disturbances. However it is a common idea that the presence of an internal representation of the motor control system and of the environment is used to predict causal relationships between motor commands and motions [189, 190, 161, 162]. This internal model hypothesis is a key factor in the motor control system because it allows for cancelling sensory events coming from self-produced motions in order to distinguish the information from disturbances and external environments. Furthermore, it can play a central role in maintaining stability in the presence of sensory feedback delay (for example, visual feedback processing takes about 150ms [118]).

The process of optimizing motor performance is thus achieved through learning and adaptation. The learning phenomenon for the CNS can be described, by borrowing expressions from control theory, as a closed-loop system with feedback and feedforward terms [51]. Mainly the feedforward control is learnt in order to account for the movement, while the feedback control corrects potential disturbances and prediction errors [21]. Trial-by-trial, the feedback (from sensory and motor commands) drives the adaptation of the feedforward internal model.

However, motor learning is still a vaguely defined term that embraces motor adaptation, skill acquisition, and decision-making [92]. Motor adaptation occurs when the CNS must react to external stimulus to regain former levels of performances, thus modifying existing motor patterns. On the contrary, skill learning involves acquiring new patterns of muscle activation for producing new performances.

Healthy humans are able to adapt trial-by-trial, driven by the prediction error (the brain's predicted movement outcome versus the observed output), and this phenomenon works even implicitly, when the subject is not aware of the learning process [164]. In addition, it has been observed that adaptation occurs faster when the stimulus are represented on a second time, meaning that memory is implied as well [92]. On the other hand, skill learning is a slower process, since it requires, for any generic task, an improvement of the speed-accuracy trade-off, which is generally a constant ratio in human beings (if speed increases, accuracy goes down [48]).

Motor impairments of the upper-limb, particularly those due to lesions of the central nervous system, strongly modify the properties of the motor control, producing, among others impairments, decrease of smoothness, disruption of natural synergies, delays in motor adaptation and learning. Clearly, all these impairments reduce the independence of the patients: they generally lack of functional abilities, requiring external assistance in the everyday life. Among others diseases, in this thesis we focused on the consequences of stroke, a brain damage which generally causes neurological issues and provokes hemiparesis and upper-limb motor control deficit.

1.2 Stroke and Rehabilitation

1.2.1 Stroke: a neurological disease

Stroke, also known as *cerebrovascular accident* (CVA), is a neurological disease occurring when the brain is not fed with sufficient blood flow for a period of time long enough to cause brain cell death and, as a consequence, persisting neurological deficit. This disease is the second leading cause of death in the world (a person dies from stroke every 4 minutes, as estimated by the World Health Organization [2] and the National Stroke Association [1]) and moreover the leading cause for acquired disability in adults [5].

Hippocrates (460-370 B.C.) was the first describing the phenomenon of the *apoplexy*, from the Greek word meaning “struck down with violence”, referring to the paralysis following a stroke. The ancients believed that someone suffering a stroke (or any sudden incapacity) had been struck down by the Gods. The word *stroke*

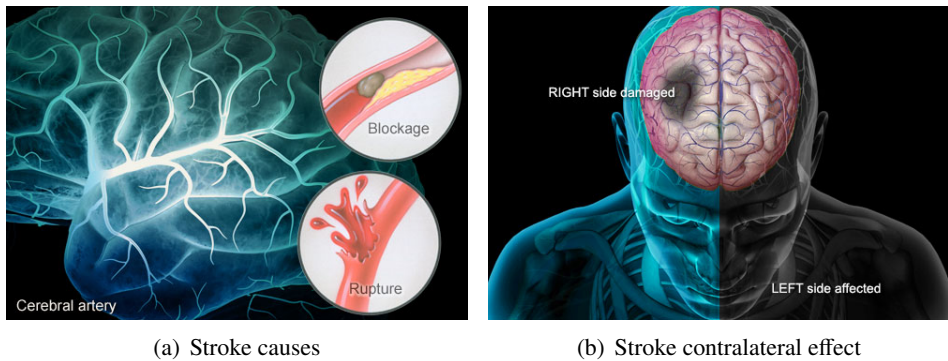


Figure 1.2: Stroke causes and effects. Images by webdm.com/stroke.

became a synonym for apoplectic seizure at the end of 16th century, and in the 1970s the WHO defined stroke as a “*neurological deficit of cerebrovascular cause that persists beyond 24 hours or is interrupted by death within 24 hours*”. This definition was supposed to reflect the reversibility of tissue damage and was devised for the purpose, with the time frame of 24 hours not being chosen arbitrarily. In fact, the 24-hour limit categorizes stroke from *transient ischemic attack*, which is a related syndrome of stroke symptoms that resolves completely within 24 hours.

There exist two forms of stroke: *ischemic* and *hemorrhagic*. Ischemic stroke (87% of cases) is caused by blockage of the flow in blood vessel by an obstruction (*thrombosis* — blood clot forming locally — or *embolism* — a clot from elsewhere in the body). Hemorrhagic stroke is caused by bleeding and thus the accumulation of blood anywhere within the cranial vault, usually due to blood vessel rupture.

Stroke survivors are usually left with neurological deficits, resulting in paralysis on the half of the body on the opposite side of the lesion (*hemiplegia*), memory loss, visuospatial problems as altered perception of both themselves and the surrounding environment, balance problems, numbness and cognitive issues, and other consequences depending on the affected side of the brain. According to the National Stroke Association, among the stroke survivors:

- 10% of the stroke survivors recover almost completely,
- 25% recover with minor impairments,
- 40% experience moderate to severe impairments that require special care,
- 10% require care in a nursing home or other long-term facility,
- 15% die shortly after the stroke.

However, generally, half of the stroke survivors show severe disability and marked limitation in activities of daily living, necessitating special care, 20% need assistance with ambulation, and about three quarter of the patients decrease their employability because of their disability.

1.2.2 Stroke effects: hemiparesis and hemiplegia

A common issue for post-stroke patients is motor disability, that is moderate to severe impairments on both lower and upper-limb movements (*hemiparesis*), together with a loss of hand dexterity. Hemiparetic patients can exhibit paralysis at different levels and the most severe form, meaning complete paralysis of half of the body, is named *hemiplegia*. Different medical issues (traumas, tumors, etc.) can cause this disability but stroke is the most common one. Both hemiparesis and hemiplegia are not related to issues with the musculoskeletal system, but they are problems concerning the motor command. However, when lacking the voluntary/involuntary

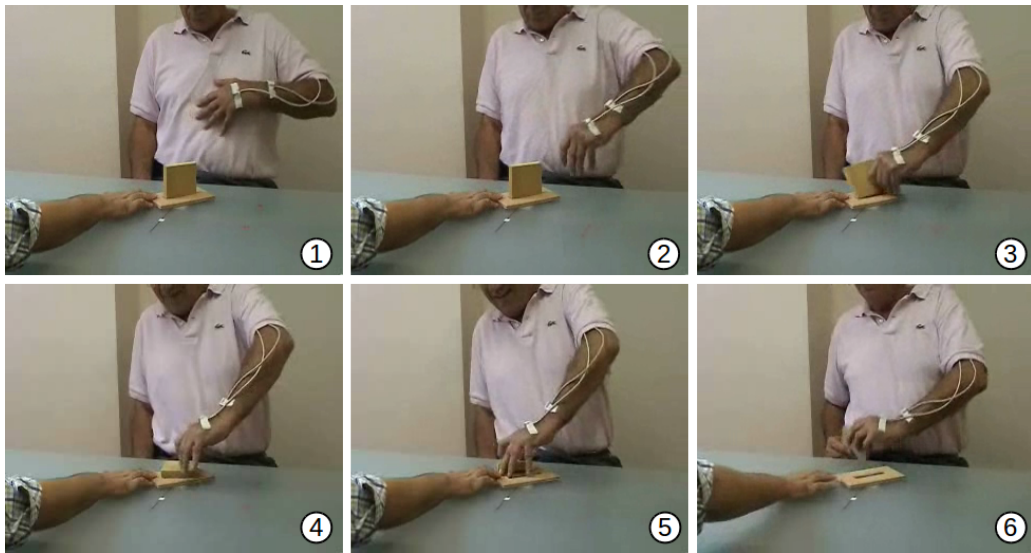


Figure 1.3: Example of a pathological reaching movement in a patient with a right brain lesion. The shoulder flexion and elbow extension are limited but there is an involuntary simultaneous shoulder elevation and abduction, indicating a pathological synergy (photo 4-5). The patient needs to compensate with a trunk movement. The dexterity is also affected (in this case, the patient fails at grasping the object with the impaired hand and utilizes the healthy side to achieve the task, photo 6).

control of the movements, different body musculoskeletal issues can appear (as, for example, humeral joint inflammation, muscle wasting, etc.).

Movement of the body is primarily controlled by the *pyramidal tract*, a pathway of neurons that begins in the motor areas of the brain, and travels through the brainstem and the spinal cord. This aggregation of nerve fibres of upper motor neuron allows the voluntary motion command from the brain to be directly fed into the motor neurons that control each muscle. Hemiparesis and hemiplegia are thus conditions following lesions at the pyramidal tracts, resulting in *contralateral* hemiparesis (affecting the body on the opposite side of the injury), as shown in figure 1.2(b). Hemiparesis and hemiplegia consequences, other than decreased movement control, endurance, and strength, may include spasticity (excessive muscle contraction) and could be associated with impairments of the somatosensory system on the contralateral side. Together, these impairments and the abnormal contractions result in a disruption of goal-directed upper-limb movements and hand dexterity. The consequent disability is also worsened by both altered moving coordination and walking gait.

Upper-limb motor control in post-stroke patients

When referring to the specificity of the impairments to the upper-limb motor control in post-stroke patients, the word “synergy” is redefined. Indeed, this term is also used to refer to the pathological coupling of movements observed in patients [38]. The global and stereotyped patterns of movements that occur when stroke patients make any effort to move are described as *pathological synergies*, see figure 1.3. Couplings of shoulder elevation movements with elbow flexion (*flexor synergy*) or shoulder adduction/internal rotation with elbow extension (*extensor synergy*) have been reported [20]. These abnormal synergies have been documented using quantitative experimental methods. Tasks involving the isometric generation of force have demonstrated that abnormal muscle coupling induces involuntary elbow flexion during voluntary shoulder abduction [39, 38]. During forward reaching movements, shoulder flexion and elbow extension tend to be reduced and shoulder abduction increased [154]. This elevates the elbow and alters the plane of arm movement [117]. The analysis of arm coordination is complicated by the fact that stroke patients develop compensatory trunk flexion in order to reach targets in front of them, due to the impairment of the upper-limb extension [26, 153]. A study based on Principal Component Analysis (PCAs) showed that, when the trunk is fixed, patients with higher levels of impairment use fewer synergic joint combinations to carry out reaching tasks, suggesting that there is a reduc-

tion in the flexibility of synergies [147]. Automatic error compensation between joint rotations is also impaired in stroke patients but appears to be task dependent since it is relatively preserved when the trunk is fixed [147] but not when trunk movement assists the reach [148]. When the trunk is free, stroke patients use more synergic joint combinations than healthy subjects [175].

As a consequence of the disordered motor control, other phenomena at the upper-limb motor control have been observed in stroke survivors:

- During reaching movements in the horizontal plane at the shoulder level, target dependent perturbations of reaching kinematics and kinetics occur. These are reduced when the arm is supported against gravity [12, 44, 169].
- The available reaching workspace depends on the degree of shoulder loading [169, 44].
- Kinematic analysis of the time course of joint rotations showed a disruption of the relative timing between shoulder and elbow movements during reaching [27, 100, 175].

At the kinematics level, the properties of smoothness and the characteristics of the end-point trajectories, described in section 1.1, are also strongly impaired [26]. Studies have shown that in stroke patients multi-joint pointing movements are characterized by decreased movement speed, by increased movement variability, by increased path length of the hand trajectory, and by increased movement segmentation [100, 89]. The peculiar symmetric bell-shaped profile of the hand speed of a healthy person is replaced by an irregular multi-peak profile, corresponding to multiple zero-crossing for the acceleration profile. Most studies have analyzed reaching with the arm supported and found that stroke subjects have decreased elbow velocity [184], initial movement direction error [13], and increased trajectory curvature [100].

All the mentioned compensatory strategies, as for example the trunk flexion when performing reaching of a target in front of the patients, help stroke survivors to perform tasks in the short term. Unfortunately these compensations can be associated with long-term harmful complications [101]. The main problem is that they can lead to a pattern of *learned nonuse*, limiting subsequent recovery [74, 170]. It is therefore important for the post-stroke therapy, generally named *neurorehabilitation*, to target motor recovery, functional independence, and improvements of sensorimotor impairments.

1.2.3 Post-stroke care: neurorehabilitation

Neurorehabilitation is a long lasting therapy, related to and acting on many different aspects of everyday life, strongly dependent on the patient and his disability. Stroke rehabilitation is “*a progressive, dynamic, goal-oriented process aimed at enabling a person with impairment to reach their optimal physical, cognitive, emotional, communicative, and/or social functional level*” [34].

Neurorehabilitation is provided in clinics and hospitals by *physiotherapists* and *occupational therapists*. Physical therapy tends to focus on evaluating and diagnosing movement dysfunctions as well as on treating the impairment: in this case the therapy aims, for example, at producing elementary voluntary movements while reducing motor impairments through passive mobilization and stretching, avoiding contractures and articular stiffness. On the other hand, occupational therapy focusses more on evaluating and improving functional abilities: occupational therapists train impaired subjects to perform ADL and other rehabilitative exercises, in order to increase subjects independence. Of course there is much crossover between these two kinds of therapies.

1.2.4 Key factors for efficacious rehabilitation

The human brain is a powerful organ, naturally capable of reorganizing cortical representations, in order to access latent circuits, to create new ones, and/or to bypass damaged pathways. This innate brain capacity names *neuroplasticity* and it underlies all learning and memory related phenomena in both healthy and damaged brains [185]. One important pursuit of post-stroke treatment, and thus of neurorehabilitation, is to induce

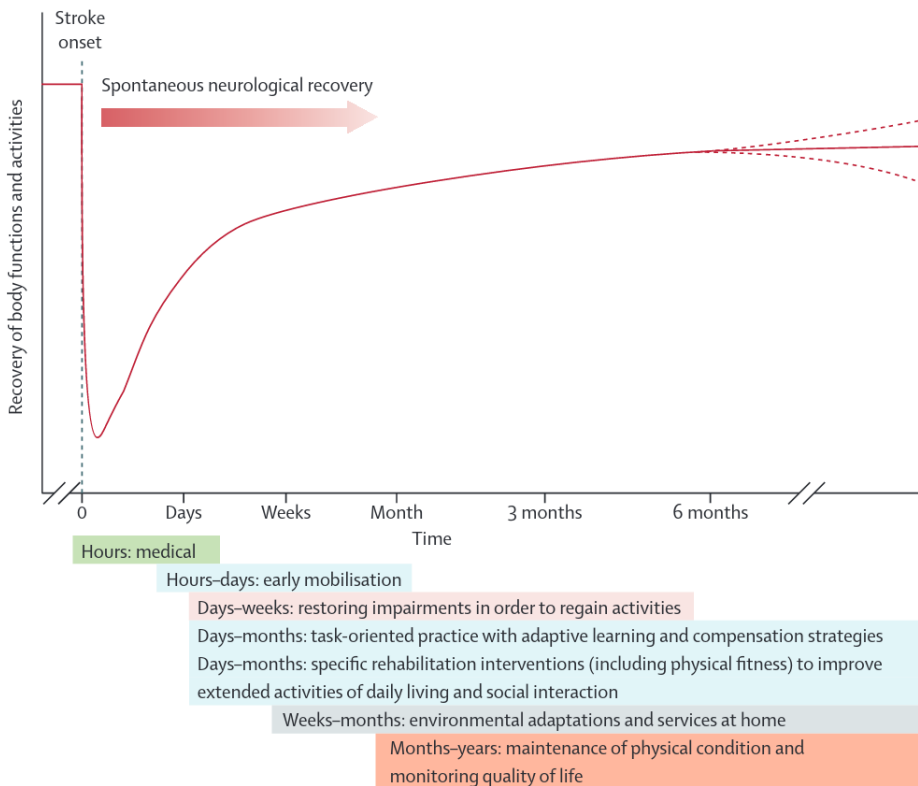


Figure 1.4: Hypothetical pattern of recovery after stroke in humans. Reproduced from [98].

neuroplasticity in stroke survivors, in order to recover voluntary control of movements. Until the late 90s, stroke recovery was believed to be only due to spontaneous biological phenomena, and to occur partially only during the sub-acute period. Recently, these classical assumptions were reviewed, and nowadays it is known that rehabilitation can induce activity dependant cortical plasticity [128] and that recovery may occur also during the chronic period [167]. Figure 1.4 presents a hypothetical pattern of recovery after stroke in humans, reproduced from Langhorne *et al.* [98]. The stroke recovery is characterized by the presence of a quick improvement immediately after the stroke, during the so-called *acute phase* (days and few weeks after the neurological deficit), followed by a *plateau* of relearning, where improvements is slower, during the so-called *chronic phase*, few months after the start of the disease. It is interesting to underline that only less than 10% of motor rehabilitation control trials have enrolled survivors at early-stages (during the first month after stroke) [168] and thus there is still a need to improve the general understanding of the interaction of the therapy with the spontaneous recovery process and the possibly positive effects of early treatments. Indeed, in the acute phase, the ambulatory treatment is focused on stabilizing the vital functions. Only in the following six to twelve weeks, neurorehabilitation is provided at the hospital, in the form of one-on-one therapy with physiotherapists. Due to the limited financial resources, patients are usually sent home when they are able to walk, although their upper-limb functionality might still be severely impaired, directly affecting patients independence and quality of life [178, 107]. However there is evidence that more therapy would improve patients motor function [72, 180]. Recently, a new emerging field, *computational neurorehabilitation* [143], is addressing the possibility to model plasticity and motor learning in stroke survivors, in order to improve movement recovery. Indeed the emergence of robotics and wearable sensors for rehabilitation is providing an important amount of new data, never really available before, to develop and test new models of recovery.

Many techniques have been tested for improving motor recovery after stroke and these are still subject of research (among others, repetitive task training, constraint-induced movement therapy, robotics and virtual reality, motor imagery, noninvasive brain stimulation). However, nowadays, there are some accepted key factors,

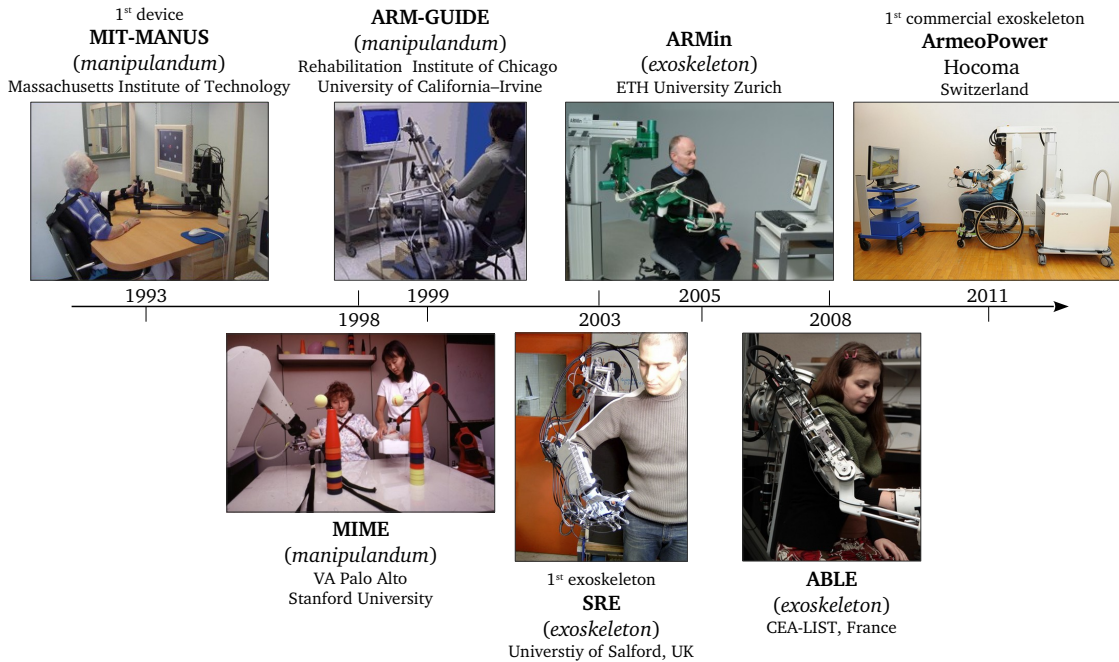


Figure 1.5: Overview of upper-limb rehabilitation robotics timeline.

shared within the medical and research community, recognized as necessary to promote efficacious therapy. These factors are all equally important and they are described in the following list [185, 186]:

- *intensity of training*, meaning that the dose, the frequency, and the duration of the practice should be considered as important parameters of the therapy,
- *involvement and motivation of the patient*, as necessity of engaging the subject with active participation,
- *minimal necessary ad-hoc assistance to reduce failures*, in order to induce confidence to use the impaired limb and to keep the motivation high,
- *goal-directed task-specific activities*, as an increase of efficacy working in a normal daily context on activities of daily living, more than in simulated or reproduced environments,
- *progressive, customized, challenging practice*, following the idea that practice should be “difficult but not too difficult”, thus not repetitive and meaningful for optimal engagement,
- *early participation*, to avoid the time course of recovery, thus the appearing of negative compensatory approaches and the growing lack of confidence in using the impaired arm.

1.3 Rehabilitation robotics

Starting from the mid 90s (see figure 1.5), there has been a burst of research on and development of robotic devices for rehabilitation, particularly for treating the impairments of the upper-limb following a stroke. Robotics has been identified as one possible solution to provide intensive goal-directed assisted training, increasing the number of repetitions which any human-led therapy could impose, as well as to improve involvement thanks to technology appeal and virtual reality [160, 185]. Furthermore, robotics could be used to treat the patients without the presence of the therapist, allowing for more frequent training with, potentially, reduced costs.

The first robots developed, also referred as *manipulanda* or *end-effector robots*, were only able to guide the motion of patient’s hand in the plane (for example the MIT-Manus [78], the ARM-Guide [145], or the MIME

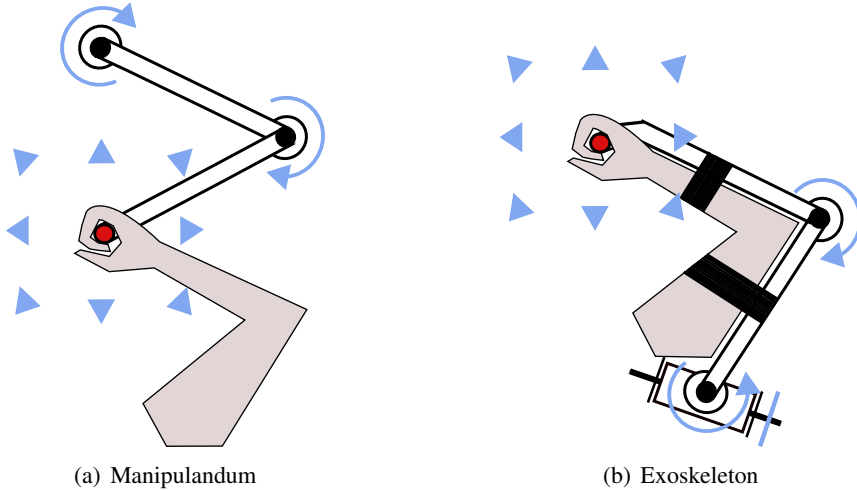


Figure 1.6: Comparison between manipulandum and exoskeleton. The most important and evident feature is that the exoskeleton usually controls more DOF than an end-effector robot, which is usually planar, that is maximum 2-DOF. Furthermore, the exoskeleton usually has more contact points with the human wearer. These two characteristics allow the exoskeleton to fully determine the upper-limb posture, applying torques to each joint separately, and to enable a distributed interaction on the whole limb. Obviously, these advantages comes with generally more complex controllers and higher manufacturing costs.

platform [22]). Extensive testing of these devices [96], simultaneously to clinical testing on the ARM robot (© *InMotion*, the commercialized version of the MIT-Manus) resulted in improvements of the motor capacity of the impaired arm, after sessions of robotic therapy [179]. However, despite their potentiality, the use of end-effector robots has not shown yet qualitative benefit (*i.e.* improved functional recovery) over conventional therapist-led training session, performed on the same quantity of movements [103, 82, 144].

These preliminary results for rehabilitation robotics, together with the technological progress, pushed the researchers to develop more complex wearable robots, named *exoskeletons*. A schematic of the differences between manipulanda and exoskeletons is shown in figure 1.6. These multiple degrees of freedom structures, allowing distributed physical interaction with the whole limb, provided new capabilities within standard rehabilitation sessions. Indeed exoskeletons allowed to address natural 3D movements and activities of daily living, plus supported the analysis of the inter-joint coordination of the human arm. Besides these devices could be adopted as a detailed source of joints movement measurement, to perform quantitative assessments and analysis of patient recovery [82].

Therefore numerous upper-limb exoskeletons have been recently developed but their effects have been still little studied, especially clinically. Indeed, the first and only commercially available upper-limb exoskeleton for rehabilitation (the ArmeoPower by *Hocoma*, based on ARMinIII robot) was only released at the end of 2011 [151]. Moreover, the first results on a randomized controlled trial with the ArmeoPower and more than 70 post-stroke patients showed not significant improvements with respect to conventional therapy, making the clinical relevance of exoskeleton-led therapy questionable [93].

1.3.1 What is an exoskeleton?

An exoskeleton is a mechanical structure, either passive or actuated, designed for physically interacting with one or more parts of the body. Through the interaction points with the body (*fixations*), the exoskeleton can interact directly at the joint space of the subject's body. This interaction has different functional purposes in terms of force (scaling factor, thrust force applied directly to the wearer body, replication) or movement (monitoring, correction, prevention, assistance, compensation).

An exoskeleton can be therefore considered as an articulated mechanical orthosis, since, as the latter, it is a device which compensates for an absent or a deficient function (to allow the gait of a tetraplegic patient, for example), assists a musculoskeletal structure (to boost the carrying capacity for military applications, for

example), stabilizes a body segment during a rehabilitative period (the example of exoskeletons for neurorehabilitation of stroke patients), or allows to replicate body motions (for example in teleoperation).

As for any robotic device, the nature of the requested task and, thus, the necessary physical interaction, influences the mechatronic specifications: for example, the effort capacities of the exoskeleton, the presence and type of actuation, or the device kinematics and workspace. Normally, the operator physical condition imposes the interaction and the level of shared control with the robotic structure.

Three main kinds of exoskeleton are then available based on the required performance:

- *augmenting* exoskeletons, mainly for healthy operators, to increase the natural capability of the human body,
- *passive* exoskeletons, without actuators but sensorized, principally used in a master-slave configuration to replicate human operator actions,
- *substitutive* exoskeletons, to recreate lost or damaged body features, in case of impaired subjects.

Furthermore, this categorization can be enhanced by considering that each device can be either actuated, thus robotic exoskeletons, or can be a pure mechanical structure. For example, an augmenting robotic exoskeleton is used for assistance to improve human load capacity in [157], while in [181], an augmenting mechanical device is used as a solution to reduce kinetic energy consumption during walking.

1.3.2 Robotic exoskeletons for rehabilitation

Exoskeletons for neurorehabilitation are specific devices involved in manoeuvring weak impaired people. The particular physical situation of the exoskeleton wearer requires compliant devices, completely backdriveable. *Backdriveability* is an inherent mechanical property that reflects the capacity of providing almost null resistance to the operator movement, when needed. This feature is fundamental to deal with post-stroke patients who should not apply any unnecessary force to move their impaired limb. In addition, it is a useful property for helping physiotherapists, who need to directly manipulate the robotic joints for showing the correct movements to the subjects.

The issue with a device lacking of mechanical backdriveability, for example because of friction in the gears of the actuators, can be overcome at the control level, by detecting the operator motor intention and the physical human-robot interaction, and therefore by moving the robot accordingly (similarly to an admittance control scheme). Nonetheless, this solution requires numerous sensors to measure the operator movements and it will certainly suffer from control limitations (robustness to noise, stability, etc.). Moreover, the interaction with the robot should be done through sensors only, making difficult, for example for a therapist, to manipulate the robot if not applying any input directly to the sensors [84].

The resulting transparency, either thanks to mechanical backdriveability or to an implemented control strategy, provides to exoskeletons another important characteristic for rehabilitation, that is the capability to produce reliable, distributed, and specific measures of the impaired limb motions, to obtain significant data for the analysis of the process of recovery.

However, while pursuing transparency, the rehabilitative therapy and the necessary assistance must be provided through the exoskeleton, through forces or imposed displacements. Furthermore, as said before in section 1.2.4, one aim of the therapy is to maximize stroke survivors engagement. Thus a fundamental property for rehabilitation exoskeletons is the necessity of allowing for shared control modes, between the robot and the human wearer. Sharing control grants the possibility for the subject to be highly involved in the motion of his own limbs, but, simultaneously, it enables the necessary assistance for correcting wrong motions and avoiding task failures.

Finally, in order to increase the involvement during the rehabilitation therapy, an emerging requirement is the possibility to interface these devices with virtual reality, to include the impaired upper-limb, and therefore the stroke patients, in immersive interactive video games.

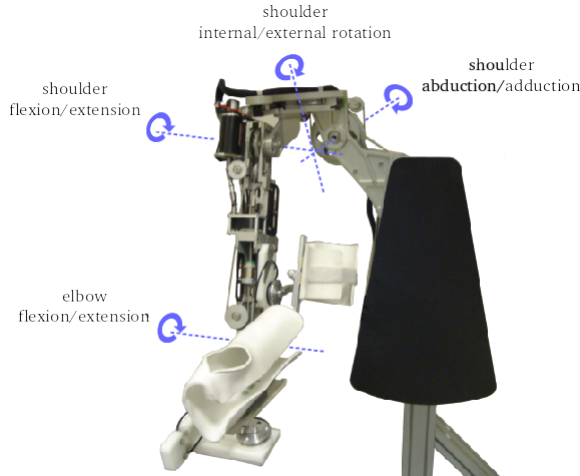


Figure 1.7: The 4-DOF ABLE exoskeletons.

Joint	Axis 1	Axis 2	Axis 3	Axis 4
	Abduction/Adduction	Internal/External Rotation	Flexion/Extension	Flexion/Extension
	Shoulder			Elbow
Amplitude	110°			130°
Motors	DC Faulhaber type			
Controller	RTLinux (1KHz)			
Transmission	Screw-Cable System (SCS)			
Speed (cartesian)	> 1m/s			
Joint torque	18Nm		13Nm	
Equiv. Force (hand)	50N		40N	
Weight	3kg		10kg	

Table 1.1: ABLE exoskeleton main specifications.

1.3.3 The ABLE exoskeleton

The ABLE exoskeleton is the robotic device used in this thesis for all the experiments, see figure 1.7. This exoskeleton, built by CEA-LIST [60], is a four active DOF robot, with 3-DOF at the shoulder (for abduction/adduction, internal/external rotation, and flexion/extension) and one at the elbow (for flexion/extension). It was initially developed as a master robotic arm for teleoperation in nuclear plant environments. However, ABLE has interesting features for rehabilitation robotics, among which, a large workspace, force/torque ranges compatible with human ones, and above all high backdriveability, thanks to a patented screw-cable mechanical transmission [59], which is acting together with a model-based gravity software compensation to allow a transparent behaviour. ABLE is equipped with a real time controller (RTLinux) running the control loop at 1kHz, controlling and actuating the 4 available DC Faulhaber electric motors. It allows 110° of rotation at the first three axes, and about 130° at the elbow. It can generate a force of about 50N at the hand, which can be used to impose some particular movements and distributed constraints to the whole upper-limb. The total weight of the arm structure is about 13kg. A summary of all the most interesting characteristics of this exoskeleton is presented in table 1.1.

Experiments with this device have been validated by a CPP and AFSSAPS in 2009. In addition, each experimental study within this thesis (therefore the exoskeleton itself and all the instrumentation, the protocols, the developed control laws, etc.) has been validated by the ethics committee of the Paris Decartes University (*Comité d'Éthique de la Recherche En Santé - CERES* - IRB number 20162000001072). The certificate is provided at the end of the dissertation.

1.4 Thesis objectives

Despite the large number of robotic devices for neurorehabilitation, modern exoskeletons have so far not brought any major improvement to the results achieved with planar robots or to the standard post-stroke therapy. Indeed the first and only results on a randomized controlled trial with the ArmeoPower (© *Hocoma*) and 77 post-stroke patients did not produce significant improvements with respect to the traditional therapy [93], making the clinical relevance of robotics, and of exoskeletons especially, questionable. The main causes of this unexploited potentiality are multiple.

On the one hand, the technological and scientific step, which pushed the research directions from simpler planar robots to complex multi-DOF exoskeletons, did not occur simultaneously to a development of innovative control strategies, adapted to these multi-DOF joint space based devices. Indeed, most of the available controllers for exoskeletons are often implementation of 2D control laws on a 3D device (mainly end-effector controllers adapted to exoskeletons). Robotic exoskeleton state-of-the-art almost completely lacks of controllers addressing the upper-limb coordination, which is heavily impaired in post-stroke survivors and strongly reduces the long-term motor improvements, although exoskeletons were introduced above all to address intermediate joints issues, problems that could not be faced by end-effector based robots.

On the other hand, using robots often corresponds to the prescription of standardized therapies which cannot deal with the necessities of different patients and the variation in the evolution of their recovery. Indeed, the effects of the above mentioned controllers generally consists in a partial and fixed assistance of the upper-limb, where the level is often manually set, which limits the freedom of the patients movements, *i.e.* the respect of their motor intentions, and consequently decrease their involvement in the action.

One important feature which could unleash the potentiality of robotics is therefore adaptation. Adapting the assistance provided by the robots, in order to maximize the subject engagement and to progress with the patient recovery, correctly challenging him to increase the physical effort, is a key to improve the efficacy of the therapy. Physiotherapist naturally adapts to the patient necessities, when leading the physical therapy, by varying, among others, the interaction forces with the patients limb and the rehabilitation exercises. For this reason, this thesis aims at better understanding the process of reciprocal adaptation in a context of physical human-robot interaction, in order to develop innovative control strategies for neurorehabilitation robotics. We try to find the best solution to finely guide the adaptation of the robot with respect to the human performance, but at the same time, we need to study the way this motor behaviour is constrained and adapted when the robot control action is performed and when it is removed (post-effects).

Therefore we developed two main sections, corresponding to the two simultaneous aspects of the human-robot adaptation due to the physical interaction: the first about *the adaptation of the robot* with respect to the human action, and the second on *the adaptation of the human action* with respect to the robot control action.

Robot control adaptation The objective of this section is to study optimal ways to adapt the exoskeleton action, based on the subject performance. In the current literature, there exist different solutions which discretely map the successive stages of the patient recovery, and which will be the topic of the next chapter: from passive control, which zeros the compliance of the robot, to partial assistance, which requires some effort from the operator, to active modes, in which the robot is only compensating for its weight. However, these are only separate controllers and it is usually the therapist who decides to change among these control modes. An important effort must be done in order to understand how to produce a continuous automatic adaptation through these stages. Therefore, we developed and tested a new adaptive controller, which assists the subject “as-needed”, by adapting its interaction throughout trials. The better the subject is able to perform the task, the less the robot helps, and vice versa, mainly pursuing the maximization of the human involvement. This idea is not new in the state of the art, but the simplicity of our paradigm permits to implement this strategy with most of the existing controllers for exoskeleton. At the same time, we compared different strategies and signals driving this adaptation, in order to better following the functional recovery level of the patients.

Human adaptation While the control action is performed by the exoskeleton, the subject is also adapting his movements. Although human adaptation has been extensively studied when perturbing the end-effector on 2D movements through a planar robot, there is still a need to understand and describe this adaptation when dealing with 3D movements and exoskeletons, in a redundant situation. The literature on the adaptation of the inter-joint coordination of the upper-limb, when constraints are produced by an exoskeleton, is scarce. However, the analysis of the upper-limb synergies is one critical issue with post-stroke rehabilitation: in fact, the presence of pathological and stereotyped unnatural patterns of movements on the upper-limb coordination is frequent in stroke survivors. If healthy people can adapt to novel joint force fields, it may be possible to manipulate the training environment to have after-effects, resembling healthy coordination, in patients [82]. For this reason, we exposed human free motions to joint resistive viscous force fields, generated by the exoskeleton to produce unnatural inter-joint coordination. This corrective control mode helped us to analyse the effects of the exposure to joints distributed constraints on the upper-limb coordination during the experiment and the post-effect when these force fields were removed. This is a first step towards understanding the human-exoskeleton physical interaction, which could provide insights on innovative ways to develop rehabilitation controllers for improving post-stroke motor recovery with these devices.

1.4.1 Structure of the thesis

The next chapters are organized in the following way: Chapter 2 concerns a detailed and structured state of the art of available control strategies for stroke rehabilitation, in addition to a list of the current developed exoskeleton devices. It provides a discussion section, in which we tried to underline what we believe is constraining nowadays rehabilitation robotics with exoskeletons and it extends the concepts summarized in section 1.3 of this introduction. Chapter 3 deals with the development and testing of our adaptive control mode, and thus the analysis of the adaptation of the robot to the human behaviour. Chapter 4, instead, addresses the adaptation of the human behaviour to the robot control action, and it also contains the related experiment on the upper-limb inter-joint coordination modification. Finally, Chapter 5 provides some perspective of our work and conclusions on this thesis. This document is also made of few appendixes and some additional materials, provided to help the general comprehension of the dissertation.

Chapter 2

Control strategies for robotic exoskeletons: a state of the art

Contents

2.1	Review methodology	23
2.2	Available devices	24
2.3	Control strategies for stroke rehabilitation	25
2.3.1	Assistive modes	27
2.3.2	Corrective modes	32
2.4	Discussion	33
2.4.1	Hardware limiting control possibilities	33
2.4.2	The problem of reference definition	34
2.4.3	Addressing coordination control	35
2.4.4	Clinical testing issues	35
2.4.5	Lack of adaptation	36

As shown in section 1.3, the two major features of the robotic exoskeletons are their abilities to apply forces distributed along the assisted limbs and to provide reliable joint measurements [82]. Although the physical interaction through multiple contact points raises interest and fundamental questions from the control point of view, most of the existing control approaches have been developed by only considering the end-point interactions.

While many reviews on robotic exoskeletons are available, most of them are focused on their mechanical features, as for example [109, 25, 104]. We believe that the key characteristic of exoskeletons addressing neurorehabilitation stands in their control strategies which, on top of intrinsic mechanical behaviour of the devices (inertia, friction, backdriveability, etc.), dictate the human-robot interactions. Reviews on high-level control strategies for neurorehabilitation robots, including both manipulanda and exoskeletons, exist [113, 11], but since these were not targeting the specificities of exoskeletons, many devices and control approaches are missing.

2.1 Review methodology

We searched related literature in the main scientific databases (in particular *PubMed*, *ClinicalTrials*, *IEEE Xplore Digital Library*, *Science Direct*, and *Google Scholar*) using different combinations of these keywords:

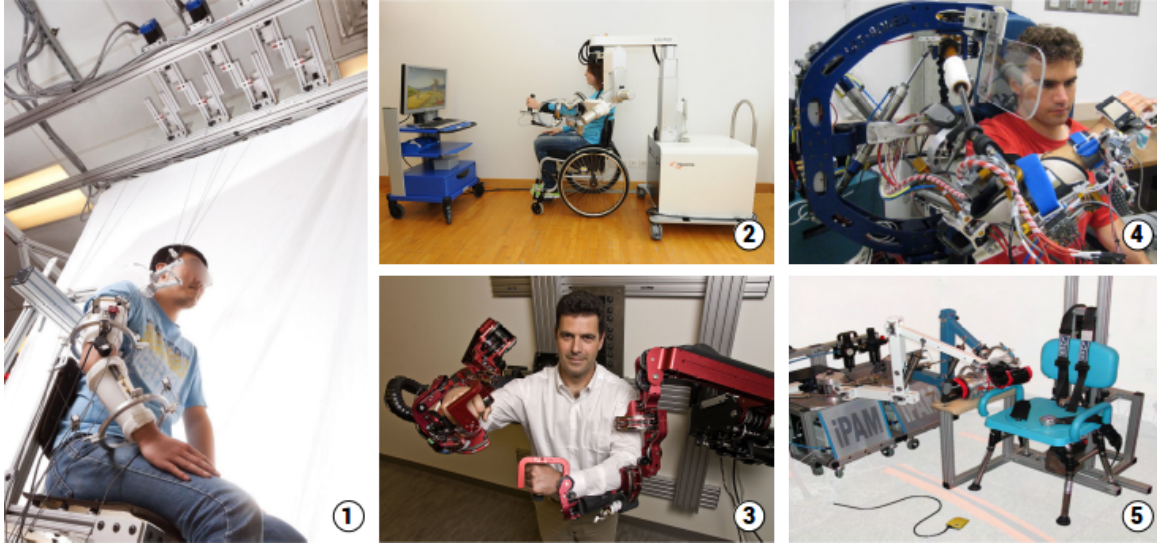


Figure 2.1: Examples of available exoskeletons for rehabilitation. ① CAREX [110]: cable-driven exoskeleton. ② ArmeoPower [151]: based on ARMInIV, it is the only commercially available upper-limb exoskeleton for neurorehabilitation with more than 3-DOF. ③ EXO-UL7 [163]: a two-arm exoskeleton. ④ BONES [94]: example of pneumatic exoskeleton. ⑤ iPam [83]: multi-contact multi-robot system.

upper-limb, rehabilitation, robot, exoskeleton, shoulder, elbow, wrist, arm, therapy, assisted, training, stroke. Besides, we also conducted a free search in the above-mentioned databases for references listed in keywords-based findings to include larger context. This review has been published in the *IEEE Reviews in Biomedical Engineering* [139]. For a purpose of feasibility, we focused our analysis on the subset of minimum 3 degrees of freedom (DOF) actuated upper-limb exoskeletons for rehabilitation, with control over at least two upper-limb joints among shoulder, elbow, and wrist. This reflects the aim of characterizing the available control strategies for multi-DOF devices, which apply forces along the assisted limb rather than acting only at the end-effector. Also, a review including most of the planar robots is already available in literature [11]. In the following review, we briefly illustrate every available control solution, providing more details on the ones which were clinically tested.

2.2 Available devices

32 robotic exoskeletons for upper-limb rehabilitation have been identified, considering only the devices with 3-DOF or more controlling the motions of minimum two out of the shoulder-elbow-wrist joint groups (see Table 2.1). Four devices [122, 83, 155, 173] composed by multiple robots acting on multiple contact points were not included in this review. Among the 32 exoskeletons, to the authors' knowledge, 10 devices were tested on post-stroke impaired subjects, but only 6 test provided comparisons with impaired subject control groups which tested different rehabilitation therapies. In addition, roughly one third of the existing structures seems not to be currently subject of study, *i.e.* no results have been published in the main journals and conferences for at least three years.

On average, full arm exoskeletons are 7 DOF robots, with at least 3 physical interfaces with the human operator, while, when controlling upper-arm or lower-arm only, the degrees of freedom are reduced to 4, with 2 contact points. Figure 2.1 shows different features of available devices. In particular, we can see differences in the actuation systems (more frequently these robots are driven by electrical DC motors, sometimes by pneumatic or hydraulic actuation, less used mostly because of the characteristics of the task — interaction with weak people — plus usually more bulky and complex to control), differences in mechanical characteristics (cable-driven versus directly controlled, 2-arm structures versus single ones, light “wearable” devices versus

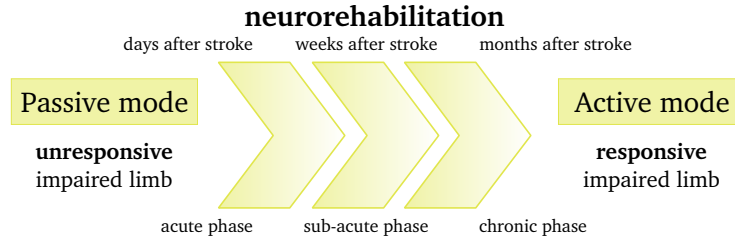


Figure 2.2: General neurorehabilitation timeline. Robot controllers should adapt to the correct phase of the therapy of the stroke survivor. *Passive* and *Active* are traditional terms to indicate the involvement of the subject in the training.

heavy wall- or ground-fixed systems, etc.).

2.3 Control strategies for stroke rehabilitation

Robot-mediated neurorehabilitation therapy mainly leverages on the same schemes of classical human-directed rehabilitation, by substituting a robotic device to the therapist, in order to help a patient to train arm movements. The rehabilitation process depends on subject capacities and phase of the injury, but it generally progresses from a very initial step of *passive* training — the subject is not able to move by himself, the therapist performs the motion for the subject — to a final step of *active* training, in which the subject has relearnt how to control his own limb, and can achieve simple to complex tasks alone (figure 2.2). The effectiveness of pure passive motions for stimulating motor recovery is known to be limited [108], since the patient is not involved in making any effort to perform the task. On the other hand, at least at the beginning of the rehabilitation, assistance is needed in order to reduce failures, to maintain subjects motivation and the intensity of the training, to increase patients confidence in using the affected limb, and to avoid negative reinforcement [82].

In between the passive and the active modes, there is a sufficiently wide variety of training modalities an expert therapist can apply. Inspired by the categories presented in [11], we defined three main global strategies for robotic-mediated rehabilitation: *assistance*, *correction* and *resistance*, see figure 2.3.

- *Assistance* means that the robot is supporting the weight of the impaired limb and providing forces to complete the task. If the patient does not produce any effort, task completion can be still achieved depending on the level of assistance.
- *Correction* defines the rehabilitation situation in which the robot is only acting when the patient is not performing the movement correctly, forcing the impaired limb to recover a desired inter-joint coordination.
- *Resistance* represents the techniques in which the robot opposes forces to the motion (potentially increasing the current error, for example) in order to make the task more difficult for the subject, and to train his ability to correct the movement and to adapt to external perturbations.

Contrary to assistance, correction does not assist the patient in achieving the task. Obviously, pure correction is an ideal case of neurorehabilitation therapy, as well as the former categorization. More often, the therapy involves several strategies combined [82].

While resistive controllers do exist for manipulanda (for example, resistive force-field in [161], or error augmentation in [183]), to the authors' knowledge, to date there are no available resistive controllers developed for exoskeletons. This could be a consequence of the fact that exoskeletons often target early stage chronic patients who rarely have recovered enough motor capabilities to undergo resistive therapies. However, most control strategies developed for manipulanda could be translated to exoskeletons, by considering only the end-effector control; though this solution would not take the full advantages of dealing with multi-contact systems like the exoskeletons.

project name	main university/company	first appearance	a	p	DOF type	pHRI	clinical testing
supported motion of shoulder-elbow-wrist							
ARAMIS [137]	Istituto Sant'Anna, Crotone, Italy	2009	6	0	e	2-sfh	[137]
ARMinIV [64]	ETH Zurich, Switzerland	2007	7	0	e	ufh	[93]
ArmeoPower ¹ [151]	Hocoma, Switzerland	2011	6	0	e	ufh	¹
ARMOR [116]	Abteilung fur Neurologische, Austria	2008	8	4	e	2-uffh	[116]
BONES+SUE [94]	University of California Irvine, USA	2008	6	0	p	ufh	[120]
BOTAS [156]	NRCD, Japan	2013	6	0	e	2-ufh	
ETS-MARSE [141]	Ecole de Technologie Superieure, Canada	2010	7	0	e	ufh	
EXO-UL7 ² [163]	University of California Santa Cruz, USA	2011	7	0	e	2-uffh	[163]
IntelliArm [149]	Rehabilitation Institute of Chicago, USA	2007	7	2	e	ufh	
NTUH-ARM [35]	National Taiwan University, Taiwan	2010	7	2	e	uf	
RUPERT IV [8]	Arizona State University, USA	2005	5	0	p	sufh	
SRE [23]	University of Salford, UK	2003	7	0	p	fh	
SUEFUL 7 [63]	Saga University, Japan	2009	7	1	e	uffh	
supported motion of shoulder-elbow							
- [124]	INSA Lyon, France	2009	4	0	e	uf	
- [105]	University of Auckland, New Zealand	2014	5	0	e	uh	
ABLE [60]	CEA-LIST, France	2008	4	0	e	uf	[29]
ALEX [138]	Scuola Superiore Sant'Anna, Pisa, Italy	2013	4	2	e	ufh	
AssistOn-SE [45]	Sabanci University, Turkey	2012	6	1	e	ufh	
CAREX [110]	University of Delaware, USA	2009	5	0	e	suf	
CINVESTAV-Robot-1 [61]	CINVESTAV-IPN, Mexico	2014	4	0	e		
L-Exos [52]	Scuola Superiore Sant'Anna, Pisa, Italy	2005	4	1	e	ufh	[55]
LIMPACT [129]	University of Twente, The Netherlands	2008	4	6	h	uuff	
MEDARM [9]	Queen's University, Canada	2007	6	0	e	uf	
MGA [24]	Georgetown University, USA	2005	5	1	e	uh	
MULOS [88]	University of Newcastle, UK	2001	5	0	e	uff	
Pneu-WREX [188]	University of California Irvine, USA	2005	4	0	p	ufh	[146]
RehabExos [176]	Scuola Superiore Sant'Anna, Italy	2009	4	1	e	ufh	
supported motion of elbow-wrist							
6-REXOS [68]	University of Moratuwa, Sri Lanka	2015	4	2	e	fh	
MAHI EXO-II [70]	Rice University, USA	2006	5	0	e	ufh	³
MAS [42]	Nara Institute of Science and Technology, Japan	2008	4	0	p	ufh	
ULERD [165]	Kagawa University, Japan	2013	3	4	e	uuff	
Wrist Gimbal [114]	San Francisco State University, USA	2013	3	0	e	fh	
multi-contact multi-robot systems							
- [122]	Universidad Miguel Hernandez, Spain	2011	6	0	p	uh	
iPAM [83]	University of Leeds, UK	2005	6	0	p	uf	[31]
NeReBot [155]	University of Padua, Italy	2005	5	0	e	fh	[115]
Reharob [173]	University of Budapest, Hungary	2004	12 ⁴	0	e	uf	[46]

Table 2.1: Exoskeletons for upper limb rehabilitation. We considered only minimum 3-DOF systems controlling at least two joints out of the shoulder-elbow-wrist chain. Number of Degrees of freedom (DOF): **a**-active thus actuated, **p**-passive thus mechanical only. Type refers to the actuation system: **e**-electrical, **p**-pneumatic, **h**-hydraulic. Physical Human-Robot Interface (fixation levels) : **2**-two arm exoskeleton, **s**-shoulder, **u**-upper arm, **f**-forearm, **h**-handle. Double letters indicates double interfaces. The last four projects are not strictly exoskeletons but rather multi-contact multi-robot systems. ¹based on ARMinII, the only commercialized exoskeleton for the clinical environment. ²based on CADEN-7 (2006) [136]. ³ongoing test, ClinicalTrials.gov identifier: NCT01948739. ⁴two 6-DoF industrial serial manipulators.

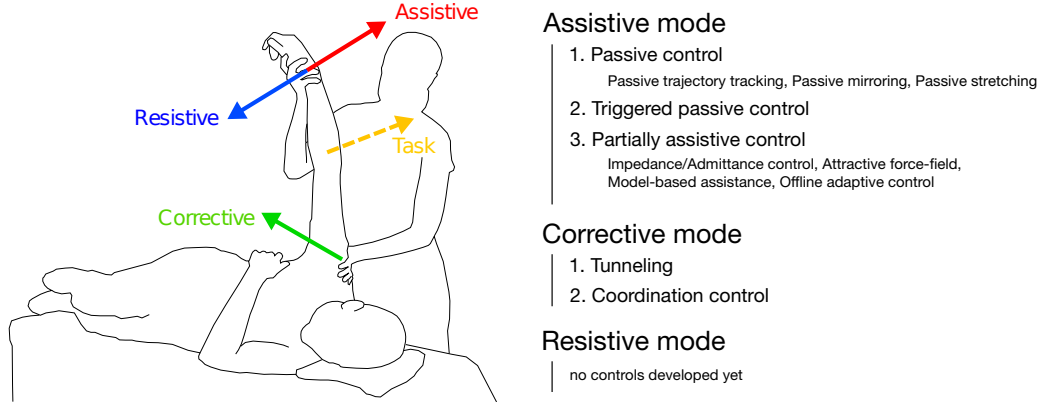


Figure 2.3: The three global strategies for robotic-mediated rehabilitation. In details, also the current implementations on robotic exoskeletons.

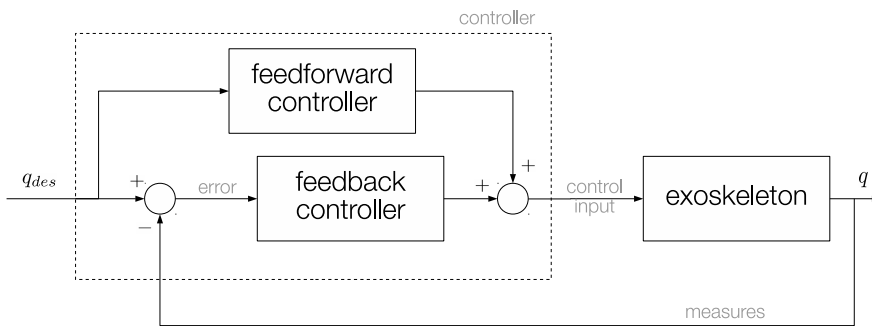


Figure 2.4: General control scheme for exoskeletons for neurorehabilitation. The control is made of a feedback term, which varies controller by controller, and a feedforward term, which is usually adopted to compensate for predictable perturbations in an anticipatory way (for example, the weight or the dynamics of the exoskeleton, and the friction forces within the joints).

Existing controllers for exoskeletons mostly combine assistive-corrective control, but there exists a variety of implementations of each category by using different control techniques. The general control scheme is made of a feedback term, which varies controller by controller, and a feedforward term, which is usually adopted to compensate for predictable perturbations in an anticipatory way (for example, the weight or the dynamics of the exoskeleton, and the friction forces within the joints), see figure 2.4. Model-based gravity compensation is one possible solution to decrease the weight of the robotic arm, and thus the effort by the subject, but it is not always simple to model the usually complex exoskeleton structures (because of, for example, moving parts within the actuation transmission). Other solutions to produce feedforward compensation usually involve adaptive control [187], neural networks [193], or iterative learning [7].

2.3.1 Assistive modes

Within this type of control approaches, three groups of assistive strategies were determined — *passive*, *triggered passive*, and *partially assistive* control — although there exist solutions which are mixed strategies. The distinction between *passive* and *partially assistive* controls is thin, since if the patient is not participating in the task, both controllers would react similarly. Also, triggered assistance generally refers to solution only different to initiate the assistance: once triggered, these controllers usually exhibit either passive or partially assistive behaviours.

Passive control

The simplest way to control an exoskeleton is to control the motion rigidly along a desired reference trajectory through position feedback control with high corrective gains. In rehabilitation this *passive* technique is common at early stages of the post-stroke therapy, when the impaired limb is usually unresponsive, and thus passive mobilization is the only feasible solution to achieve any result. Nonetheless the feedback controller gains have to be tuned carefully and the exoskeleton has to show a minimum of compliance not to hurt the subject in the presence of trajectory errors due to excessive muscle contraction, spasticity, or pathological synergies. Such compliance between the robot and the human body can also be introduced mechanically, at the fixation level with, for example, elastic straps [8] or mechanical fuses placed serially [173].

► **Passive trajectory tracking** Passive control can be achieved by adopting different techniques. The simplest is the use of a proportional-integral-derivative (PID) feedback control which usually regulates the position or the interaction force along a known reference (for example, a trajectory or a force field model), and can be applied either at the joint or at the end-effector level. Examples of these joint controllers are shown in [61, 114, 166, 24, 125, 176, 123, 129].

More complex approaches have been recently developed to improve the quality of the physical interaction during passive mobilization of patient's limb. In [141], the authors developed the *Sliding Mode Control with Exponential Reaching Law (SMERL)*, a non-linear control technique which minimizes the tracking error on a state space projection. In [102] a fuzzy logic technique is adopted: in order to deal with uncertainties and disturbances from the environment, adaptive fuzzy approximators estimated the dynamical uncertainties of the human-robot system, and an iterative learning scheme was utilized to compensate for unknown time-varying periodic disturbances. Preliminary results on healthy people showed better performances, in terms of tracking error and average control input, compared to classical PID control.

Different methods exist for defining reference trajectories. For passive strategies, these references are often created by recording the physiotherapist inputs on the subject limb attached to the exoskeleton, during a *teaching* phase. In this phase, the robot is generally set in a transparent mode (usually achieved by adopting a feedforward term to compensate for the robot dynamics) to limit any resistance to perform motions. Once recorded, the exoskeleton is ready to *replay* the trajectory with its feedback controller. *Teach-and-replay* is presented in [95]. In [166] teach-and-replay mode was tested on four chronic stroke patients during 8 weeks of training. Encouraging preliminary results were obtained (increase of Fugl-Meyer Assessment score – FMA, meaning improvement of motor functionality of the paretic arms, in addition to positive transfer to ADLs). Nevertheless, no comparisons with control group receiving traditional therapy were provided. Similarly to teach-and-replay, *record-and-replay* uses healthy limb motions, recorded within the robot, to create reference trajectories. This strategy was for example used in [137].

Instead of using external inputs or "healthy" trajectories as references, some research groups have been trying to directly detect patient motion intention by measuring muscle activity through surface-EMG. In [106] EMG and two offline-trained time delayed neural networks (one for the shoulder and one for the elbow) were used to estimate and predict the resulting torques at the joint level. By using this prediction, a reference joint position trajectory was computed and fed to a PD controller with gravity and friction compensation. In [142] an EMG-based version of the SMERL controller was provided. In this case, EMG signals, transformed to a desired position reference through a muscle model, acted as the reference for the position feedback controller.

A third strategy to define reference trajectories is to determine cost functions and to use optimization algorithms. Generally the cost function aims at minimizing the jerk. This solution is mostly used for triggered passive control (for example in [156]) or for partially assistive controls (examples in [187] or [182]). Due to the complexity and variety of possible actions of the upper-limb, generally the movements of intermediate joints either occur as a consequence of the end-effector movement in the task space (for example in [110]), or are constrained along specific dedicated trajectories, which are synchronized within the joint space (for example in [53]). However, because of the redundancy of human arm, there are no commonly accepted solution to compute joint trajectories from task space motions [67].

Beside standard passive control approach, two other passive strategies exist. Those either target two-arm exoskeletons (*passive mirroring*) or utilize a different rehabilitative training, *i.e.* the *passive stretching*.

► **Passive mirroring** Few exoskeletons have two arms (four devices in Table 2.1, column pHRI). For these robots, *passive mirroring* is a further strategy. It consists of synchronous passive mimicking of the behaviour of the healthy limb, in a master-slave configuration, as in [137] or in [116]. In [137] a clinical pilot study on 14 impaired subjects (21±6 days since stroke), based on an average of 31 sessions over 2 months, resulted in applicability and tolerability of the robot-mediated treatment, with similar improvements to other robot-assisted rehabilitation therapies. In [69] passive-mirroring was implemented on a single-arm robot in a master-slave configuration with an external haptic device to control the master side of the system.

► **Passive stretching** A different rehabilitative passive training is the so-called *passive stretching* [149]. With this strategy, individual joints were passively stretched by the robot in order to identify their individual angle-resistance torque relationships. These relationships were then used to coordinate the passive stretching of multiple joints together. Feasibility test performed in 3 stroke patients showed a reduction of cross-coupled stiffness after a 40 min stretching session.

Triggered passive control

A slight variation of assistive modes consists in approaches in which the user triggers the exoskeleton assistance. This technique is frequently used to introduce brain-machine interface (BMI) into the control loop. These approaches are directly adapted from the field of assistance to patients with non-recoverable impairments (like tetraplegia). In fact, after the triggering (mainly a selection of available targets), the exoskeleton is usually controlled passively along pre-determined trajectories.

In [156] passive recorded-trajectory replication through BMI control is shown. The end-effector trajectory were computed by minimum-jerk optimization. BMI trajectory-replay triggering was implemented through SSVEP (*steady-state visual evoked potential*). SSVEP can be observed mainly from the visual cortex when a person is focusing his visual attention on a flickering stimulus. Pre-clinical testing (12 healthy and 3 upper cervical spinal cord injured subjects) were performed to show the capacity of the system to be used by subjects to activate different trajectory reproductions.

In order to extend patient's control over the task, gaze tracking methods can also be used in addition to BCI-driven control like in [54]. An eye-tracker together with a target-tracking module (a Kinect camera) gave the reference position of the target to reach to the exoskeleton controller; the BCI module estimated user's motion intention, modulating maximum joint jerk, acceleration, and speed within an admissible predefined set of values. Then a PD feedback control (helped by classical gravity and friction compensations) performed the reaching task. Pre-clinical testing with 3 healthy and 4 chronic stroke patients showed that all subjects were able to operate the exoskeleton.

In [10] a Motor Imagery based Brain Computer Interface (MI-BCI) is used to control an eight DOF exoskeleton. Three chronic stroke survivors were able to perform passive controlled tasks (arm motion towards a target, grasping and releasing of an object) by producing MI of the reaching task before the movement. Two seconds of MI activity collected, triggered the exoskeleton to replay pre-recorded trajectories. In [17] authors developed a similar approach, by controlling an ArmeoPower exoskeleton through MI-BCI. 9 healthy subjects and 2 stroke survivors were able to move the exoskeleton along pre-defined trajectories, and these motions were brain-state dependent, meaning that motion was performed only during MI phases.

Partially assistive control

The effectiveness of pure passive motions for stimulating neuroplasticity is known to be limited [108], since the patient is not involved in making any effort to perform the task. On the other hand, assistance is needed in order to reduce failures at least at the beginning of the therapy, thus maintaining subject motivation, intensity

of the training, confidence in using the affected limb, and to avoid negative reinforcement [185]. But as soon as the patient has recovered a minimal amount of motor capacity, it is essential for the robot to allow for shared control of the movements [79], [130]. Indeed, as neurorehabilitation addresses issues related to motor control, the devices must allow patients to express whatever movement they can without suppressing any motor capability [77].

Partial assistance, or *assistance-as-needed* [187], groups all those control strategies which allow the impaired subject to actively control the motion, supporting it based on performance indexes. The most common solution to provide a partial assistance to the impaired limb, is to increase the compliance of the above-mentioned passive controllers. Instead of rigid “industrial-type” position feedback controllers (with high corrective gains), many controllers for exoskeletons rely on more flexible *impedance control* [76], or its dual *admittance control*, with reduced corrective gains to exhibit “human-like” mechanical properties. These controllers allow to implement a good compromise between tracking skills and compliance of the robotic arm.

► **Impedance/Admittance control** Impedance control is a model-based force controller with position feedback while its dual, the admittance control, is a position controller with force feedback. Impedance control is efficient for lightweight backdrivable exoskeletons (often cable-driven devices). In these systems, problems arise when it is necessary to compensate for gravity and friction. For exoskeletons that lack backdrivability, admittance control may be more appropriate, because the forces at the interfaces with the human limb must be measured to move the robot, thus considering its inertia and dynamic effects. The force-tracking trade-off feature, together with the simplicity of implementation, are the reasons why these are two of the most common control algorithms currently used for rehabilitation exoskeletons [70, 95, 24, 30, 166, 174].

Adopting an admittance/impedance approach, some research groups developed slightly different and more complex strategies. In [56] the exoskeleton was controlled through two impedance control loops, one for assistance along the end-effector reference trajectory, the other to apply corrections along the orthogonal direction to the trajectory. Model-based gravity compensation was also present. The setup was supported by a virtual environment on which a reaching game was created. A therapist could directly tune tasks complexity on a therapy control unit. Pre-clinical testing (8 post-stroke subjects), three one-hour rehabilitation sessions per week for a total of six weeks, resulted in performance improvements and a reduction of position errors after the therapy for 5 patients. The same controller was tested in [55] on 9 impaired subjects performing three games (pointing task, circle drawing, and puzzle-type game). The robot-aided training induced, independently from the post-stroke phase, statistical significant improvements of kinesiologic and clinical parameters (such as analysis of reaching movements, degree of functional impairment through FMA, active range of motion, and Modified Ashworth scale), as a result of the increased active ranges of motion and improved co-contraction index for shoulder extension/flexion.

In [194], the authors developed a model-free PID type admittance control in task space to generate desired trajectories for a lower-level PID position control in task space too. The control parameters can be chosen based on kinematics and dynamics of the human arm. Besides, a simplified model-based gravity compensation was used. In [119] the authors compared task space with joint space admittance control, showing that task space control spent about 11% less of interaction energy for a peg-in-hole task. In [63] the exoskeleton was controlled by an end-effector impedance control. A joint torque fuzzy logic estimator (using signals from 16 sEMG channels and a couple of force/torque sensors) evaluated the user hand motion intention. The fuzzy set of membership functions determined which data considering from a combination of the two inputs: if the EMG values were high, the estimation was only EMG-based; if they were low, it was only force/torque based; otherwise a continuous mixed integration of both signals was adopted. In [165] admittance control was computed by substituting force sensors with springs, and their compression measured to estimate interaction force between the human limb and the robotic device. Two control techniques were implemented: respectively high stiffness mode when passive DOFs of the arm (a group of 4 springs) were locked, and resistive training when they were unlocked.

Apart from impedance-admittance controls, there exist others examples of assistive controls in the literature.

In particular, we can describe three categories of assistance respectively based on attractive force-fields, on human arm model, and on offline adaptation.

► **Attractive force-field** [91] used, among other approaches, an attractive force field to control their exoskeleton during a clinical rehabilitation therapy with 15 impaired subjects. During the trial, subjects were randomly assigned to bilateral training (BT), unilateral training (UT), and standard therapy (ST) and executed a total of 12 sessions of virtual reality gaming (8 different games in total). While in BT partially assisted mirroring of the unaffected limb was provided by the robotic exoskeleton, in the UT an attractive force-field acting only on the end-effector was determined based on the end-effector position. For the other joints of the robot, an assistive force was produced based on reference trajectories computed by using the swivel angle estimation algorithm [90]. Following these treatments all of the subjects significantly improved their fine motor control and gross control across all the treatment modalities. BT showed better results compared to UT but this might have been because of more assistance from the robot to the impaired limb. However robot-mediated therapy exhibited comparable outcomes than standard therapy.

► **Model-based assistance** In [42], after an offline posture measurement through motion capture, authors derived a muscle force estimation to maintain a desired pose, by using a musculoskeletal human model. The reference muscle force was then fed into the device controller together with the current force, estimated through 3 EMG sensors, and a proportional control drove the pneumatic actuators to provide only the necessary force. In [41] the former method was improved to reduce non-target muscle efforts through an optimization algorithm, and tested for controlling quasi-static posture-by-posture human motion.

► **Offline adaptive control** Adaptation trial-by-trial is also a solution to modulate robot assistance based on different performance indexes. In [8] the authors implemented an iterative learning control: a feedforward assistive term was learnt using trial-by-trial adaptation, based on the error of the previous trial and on a fuzzy logic based non-linear function of the tracking error statistics. The feedforward term was then added to a PID feedback controller at the joint level. Pre-clinical testing with 6 impaired subjects to test its usability are shown in [195].

In [187] a PD controller was also used with a feedforward assistive term, which was adapted during the motion depending on the dynamics of the patients extremity, the patients neurological ability, and the patients effort, modelled through a Gaussian radial basis function neural network. Assistance-as-needed was achieved by adding a force decay term to the adaptive control law, which reduced the output from the robot when errors in task execution were small. The controller was tested with 11 chronic post-stroke patients. Results interestingly showed the “slacking” behaviour of the human motor control, meaning that, as the central nervous system (CNS) tries to optimizes its efforts, as soon as it can take advantages of the controller, it leaves the controller taking over most of the physical effort required to complete the task. By adding the force decay term, the controller was able to encourage the patient efforts.

Two different tests of the same controller on two different exoskeletons were presented in [146] (clinical testing with 27 impaired subjects) and [120] (20 subjects with mild to moderate chronic stroke). In the first study, the subjects, divided into two groups, received either the assist-as-needed robot training, or conventional table top therapy with the supervision of a physical therapist. The results were moderately better by assisting the tasks with an assist-as-needed controller. In the second study, the subjects experienced multi-joint functional training and single joint training, generally improving motor function after chronic stroke. Multi-joint functional robotic training was anyway not decisively superior to single joint robotic training.

In [140] an adaptive PD controller, acting at the joint level, together with a model-based feedforward gravity compensation, regulated the stiffness of a robotic exoskeleton. Tracking error of the reference trajectory drove the trial-by-trial adaptation of the feedback gains. In [133] a sensorless force estimator, based on a Kalman filter, was used to dynamically determine the exoskeleton operator’s capability performing the desired task, in order to provide him minimal assistance with an user-specified maximum allowable bounds on position error.

Both the two former controllers were only preliminary tested on healthy subjects, showing the applicability of the two approaches.

Finally, in [135] an assist-as-needed control algorithm tried to anticipate patients deviations from desired reference trajectories, by utilizing an adaptive model of the patient's dysfunctionality. Such a dysfunctional profile of the patient should be provided by the therapist, depending on both the specific ADL and the patient motion deficits. The anticipatory behaviour of the controller was only tested through a simulation in virtual reality by the authors.

2.3.2 Corrective modes

As described in the former section, many assistive controllers act on the trajectory followed by the subject not only in the direction of the desired motion, but also applying forces along the orthogonal direction, which is the domain of corrective control.

A key to understand the differences between the two approaches is the capability to successfully complete a motion without any effort from the subject: assistance is generally able to move the limb towards the final target, if the subject does not participate, while ideal corrective strategies cannot.

A similar concept can be expressed by considering the time-dependency of the references. Assistive controller are usually fed with desired trajectories, *i.e.* time-dependent speed profiles. Pure corrective strategy is linked to the idea of time-independence of the references, for example feeding the controllers with desired path instead of trajectory. The time-independence allows the robot to only act on the current position to correct it along the orthogonal direction.

However, it is often difficult to make a clear distinction between pure assistive control laws and pure corrective ones. Currently there exist two approaches which provide pure correction, or at least, in which assistance is clearly decoupled from correction.

Tunneling

Tunnelling consists in creating virtual channels for the end-effector or the joints of the exoskeleton, in which the subject moves: once he/she goes out of the channels, the feedback control takes him back into the channel, as if a spring impedance was attached from the limb to the center of the virtual channel. In addition, to prevent the subject from getting stuck during the motion, a supporting force in the direction of the channel is generally added. Therefore, tunneling strategies can be seen as an impedance control with a path-centred no-action zone, *i.e.* one can clearly consider the supporting force field as an *assistive* term, and the spring-damper-like force in the direction of the centre of the channel as a *corrective* term.

In [64] the channel was acting on the end-effector position and the supporting force field was adapted depending on minimally desired mean velocity of the subject's limb. The system was also fed with control inputs from the gravity and friction feedforward compensator. The reference trajectory was divided in subtrajectories, and a trajectory generator algorithm updated the tunnel direction every time the subject achieved a subtask. Pre-clinical testing on healthy and 3 impaired subjects showed the feasibility of such control paradigm. The same controller was tested in [93] in a clinical experiment with 77 stroke survivors. Various games and ADLs were tested in a virtual reality environment, augmented with online audiovisual information to increase subjects motivation. After 8 weeks of training, small improvements in FMA scores were higher in patients assigned to robotic therapy than in those undergone conventional therapy. A similar approach was adapted by [112]. Due to the cable-driven system, simultaneously to the high-level tunnelling controller, a low-level PI plus feedforward control kept the tension of the cables [111]. Pre-clinical testing on 8 healthy and 1 impaired subject, showed that the subjects constantly moved closer to a prescribed path in the training trials.

Coordination control

When considering corrective modes, the aim of the control law is generally to regulate the coordination (also called “synergies” [14]) during the movement, *i.e.* controlling joint positions and/or velocities relative to the others. Trying to coordinate inter-joint positions or speeds is a way to solve the reference time-dependency problem, which remain a constraining parameter of the assistive controllers.

In [18] the Time-Independent Functional Training (TIFT) algorithm was introduced: virtual joint-space walls kept the subject close to the ideal joint-space path, acting simultaneously on multiple joints motion as PD position controls. This strategy provided assistance as correction to bad motion coordination of the main joints active during the task, in particular on shoulder and elbow joints. This controller was tested on 12 impaired subjects in a 3-month pilot study [19]. Data suggested that this robotic therapy could elicit improvements in arm function that were distinct from conventional therapy (improved inter-joint coordination), and thus it could integrate to conventional methods to improve outcomes.

In [29] an alternative approach was presented, the Kinematic Synergy Control (KSC). In this work, the problem of tracking was projected from the reference trajectory space to the joint velocities synergy space through Principal Component Analysis (PCA). The exoskeleton generated reactive viscous joint torques to impose specific patterns of inter-joint coordination without constraining the hand motion. This controller was tested with healthy subjects and, preliminarily, with hemiparetic patients, and showed its the ability to impose constrained synergies without altering the hand motion.

[65] developed an approach based on correction of the pathological involuntary flexion torque, which occurred at the elbow during shoulder abduction. During an evaluation session with the robot, the patients pathological involuntary torque was measured and a counter-active, just-as-needed torque was then calculated and applied during the therapy. A case study on one patient showed a reduction of elbow involuntary elbow flexor torque during shoulder abduction. [149] used a similar approach to develop a passive stretching controller for multiple joints. However no active modes of therapy, during which the subject is actively participating in the movement, based on previously identified angle-torque relationships, have been developed to target patterns of inter-joint coordination.

2.4 Discussion

We reviewed the currently available control strategies for robotic exoskeletons for neurorehabilitation, among about 100 publications and about 30 existing devices. This review allowed us to identify several issues and scientific barriers potentially limiting - to the authors’ opinion - the rehabilitative performances of current exoskeleton devices. In the following section, we discuss some of these analyses.

2.4.1 Hardware limiting control possibilities

One of the performance indexes that quantifies an exoskeleton ability to precisely produce a programmed assistance to the subject, is its transparency. This may seem contradictory, since transparency measures the robot ability of not applying any assistance/resistance to free motion. But this property is a good indicator for force precision, since any failure to reach transparency during a zero-resistance experiment will be reproduced and act as a bias in a non-zero force experiment.

As seen in section 1.3.2, transparency therefore qualifies the mechanical properties of the structure (weight, inertia, friction, etc.), of its actuation (backdriveability, friction, etc.), and of the performances of the low level control dedicated to the compensations of these perturbing phenomena (feedforward compensation of the gravity and friction, for example).

A lack of transparency can generate undesired resistances during the upper-limb motion of subjects (even healthy), from which excessive muscle efforts can arise to complete even simple motions. This, obviously, can be negligible for healthy subjects, even if it is already highly perturbing [86], but it cannot be allowed with impaired patients during rehabilitation. Moreover the lack of transparency can make almost impossible to

develop pure corrective strategies on the exoskeletons, since it does not really allow shared control (the human on the motion, the controller on the corrective part).

The transparency level directly influences the physical behaviour of the robot, and possibly perturbs the rehabilitative control strategy of the robot. Therefore it would be necessary to assess exoskeletons standard features. For example, simply showing comparisons of motion ability (like range of motion) of healthy subjects with and without the exoskeleton, almost always lacks in exoskeleton design papers. Such an analysis was recently performed on the only commercially available exoskeleton for neurorehabilitation, and shows that it significantly affects the reaching movements of healthy subjects [50].

Clinical results obtained with any platform are possibly not qualifying the rehabilitation capacity of a control strategy but rather the global performance of the system. A specific care should therefore be given to draw general conclusions on rehabilitation approaches with exoskeletons.

Similarly, while researchers are starting to consider exoskeletons' sensors as a direct source of data to evaluate patient state and recovery evolution [127], it is important to highlight the fact that the capability of modern exoskeletons to provide correct assessment of quality of human motion, directly lies on their ability to be transparent.

2.4.2 The problem of reference definition

As showed in section 2.3, a central issue for most research groups is related to the generation of reference trajectories and thus, to the computation of error profiles to supply the feedback controllers. Physiotherapists also share the necessity of defining references for applying correct torque profiles on the impaired arm and, more generally, evaluating subject movements. With the experience, they learn how to correctly manipulate impaired limbs to induce neuroplasticity and recover motor control. Translating this qualitative feature into a quantitative reference for the robotic devices is a key issue, especially for 3D movements when considering interaction at the joint level.

The reference generation is a two-level problem. At the low level, the exoskeleton must be fed with human arm suited feasible trajectories to successfully complete the desired task, but taking into account the natural redundancy of human arms, at the high level, the issue is to select one of the many correct possibilities to perform the motions and achieve the task. Additionally, the ideal reference trajectory should be customized on the patient features, taking care of the specific arm physical characteristics and impairments, such as paralysis, spasticity, and joint limitations.

It is important to underline how the reference generation is a different problem from controlling the exoskeleton. Indeed, the same controller may lead to different rehabilitative performances being fed with references computed by using different techniques (an example of this phenomenon is given in the next chapter, section 3.4).

In section 2.3, we described mainly three different approaches for generating motion references. The simplest technique is about directly recording the motion of the human limb (*teaching/recording*). This generation process of recording and extracting a trajectory is time-consuming and not generalizable to multiple tasks, but it produces always feasible and customized references.

A second common technique is about using *optimization algorithms*. Computational models usually exploit minimum jerk optimization to generate the desired smooth feasible trajectory. This optimization technique has its advantages in the quickness of providing a solution, but this solution is still valid for one-single task. The last technique is about the possibility of anticipating the human CNS by detecting motion intentions, or more simply by detecting, in a set of predefined trajectories, the one to be performed (*motion intention detection*). This approach is spreading as a common solution for many research groups, even if there exist generic technical issues concerning, for example, discrete signal extraction (either from the brain or from the muscles), noise deletion, etc. Motion intention detection can be realized through force/torque sensors (for example in [177]), EMG (examples in [106, 63]), or through oculography and EEG (examples in [54, 156]). The resulting controllers appear often to be passive-triggered controllers which replay pre-determined reference trajectories, either recorded or computed through optimization algorithms.

A fourth solution to produce motion models is the generation of feasible trajectories through the evaluation of statistically consistent patterns performed by a sufficient number of healthy subjects. Nonetheless, due to its complexity, this technique is not commonly used for rehabilitation robotics and only one example can be found in [135].

Despite the above-mentioned strategies, it is important to underline that relying on a reference trajectory limits the efficacy of the rehabilitation therapy since these trajectories are generally position and time dependent and, therefore, they are complex to generalize for different movements, targets, or tasks. This means that the patients freedom of movement, within the exoskeleton, is limited to specific movements. These interactions, constantly imposing constraints (more or less rigidly), are less physiological than conventional therapy (like, for example, the Bobath therapy, during which the patient is active, occasionally guided or corrected, but not constantly constrained to follow a fixed gesture) and therefore their efficiency is questionable [85].

In order to increase human involvement in the rehabilitative therapy, thus increasing the efficacy of the therapy itself, exoskeletons controllers should target goal-independent strategies. Ideal goal-independence is a solution which allows multiple targets reaching and tasks achievement, without acting on the controller, neither the control law nor the reference. Thus, in this case, the reference is necessary described at a higher level of abstraction than the simpler common trajectory reference. Together with goal-independence, time independence, as defining path references rather than trajectories, is a key factor to allow the subject to actively make an effort to achieve the task, not being constrained by following rigid planned trajectories [85].

2.4.3 Addressing coordination control

Time independence translates into a necessity to develop inter-joint coordination controllers, more than trajectory trackers. In fact, this kind of controllers requires relative references (for example, speed profiles of joint synergy coordination) more than absolute ones, as, for example, joint positions profiles in the case of trajectories. The importance of measuring and controlling joint synergy is primary to better understand quality of movements during rehabilitative therapy. Post-stroke patients frequently adopt pathological compensatory strategies that are difficult to be analysed without coordination assessment. In [127] authors review current assessment strategies for motor recovery with robotic exoskeletons after stroke. Their emblematic conclusion says that most assessments for robotic-mediated therapy addresses end-point movements, ending in a minimal measure of compensatory joint synergy strategies. Without the latter, it is complex to distinguish between genuine motor recovery and dangerous compensation.

Few research groups developed solutions aiming at controlling synergy joint coordination [65, 149, 18, 29], as described in section 2.3.2. However, for all these approaches, only preliminary results exist.

2.4.4 Clinical testing issues

What arises from the general overview of this state of the art and of Table 2.2, is the limited number of studies and experiments both on healthy and impaired subjects. Indeed, among all the devices, only 8 of them were clinically tested, *i.e.* providing comparisons between different developed control strategies and/or standard therapies, including impaired subjects control groups. Furthermore, only three studies out of those eight involved simultaneously 20 or more stroke survivors [93, 146, 120]. For all these studies, robotic-mediated therapy generally produced small improvements in impairments measures and motor recovery compared to standard therapy on the same number of repetitions. These improvements were usually detected by FMA, range of motion tests, and measurements of strength. Only one study [120] described functional improvements after robotic training. Clearly, neither motor recovery nor functional improvement alone necessary translate to improvements in ADLs or in quality of motion, since there may still be unhealthy compensations (in case of functional improvements) or no real-life relevance (in case of motor recovery) [82].

A problem arising is the absence of a standard assessment method of the results of the robotic-mediated therapy, especially with exoskeletons (*i.e.* with multiple interaction points): the chosen kinematic parameters specify too often end-point movements only and are not able to address directly motion coordination. Moreover,

Ref.	Device	Year	No. of subjects	Control strategy	Summary of the results
[93]*	ARMin III	2014	77	Tunneling	Small improvements in FMA score
[146]*	Pneu-WREX	2012	26	Assistance-as-needed	Small improvements in FMA score
[120]*	BONES	2013	20	Assistance-as-needed	Improvements in FMA and functional tests (like WMFT), no differences between multi-joint/single-joint training
[91]*	EXO-UL7	2013	15	BT (mirroring), and UT (partial assistance)	Improvements in score of few efficiency indexes but small improvements in FMA score, BT better performing than UT
[137]*	ARAMIS	2012	14	Rec-and-Replay	Proof-of-concept test, similar score as other test with exoskeletons
[55]*	L-Exos	2012	9	Partial assistance	Small improvements in FMA score
[195]	RUPERT IV	2011	8	Passive	Feasibility test
[29]*	ABLE	2012	7	Coordination control	Preliminary results on improvements on shoulder-elbow coordination
[163]*	EXO-UL7	2013	5	BT (mirroring), and UT (transparency)	Same improvements as standard therapy, UT less performing than BT
[149]*	IntelliArm	2013	3	Passive stretching	Reduction of cross-coupled stiffness
[156]	BOTAS	2013	3	BMI	Feasibility test
[112]	CAREX	2014	1	Tunneling	Preliminary results on better trajectory tracking

Table 2.2: Control strategies tested on stroke survivors with robotic exoskeletons. The asterisk * indicates clinical testing, meaning results provided comparing different control strategies.

these parameters show insufficient correlation with standard clinical assessment [127], thus they are difficult to be used as predictor to the clinical outcomes of robot-mediated therapy.

However, it is important to underline that each single clinical result is strictly linked to the device and the selected control strategy. In fact, every test is the result of a combination of the mechanical properties of the available exoskeleton, its transparency level, the chosen control strategy, and the type of generated reference. Thus, it is yet difficult to produce generic conclusions about the results of exoskeleton-mediated therapy.

2.4.5 Lack of adaptation

As mentioned in section 1.2.4, rehabilitation efficiency increases when patients are involved and motivated to actively perform physical exercises [150], but at least at the beginning of the therapy, upper-limb assistance is necessary to increase patients confidence in using the affected limb [82]. Nonetheless, refining the level of challenge of the practice, based on the recovery phase of the patient, may lead to improved results [185].

The existence of this trade-off between requested involvement of the patients and necessary assistance by the therapist is clearly an issue for neurorehabilitation. In 2008, two studies, respectively by Wolbrecht *et al.* [187] and Franklin *et al.* [51], showed the existence of a “slacking” behaviour by the human CNS, meaning that persistent over-assistance of the upper-limb leads to a minimization of the active physical involvement of the subject, thus mostly transforming partial assistance into passivity, with the consequence of reducing the motor improvements by the patients.

However, when considering the current state of the art, most of the available control strategies tends either to partial fixed assistance through impedance/admittance control or to complete passivity of the patients. There

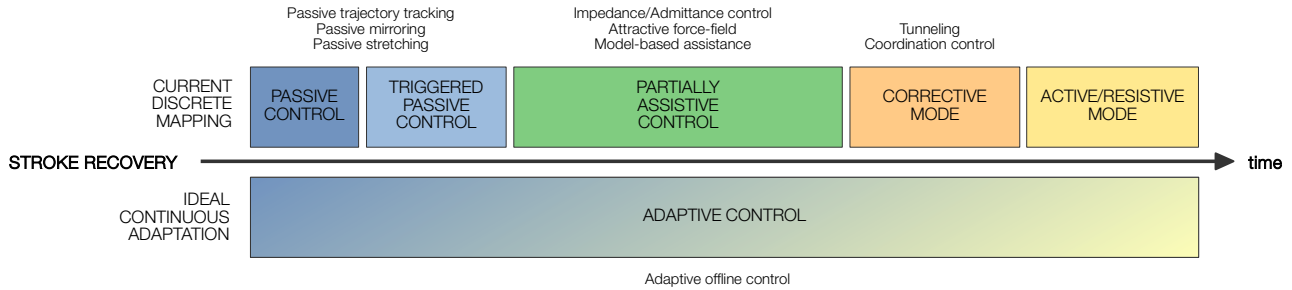


Figure 2.5: Existing discrete mapping between patient recovery and control strategies. As shown, the assistance provided by the robot is discretely, and generally manually, updated. An ideal adaptive controller would be able to finely continuously modify its level of assistance, better following the patient capabilities. Resistive controllers are not yet available for robotic exoskeletons.

exist different solutions which discretely map the successive stages of the patient recovery: from passive control, which zeros the compliance of the robot, to partial assistance, which requires some effort from the operator, to active modes, in which the robot is only compensating for its weight, finally to resistive modes, which fight against the user motion intention, see figure 2.5. However, these are only separate discrete controllers, which perform rigid assistance, generally manually programmed and updated.

Therefore an important effort must be done to understand how to produce a continuous and finer adaptation through the different stages of recovery, automatically retrieving the data from the robot reliable measurements and deriving the information to interact with the therapy. Consequently exoskeletons could improve their performance by providing explicit reactions to patient behaviours during interaction [58] and could even account for differences between stroke survivors, avoiding one great mistake of modern rehabilitation robotics, that is the prescription of standardized therapies to the different patients, as in the case of the lower-limb exoskeleton *Lokomat* (© Hocoma) which has been found to alter healthy walk patterns due to poor adaptability to the specific human user [73, 75, 134].

Chapter 3

Robot adaptation to the human action

Contents

3.1	Introduction	38
3.2	Adaptive control	39
3.2.1	Working principle	39
3.2.2	Control algorithm	40
3.2.3	Performance metrics	41
3.3	Proof-of-concept	42
3.3.1	Preliminary test: mimicking relearning	42
3.3.2	Advanced test: more dynamical behaviour and different adaptation rates	44
3.4	Comparison of different error signals driving the adaptation	47
3.5	Conclusions and perspectives	53

3.1 Introduction

The existence of a trade-off between requested involvement of the patients and necessary assistance by the robot is clearly an issue for neurorehabilitation, above all because of the so-called *slacking* behaviour [187, 51], as mentioned in the former chapter. There exist several different solutions to map the successive stages of the patient recovery, but these are mostly discrete, meaning that they need to be manually configured and updated. A rather simple improvement to this issue would be the use of adaptive control techniques to produce *Assist-As-Needed* (AAN) modes. Adaptation can allow the robot to modulate its assistance level based on the user necessities, potentially leaving the patients expressing the most of their possible effort to train their upper-limb, fitting into the necessity of progressively increasing the engagement of the subjects. Adaptation can also tune the controller to account either for differences between stroke survivors, or for the level of motor recovery on the same patient during multiple training sessions. A major contribution of robots is the capability to collect reliable measurement of the patient performance and therefore exoskeletons have the features to provide a customized *ad-hoc* therapy. Adaptation of the assistance could potentially lead to an increase of the efficacy of modern rehabilitation robotics.

AAN controllers have been already developed in order to maximize patients involvement by minimizing robot necessary intervention. There exist few different implementations to produce AAN – as detailed in section 2.3.1 – and the results are generally preliminary (only [146, 120] tested their AAN strategies with patients, observing small improvements in FMA score). AAN usually involve a feedforward assistance in addition to a

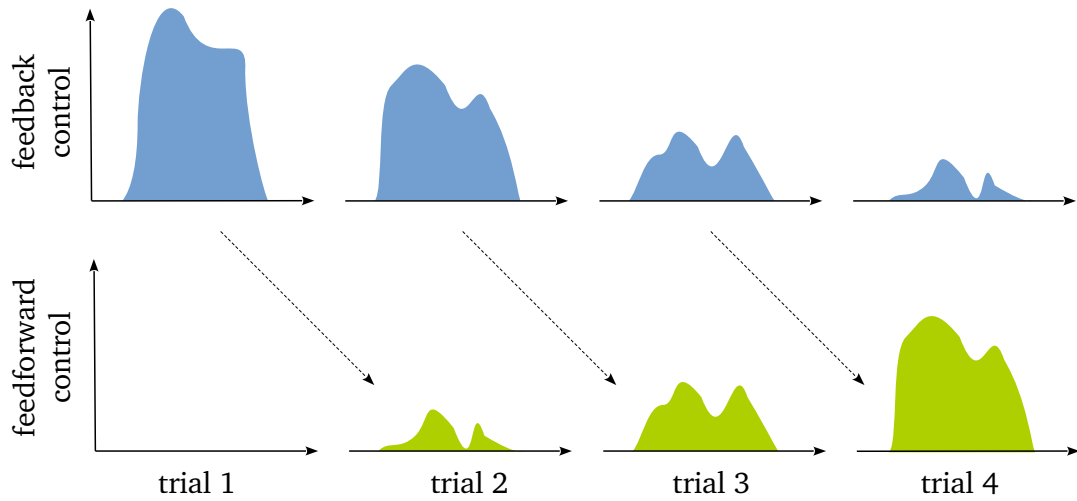


Figure 3.1: Example of typical trial-by-trial offline adaptation of feedforward control based on former trial feedback values, in the human CNS. The more the CNS learns the kinematic and dynamic of the task, the more it controls the upper-limb through feedforward motor commands, keeping feedback control to modify the inputs to face, for example, unexpected disturbances. Reproduced from [21].

feedback controller, with the adaptation generally running offline trial-by-trial, based on the user performance, see figure 3.1. This strategy is naturally present in the human motor control, where it is generally assumed that each motor command $\mathbf{w} \equiv (w_1 \dots w_n)^T$ to the n muscles involved in a movement is composed of a feedforward term \mathbf{u} and a feedback term \mathbf{v}

$$\mathbf{w} = \mathbf{u} + \mathbf{v}. \quad (3.1)$$

This fact is probably a direct consequence of the presence of sensory feedback delay in the human CNS. In fact, we are able to sense the environment and our movements quickly, but transferring the signals from the sensors to the CNS and processing them, introduces a delay of between 100ms and 200ms (visual feedback is about 150ms for example). Hence, in a sensory feedback delayed system, the use of an internal model to predict and control in feedforward the upper-limb, becomes crucial. The feedback control is still fundamental to improve the performances, for example by taking into account unpredictable disturbances, unexpected obstacles, or new, *i.e.* unknown, environments.

When considering the implementations of adaptive controllers on current exoskeletons, the adaptation can occur either at the feedforward level (adaptation of the feedforward term to address repetitive consistent errors [182], or through an additional neural network to model the subject capabilities [187]) or at the feedback level (gains adaptation to modify the compliance of the robot with an adaptive forgetting factor, to decrease these gains in case of poor performance by the subject [6], or with sensorless force estimation, in order to model subject's capabilities and to avoid the forgetting term [133]).

In our case, we developed a simple AAN solution which performs active modulation of the stiffness of the robotic device, thus acting at the feedback level, as a function of the user performance. One interesting feature of this strategy is its simplicity, which could help to directly apply this adaptive paradigm to most of the common current feedback controllers for exoskeletons, potentially improving their applicability to rehabilitation.

3.2 Adaptive control

3.2.1 Working principle

The desired behaviour for our robotic exoskeleton is depicted in figure 3.2. The principle is simple: the controller should be able to tune automatically and continuously its level of assistance based on the performance of

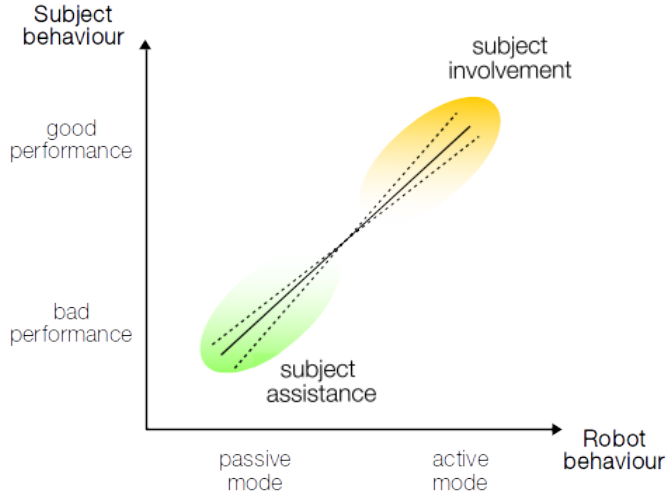


Figure 3.2: Desired behaviour for our adaptive controller. The exoskeleton should adapt, reacting to the user performance. The multiple lines represent different rate of adaptation, that is different trade-off between assistance and involvement, that should be consequence of the level of recovery of the patients.

the exoskeleton operator. In particular, if the performance worsens (green zone in the above mentioned figure), the exoskeleton should help the subject, by increasing its assistance and thus moving toward a “passive” control of the arm. Vice versa, if the performance improves (red area), the robot should excite the subject to work more by reducing its cooperation.

This general behaviour is particularly well suited for early rehabilitation therapy, when stroke survivors are usually too weak to produce important physical effort. Indeed, an AAN solution could better follow the recovery of the patients automatically and continuously, with respect to passive or partial assistive strategies, with their fixed level of assistance.

For the following experiments in this chapter, we decided to refer to the performance of tracking a desired pre-defined upper-limb trajectory (which is yet the most common rehabilitation control algorithm implemented in commercial robots). However, this paradigm is not necessarily constrained by computing the performance index on a trajectory tracking problem, but it could be computed on any performance variable of interest. For example, one could apply this paradigm by directly measuring the muscle activity of the patient and performing adaptation based on the weakness/strength of the subject, obtaining the same working principle. We therefore tested several adaptation variables and conducted experiments on healthy subjects, asking to modulate their participation within a motor task, in order to evaluate the adaptation of the assistance provided by the exoskeleton and to study the potential interest of each condition for rehabilitation purposes.

3.2.2 Control algorithm

The proposed robot controller involves a feedforward term and a feedback one as in equation 3.1, where now $\mathbf{w} \in \mathbb{R}^4$ stands for the overall control torque to the four actuators of the ABLE exoskeleton. The feedforward torque $\mathbf{u} \in \mathbb{R}^4$ is a model-based gravity compensation, which helps the subject not to feel the weight of the robot while inside the exoskeleton (about 13kg for ABLE). The feedback torque $\mathbf{v} \in \mathbb{R}^4$, instead, is provided by a PD controller, thus similar to an impedance control without the inertial term:

$$\mathbf{v} = \mathbf{K}_p \mathbf{e} + \mathbf{K}_d \dot{\mathbf{e}}, \quad \mathbf{e} = \mathbf{q}_r(t) - \mathbf{q}(t), \quad (3.2)$$

where $\mathbf{q}(t) = [q_1(t) \ q_2(t) \ q_3(t) \ q_4(t)]^T$ is the joint position vector, and error signals \mathbf{e} and $\dot{\mathbf{e}}$ are calculated with respect to the reference joint trajectory $\mathbf{q}_r(t)$ and the reference joint velocity $\dot{\mathbf{q}}_r(t)$. \mathbf{K}_p , the stiffness term, and \mathbf{K}_d , the damping term, are positive diagonal matrices of gains.

Through this simple control scheme, the robot imposes the reference trajectory $\mathbf{q}_r(t)$ to the subject's joints when the stiffness is high (large values of \mathbf{K}_p and \mathbf{K}_d), which is suited for early rehabilitation exercises, when the subject cannot provide large forces. In this case, the robot torques are large and the subject is mostly passive in the exoskeleton. During the recovery, as soon as relearning is occurring, the subject is expected to be able to provide more energy in order to complete the task more autonomously and thus the robot needs to decrease its assistance. In our control, this is achieved by decreasing the stiffness of the robotic arm (small values of \mathbf{K}_p and \mathbf{K}_d). At the lowest limit, *i.e.* when null \mathbf{K}_p and \mathbf{K}_d are reached, the robot is only compensated for the gravity by the \mathbf{u} feedforward term, thus leaving the exoskeleton in a transparent mode (no assistance/resistance to the free motion of the subject), and the subject completely active and free to perform any movement.

To achieve this adaptive behaviour, the gains of the PD controller are adapted trial-by-trial, based on the former performance of the subject, similarly to what is proposed by Yang *et al.* [192]. If the subject is performing the requested task correctly, the robot should try to reduce its assistance, and vice versa if the performance is not satisfying, the robot should rather increase its assistance. Namely, at a given trial k , the controller proportional gain $K_{p,i}$ for the i -th joint of the exoskeleton is computed by:

$$K_{p,i}^k = K_{p,i}^{k-1} + \beta_i z_i^{k-1} - \gamma_i \quad (3.3)$$

where the *learning parameter* β_i and the *decay* γ_i are positive scalars, and z_i represents the reference parameter at trial $k-1$ to evaluate the performance of the i -th joint. In addition, to avoid large increasing of the robotic stiffness and thus awkward feelings on the arm of the human operator, the $\Delta K_{p,i} = \beta_i z_i^{k-1} - \gamma_i$ is upper-saturated such that $\max(\Delta K_{p,i}) = \gamma_i$. At the same time the damping $K_{d,i}$ varies with the proportional gain

$$K_{d,i}^k = \alpha_i K_{p,i}^k.$$

Both gains are saturated between K_{\max} and $K_{\min} > 0$, with

$$\alpha_i = \frac{K_{d,i}^{\max} - K_{d,i}^{\min}}{K_{p,i}^{\max} - K_{p,i}^{\min}} (K_{p,i} - K_{p,i}^{\min}) + K_{d,i}^{\min}.$$

3.2.3 Performance metrics

As already said, z represents the parameter to evaluate the performance of the exoskeleton operator. Given a trajectory tracking task, many indexes can be computed to assess this performance. We defined three different error signals capable of driving the adaptation process of equation 3.3: end-effector based, joint-by-joint based, and single-joint based error signal. Indeed these are typically the implicit performances variables evaluated by a physiotherapist during rehabilitation: hand kinematics and intermediate joint movements.

End-Effector Based adaptation (EEB)

One intuitive solution to drive the adaptation is by comparing, trial-by-trial, the performance of the end-effector and the desired behaviour. The error computed at the end-effector (either position, velocity or both position and velocity error¹) is then globally modifying the behaviour of the robot, that is, all the robotic joints are adapting their control laws with the same ratio. With our controller, the EEB solution is given by defining the z_i as

$$z_i \triangleq z = \sum_{t=0}^T (\|\mathbf{e}_x\| + \xi \|\dot{\mathbf{e}}_x\|) \quad i \in [1 \dots 4] \quad (3.4)$$

where ξ is a scaling factor between the position and the velocity error, $\|\mathbf{e}_x\| = \|\mathbf{p}_{des} - \mathbf{p}_{ee}\| = \sqrt{(x_{des} - x_{ee})^2 + (y_{des} - y_{ee})^2 + (z_{des} - z_{ee})^2}$ is the end-effector position error, where we removed the dependence of time (*e.g.* $x_{des}(t)$) for a matter of readability, and similarly for the end-effector velocity error $\|\dot{\mathbf{e}}_x\| = \|\dot{\mathbf{p}}_{ee} - \dot{\mathbf{p}}_{des}\|$.

¹Since AAN controllers usually address early post-stroke therapies, faster correct movements than the desired one are unlikely to happen. Thus the robot should also take care of the speed of the motion, correcting too fast or too slow movements, which are likely to be the results of unnatural and undesired strategies. However, when considering more advanced therapies with chronic subjects, the constraint on the velocity could decrease the freedom of the patients, and so these could be removed.

Joint-By-Joint based adaptation (JBJ)

In JBJ, the error signal in equation 3.3 is locally computed for each joint. In fact, the error takes into account the single joint performance to adapt its stiffness. Therefore, with this strategy, each joint may evolve differently. The JBJ performance index z_i , for the i -th joint, is given by

$$z_i = \sum_{t=0}^T (|e_i| + \xi|\dot{e}_i|) \quad i \in [1 \dots 4] \quad (3.5)$$

where $|e_i| = |\theta_i^{des}(t) - \theta_i(t)|$ is the joint position error norm and $|\dot{e}_i| = |\dot{\theta}_i^{des}(t) - \dot{\theta}_i(t)|$ is the joint velocity error norm, both for the i -th joint.

Single-Joint Based adaptation (SJB)

In SJB, the performance of one specific joint drives the adaptation of the joints of the exoskeleton. Therefore, similarly to EEB, the SJB globally modifies the compliance of the robotic arm by considering the same error for the different joints. We defined the driving variable as the flexion/extension of the elbow angle α_{HF} , described by the International Society of Biomechanics [191], that is the angle between the upper-arm and the forearm. The coordination between these is often impaired in post-stroke survivors [152], and thus focusing on the resulting angle at the elbow could be interesting for the therapy. The error on this angle is computed as

$$z_i \triangleq z = \sum_{t=0}^T (|e_\alpha| + \xi|\dot{e}_\alpha|) \quad i \in [1 \dots 4] \quad (3.6)$$

where $|e_\alpha| = |\alpha_{HF}^{des}(t) - \alpha_{HF}(t)|$ is the the α_{HF} angle error, and $|\dot{e}_\alpha| = |\dot{\alpha}_{HF}^{des}(t) - \dot{\alpha}_{HF}(t)|$ is the α_{HF} angular velocity error.

3.3 Proof-of-concept

The preliminary experiments we performed consisted in testing the capabilities of our controllers in adapting to dynamical behaviours when the exoskeleton was operated by healthy subjects. We run the adaptive control with the joint-by-joint based adaptation paradigm of equation 3.5.

3.3.1 Preliminary test: mimicking relearning

The first experiment we conducted was about testing the working principles of our control law. The experiment consisted in mimicking a simplified process of relearning by a post-stroke patient who undergoes an ideal neurorehabilitation therapy. The main difference with the standard rehabilitation — thus simplified — was the duration of the therapy, since our experiment lasted just 35 trials, in one session only. Within this amount of motion, the person was asked to perform the desired tracking task several times, while increasing his participation to the movement. In particular starting from zero muscular activity, *i.e.* being fully relaxed as if he was not capable to perform the motion at all, we asked the participant to mimic an ideal relearning process, ending with full control of the upper-limb. Since it is not possible for a person to gradually increase his EMG/muscle activity, we decided to only ask for 3 distinct behaviours. In particular the subject was asked to perform the first third of trials with 0% of activation, *i.e.* staying relaxed and leaving the exoskeleton working for him, then the second third of trials with 50% of activation, *i.e.* sharing the effort of the motion with the controller, and finally to perform the task at his best, as an ideal patient who has finally relearnt how to control his limb and does not need the exoskeleton anymore.

Protocol

We tested our controller on one healthy subject. The subject was seating on a stool, in a comfortable way, within the ABLE exoskeleton. We recorded the activity of five groups of muscles through EMG, in particular

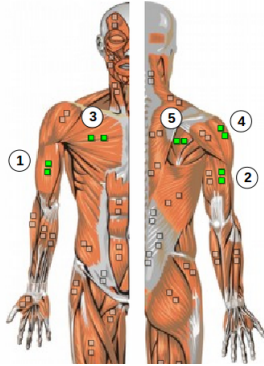


Figure 3.3: EMG sensors position on the five selected muscles. ① biceps, ② lateral triceps, ③ pectoralis major, ④ middle deltoid, and ⑤ infraspinatus. Image from MyoResearchXP (© Noraxon).

biceps, lateral triceps, pectoralis major, middle deltoid, and infraspinatus, see figure 3.3. This measure was not used in the control loop, but it was visually provided in real-time to the subject to have a direct feedback of his level of activity. The EMG was recorded at 1.5KHz with TeleMyo DTS system (© Noraxon) and the resulting values were passband filtered, between 10Hz and 400Hz, offsetted (its mean value was removed), rectified, and finally processed with Hilbert envelop function on Matlab (© The MathWorks, Inc.).

The motion task was to draw in the air, in front of the subject, two times a 4-edge polygon of side about 50cm, reaching about 80% of their maximum arm extension at the furthest position. The trajectory lasted approximatively 10s. No markers or any other visual feedback related to the desired trajectory were provided to the person, in order to make the learning process more difficult to be successfully achieved. All the recorded data from ABLE exoskeleton were low-pass filtered, during post-processing on Matlab, using 3rd order Butterworth filter.

For the control law, we chose the following values, previously tested to allow enough PD gains adaptation within the duration of the experiment, and to provide enough stiffness and compliance at the limit values. In particular, the starting gains were upper saturated to provide an initial stiff behaviour to the robot.

learning factor	$\beta_i = 0.25 \quad \forall i$
decay factor	$\gamma_i = 5 \quad \forall i$
proportional gain	$\mathbf{K}_p^{max} = [300, 200, 200, 200]$
	$\mathbf{K}_p^{min} = [10, 10, 10, 10]$
derivative gain	$\mathbf{K}_d^{max} = [10, 10, 10, 10]$
	$\mathbf{K}_d^{min} = [1, 1, 1, 1]$

Results

After an initial training with the exoskeleton in transparency mode (null PD gains and active gravity compensation), we recorded the 35 trials with the adaptive controller on. Figure 3.4 shows the total muscle activity $\Psi(t) = \sum_{i=1}^5 \psi_i(t)$ and the total current $\mathbf{C} = \sum_{i=1}^4 (c_i/\delta)$ over the 35 trials, where $\psi_i(t)$ is the activity profile of one of the considered muscle groups during one trial, c_i is the total current on the i -th actuator from the PD adaptive control, and $\delta = r_g\tau \approx 4.26$ is the product of gear ratio r_g and torque constant τ . In the same figure, the two tendencies are obtained through 3rd order linear regression. This figure shows how, as the muscles activity increases, meaning more subject involvement in achieving the task, the adaptive controller is becoming more transparent, meaning less constraints on the subject's limb. In particular, between trial 1 and trial 35, total current decreases by 25% of its initial value.

Three detailed trials, manually selected for the interesting resulting profiles, are shown in figure 3.5. First column is trial 7, second trial 20, and third column is trial 34. The first row of plots shows muscles activities,

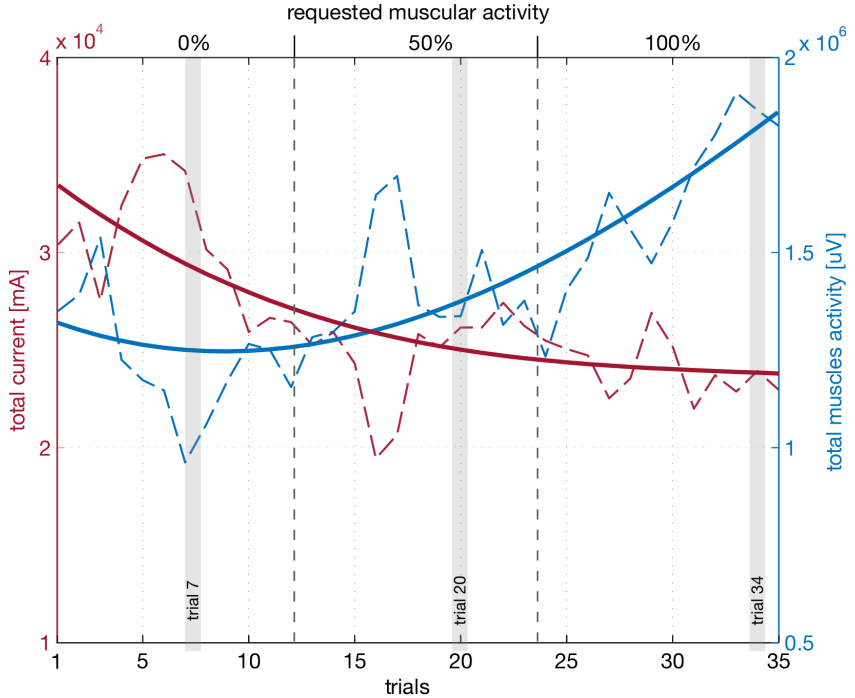


Figure 3.4: Robot adaptation to the different performance of the subject. Muscles activity (dashed blue line) and total current from the adaptive PD controller (dashed red line) over the 35 trials. The two solid lines are the two terms tendencies computed through linear regression. See figure 3.5 for details of trial 7, 20, and 34.

through EMG measurement, over the samples for the 5 different muscle groups. The second line of graphs describes PD controller torque outputs for the 4-DOF. Also, in the same plots, K_p and K_d values for the chosen trials. Finally, last row of graphs contains joint positions and desired positions for the 4-DOF. These plots clearly show how the output of the adaptive PD controller decreased while the EMG data increased, corresponding to a less constrained and more involved subject. At the final trial, $\mathbf{K}_p = [132.8, 40.2, 48.3, 45.1]$ and $\mathbf{K}_d = [4.4, 2.0, 2.4, 2.2]$ gave to the subject enough exoskeleton transparency to perform the task almost freely. As expected, less control increased the position errors, which however remained small enough to be considered negligible even at the final trial (within 5 degree at the joint level, and an increase of approximatively 1cm of the mean error at the end-effector between the first and the last trial).

3.3.2 Advanced test: more dynamical behaviour and different adaptation rates

The preliminary test, with one subject, showed us the feasibility of the adaptive principle in a pHRI context with an ABLE exoskeleton. We realized the importance and the complexity of tuning the adaptive parameters β and γ — they can be tuned differently either to achieve fast adaptation (high gains) meaning less assistance as soon as the exoskeleton operator starts improving, or slow adaptation (low gains) meaning less controller modification between trials — and we wanted to further test our controller on more subjects, plus improving the duration of the experiment and making the human behaviour more variable, *i.e.* increasing the difficulty for the robot to adapt to the human.

Protocol

The protocol was similar to the former experiment. We still recorded the muscular activity of the same 5 groups of muscles, providing these data in real-time to the subjects and not using the EMG in the control loop. Also the motion task and the trajectory duration were maintained. However this time the experiment lasted 50 trials. We tested the controller on 6 healthy people, asking the subjects to perform the pattern shown in table 3.1. With

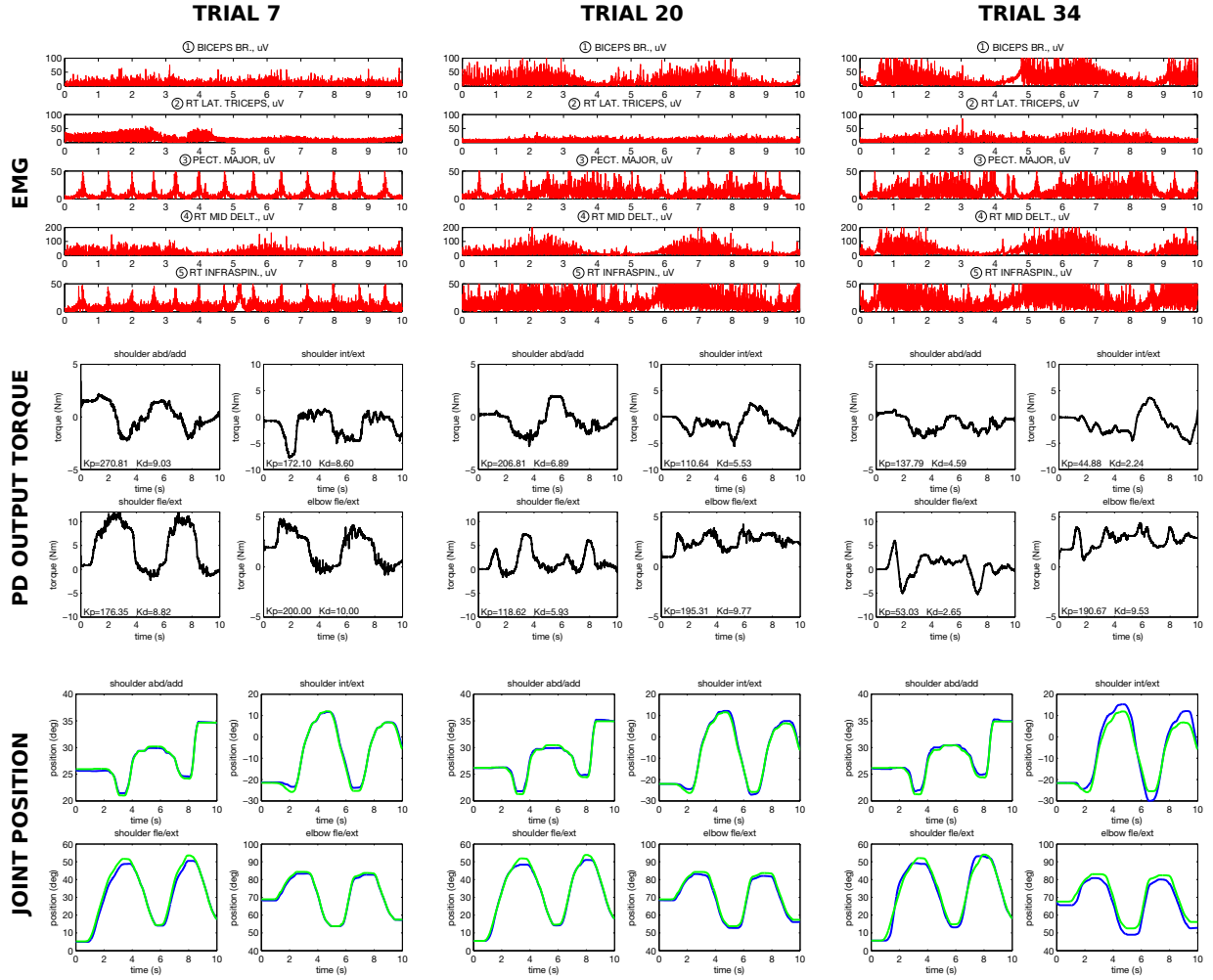


Figure 3.5: Trials details. First column is trial 7, second trial 20, and third column is trial 34. In red, muscles activity [μV] during the trial, for the 5 different muscles (from top to bottom, ① biceps, ② lateral triceps, ③ pectoralis major, ④ middle deltoid, and ⑤ infraspinatus) over the samples (sampling frequency is 1.5KHz). In black, PD controller torque output [Nm] for the 4-DOF (top-bottom, right-left, joint 1 shoulder abduction/adduction, joint 2 shoulder internal/external rotation, joint 3 shoulder flexion/extension, and joint 4 elbow flexion/extension). Also, in the same plots, K_p and K_d values for the chosen trials are shown. Finally, last line of graphs presents in blue joint position [deg] and in green joint desired position [deg] for the 4-DOF. As expected, EMG activity and joint position error are increasing with the trials, while controller output is decreasing resulting in an increase of robot transparency.

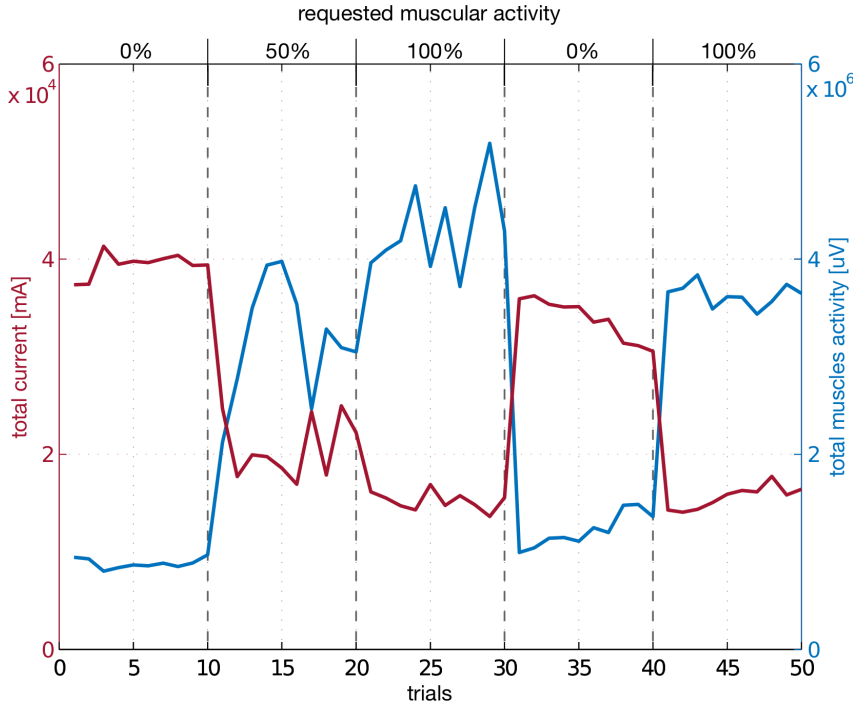
these tests, we wanted to check the ability of the controller to increase again the stiffness of the robotic arm (between trials 31 and 40), after a period of increased compliance, due to human voluntary effort (trials 0 to 30).

Besides, we also tested different adaptive parameters, with the same protocol, on the same subjects. In particular we replicated the experiment three times by using different values for the learning factor β_i , respectively fast adaptation ($\beta_i = 1, \forall i$), medium adaptation ($\beta_i = 0.5, \forall i$), and slow adaptation ($\beta_i = 0.25, \forall i$). The order of these three conditions was randomized among subjects. Clearly, the value of the decay factor ($\gamma_i = 5, \forall i$) was fixed among the three tests. We kept the same initial values and saturation for the proportional and derivative gain as in the former experiment.

Results

Figure 3.6, similarly to figure 3.4, shows total muscular activity and simultaneously total current to the exoskeleton actuators. In particular, $\Psi(t)$, the sum of the EMG signals, and \mathbf{C} , the sum of the currents from

Trials	0 - 10	11 - 20	21 - 30	31 - 40	41 - 50
Muscular Activity	0%	50%	100%	0%	100%

Table 3.1: Pattern of requested muscular activity for the advanced test of the adaptive controller.**Figure 3.6: Advanced robot adaptation to the human performance.** Muscular activity (blue line) and total current from the adaptive PD controller (red line) over the 50 trials. On top of the figure, the requested percentage muscular activity to the subject, trial-by-trial.

the four ABLE's motors, are shown respectively in blue and in red. The performance of the controller is the expected one: it reduces the stiffness of the robot in the first 30 trials, while the subject is increasing his voluntary effort along the desired trajectory, thus his muscular activity, and it increases again the stiffness of the robotic arm between trials 30 and 40, when the human is relaxing as in the first 10 trials. From trial 40 until the end, the subject tries again to perform the task by himself and consequently the adaptive controller releases the corrective term, by making the arm more compliant.

The comparison between the performances of the robot with different sets of adaptive factors, is shown in figure 3.7. In this graph different profiles of the proportional gains K_p are displayed. The four plots are, from left to right, respectively the K_p values of the first joint (shoulder abduction/adduction), second joint (shoulder internal/external rotation), third joint (shoulder flexion/extension), and forth joint (elbow flexion/extension). Each graph shows three lines: every line is relative to a whole 50 trials experiment, keeping fixed all the parameters but the adaptive parameter β , the learning factor. The red line represents the gains when $\beta = 1$, thus fast adaptation, the green line stands for medium adaptation $\beta = 0.5$, and the blue line is the slow adaptation $\beta = 0.25$. For all the experiments shown, the subjects were still following the pattern of table 3.1.

By taking into account the adaptation rule of equation 3.3, the shown behaviour is straightforward: the higher the learning factor, the higher the value of the former feedback term taken into account for the K_p updating law. Furthermore, the lower β , the larger the weight of the fixed decay factor γ , resulting in a rapid relaxation of the robot.

As expected, the adaptation process in red (fast adaptation) keeps K_p^{max} saturated on the four joints within the first 15 trials. The saturation is along the whole experiment on the first two joints and this is clearly related to the lower range of motion these joints were subjected to, *i.e.* lower proportional and derivative errors. On

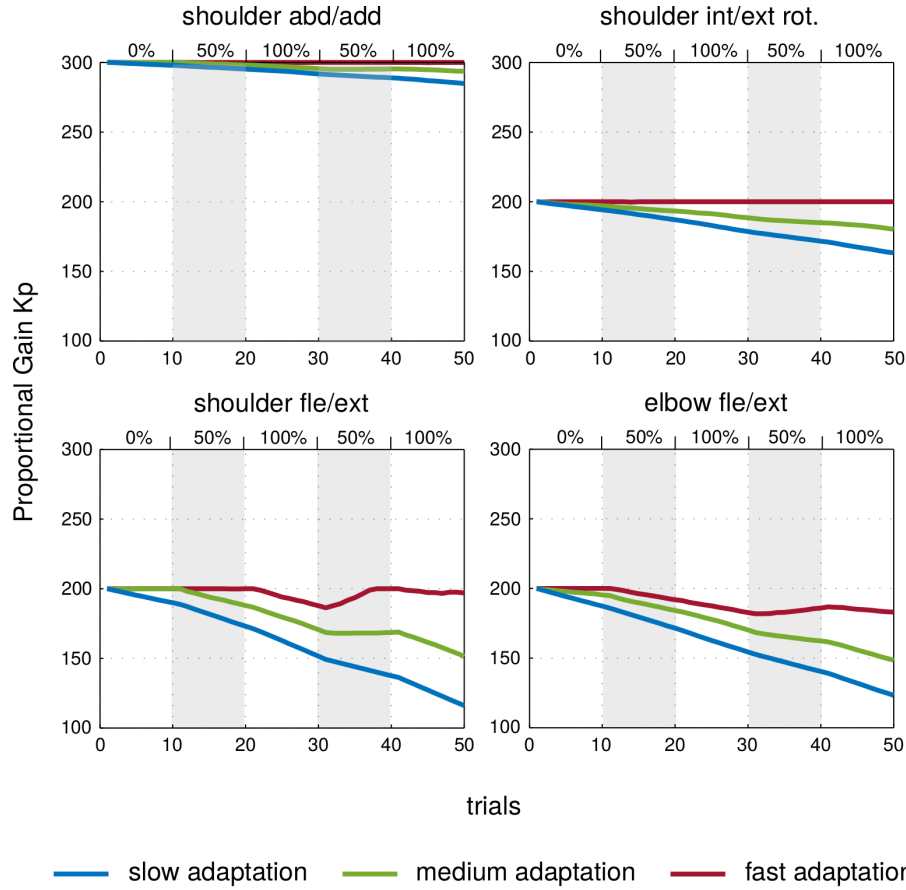


Figure 3.7: Comparison of proportional gain values by changing the learning factor β and keeping fixed the decay factor γ . In particular, in red $\beta_i = 1$, in green $\beta_i = 0.5$, and in blue $\beta_i = 0.25$, for any $i \in [1 \dots 4]$. For all the experiments shown, the subjects were still following the pattern of table 3.1.

the opposite, the blue experiment (slow adaptation) represents the situation in which the decay factor γ is over-dimensioned with respect to β : mainly, whatever the participation by the person, the controller is always trying to make the robotic arm more compliant. Finally the green line, corresponding to the medium factors – the same values used also in the proof-of-concept experiments of section 3.3.1 – represents the case in which the controller follows more carefully the dynamics of the healthy behaviour.

3.4 Comparison of different error signals driving the adaptation

We were able to provide assistance-as-needed to healthy operators performing tracking task within an exoskeleton. In the proof-of-concept of the former section, as well as in literature, however, whatever the solution adopted to provide AAN, limited attention has been yet given to the source of the adaptation, that is the error signal reflecting the performance of the operator and driving the adaptation process. In a tracking task, for example, adapting the behaviour of the robotic exoskeleton only based on the end-effector performance, rather than utilizing multiple different joint-based indexes (as we did in the proof-of-concept), can imply sufficient different adaptations and thus robot performances.

We believe that end-effector based adaptation can be the solution when functional recovery is needed (regaining of independence and functionality for performing activities of daily living), but for impairment recovery, thus addressing regaining of strength and muscle tone, range of motion, as well as joints arm coordination, for example to avoid unnatural joint synchronization and trunk compensation while extending the arm, a joint-level adaptation could be more effective. It is then clear that, in order to correctly use AAN in rehabilitation

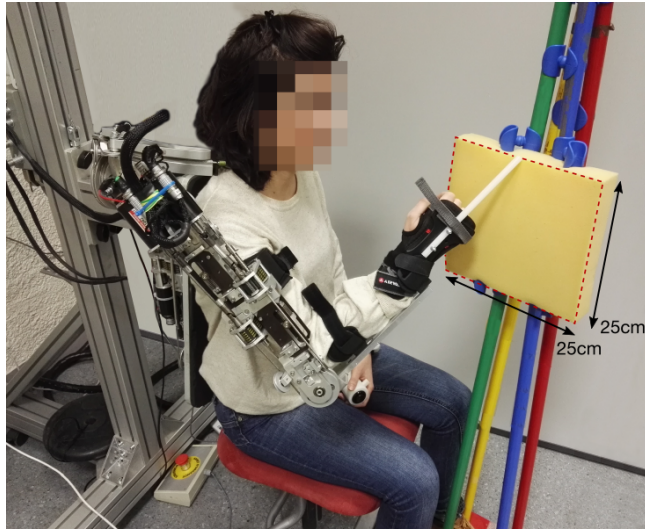


Figure 3.8: Experimental setup and ABLE close-up. The subject was told to track the outline of a foam-made parallelepiped with a plastic rod.

therapy, with neurological disease survivors, a specific analysis should be done to determine what possible sources of adaptation exist and which potentiality each of them could exhibit.

In section 3.2.3, we determined and described three different strategies for assessing the performance of the user within an exoskeleton, respectively end-effector based adaptation (EEB), joint-by-joint based adaptation (JBJ), and single-joint based adaptation (SJB). In the following part of this chapter, we will thus focus on comparing the three paradigms in order to analyse possible advantages in applying each specific strategy for neurorehabilitation.

Protocol

We asked five healthy subjects (aged 24.4 ± 0.4) to outline a $25 \times 25 \times 4 \text{ cm}^3$ foam-made parallelepiped, placed in front of them at about 80% of their maximum arm extension, while seating on a stool. The exoskeleton was connected to the right arm of the subjects through three velcro cuffs, one on the upper-arm and two on the forearm. Besides, the subjects wore a commercial wrist splint to limit wrist motion and prono-supination, not controlled and not measured by the robot, see figure 3.8.

To compute the reference trajectories to control the robot, we recorded the joint positions when the subject was pointing at the corners of the squared foam with the exoskeleton in transparency, and then we interpolated straight lines in between them to reproduce the exact contour of the tracked object. Therefore, although the end-effector position was the same for each participants, the intermediate joint trajectories varied among the subjects based on their natural inter-joint coordination.

During the experiment, we performed 40 repetitions of the task for each protocol, thus a total of 120 motions, and each motion lasted 10 seconds. By triggering a push-button with their left hand, the subject voluntarily started the motion and the trial recording.

Similarly to the former experiments, we asked the subjects for specific behaviours imitating different stages of motor recovery/abilities of post-stroke patients. In particular we determined four different phases of the experiment:

- **Trial 1 to 25** the subjects were asked to perform the task with the support of the AAN control,
- **Trial 26 to 30** the subjects were asked to relax and let the robot perform the task,
- **Trial 31 to 35** the subjects were asked again to perform the task with the support of the AAN control,

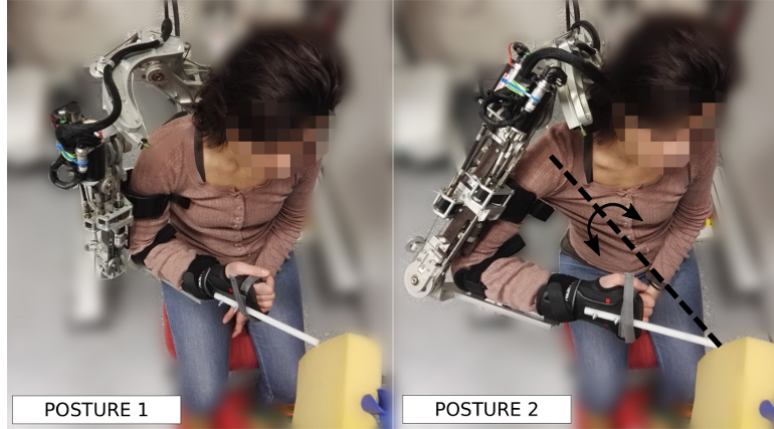


Figure 3.9: An example of *self-motion*. For a same end-effector position, the intra-joint coordination can be modified thanks to the system redundancy w.r.t. specific tracking task. This different coordination can be achieved and performed during the whole task, producing distinct joint trajectories.

- **Trial 36 to 40** the subjects were asked to perform the task with the support of the AAN control, but producing a different inter-joint motion coordination.

In the first three phases we expected to see similar behaviours for the three cases of section 3.2.3, with the robot adapting to the activity of the operator (the simple task should be easily achieved, thus the robot should decrease its assistance in phase 1 and 3, while it increases the stiffness in phase 2). We expected small differences in the adaptation strategies, apart from the structural distinction comparing global (EEB and SJB) and local adaptation processes (JBJ).

In the fourth phase, instead, when asking to change voluntarily the motion coordination, while keeping the end-effector task achievement, we expected to obtain slightly different gains evolutions due to the variation on the driving error signals. This fourth phase was crucial to observe the specificities of the different adaptation strategies in a context of modified inter-joint coordination, such as in the case of unnatural synergies of stroke patients described in section 1.2.2.

It is important to underline that subjects able to perform the fourth phase exercise thanks to the redundancy of the exoskeleton (a 4-DOF robot) with respect to the specific task (pointing in the space requires only 3-DOF). In this scenario, in fact, similarly to any pointing task with healthy human arm, there are more available DOF than the required ones and we can achieve the same task (following the squared outline) by performing different strategies at the joint level (usually named as *self-motions*, see figure 3.9).

For this experiment, the initial gains were set to $K_{p,i}^{t_0} = 200$ and $K_{d,i}^{t_0} = 6.6 \forall i$, and the gain saturations were $K_{p,i}^{\max} = 300$, $K_{p,i}^{\min} = 0$, $K_{d,i}^{\max} = 10$, and $K_{d,i}^{\min} = 0$ for all the joints. This gain definition provided an initial stiff behaviour to the robot. In addition, at the end of trial 35, we set $K_{p,i} = K_{d,i} = 0$ at each joint, in order to compare the behaviour of the controllers with the same starting gain configuration (full transparency). $\xi = 0.1$ was also set to give more importance to the path tracking, more than to the exact speed profile reproduction.

The tuning of the adaptive parameters β and γ was a crucial phase of the experiment. We wanted the robot to be transparent towards the end of the first phase (within 25 movements). For this reason, given $K_{p,i}^{t_0} = 200$, we selected $\gamma_i = 8, \forall i$. At the same time, we needed the robot to be able to react sufficiently quickly (within 5 trials) to any increase of the tracking error. To determine a useful β to reproduce this phenomenon, we recorded the error range (joint error for JBJ, α_{HF} error for SJB, and end-effector error for EEB, as defined in section 3.2.3) when the robot was performing the task alone, without any operator, respectively in rigid mode ($\forall K_p = 300$ and $\forall K_d = 10$) and in transparency ($\forall K_p = K_d = 0$). Trivially the rigid mode gave us the minimum error for each protocol, while the transparency the maximum one (indeed the robot movement was null during this test). Based on these error ranges and the selected γ , we computed the values of β for each protocol, which were: $\beta_{i,JBJ} = [0.1 \quad 0.1 \quad 0.05 \quad 0.05]$, $\beta_{i,SJB} = 0.01$, and $\beta_{i,EEB} = 0.01$ for any $i \in [1, \dots, 4]$. The different β for the

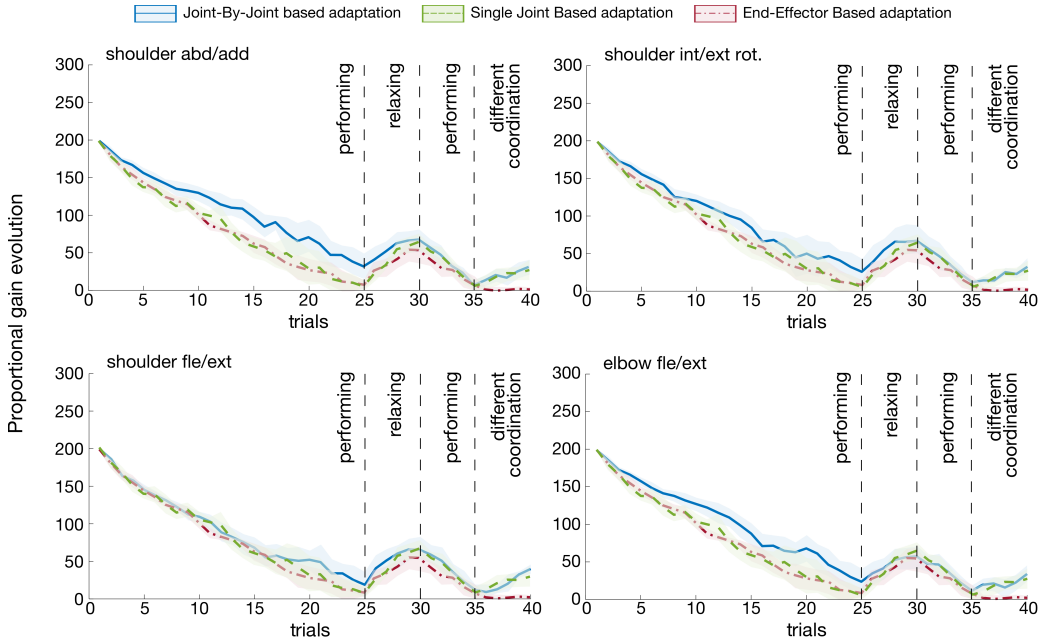


Figure 3.10: Mean evolution of the proportional gains. Evolution of the four $K_{p,i}$ during the experiment, averaged over the five subjects, for the three adaptive paradigms. At trial 35, the gains were zeroed to have the same starting configuration for the last movements. For each condition, the shaded coloured area represents the standard error.

JBJ case were due to different error ranges at the joint 3 and 4 compared to the other joints, for this specific task.

Results

Trials 1-35: adaptation to subject performance Figure 3.10 shows the average evolution of the proportional gain $K_{p,i}$ over the 40 movements and the five subjects, when using the three different error signals. At the same time, figure 3.11 shows the average errors at the joints and at the end-effector at each trial, for the five subjects. The K_p value can be considered proportional to the stiffness of the robotic arm. As expected, all the AAN controllers adapted correctly to the behaviour of the exoskeleton operators. During the first phase (trials 1-25), while the subjects were actively performing the task and consequently the errors were low, the robotic exoskeleton generally became more compliant (decreasing K_p). It is important to see the difference between JBJ local adaptation, in which the four joints adapted differently based on local performances, and the other protocols, in which the performance index was one for all the joints and therefore the gains evolved exactly the same for the whole robotic device. This different behaviour reflected into a larger mean error at each joint, during this interval.

Once the subjects relaxed (trials 26-30), the three controllers correctly increased the stiffness of the robotic arm producing better assistance to the movements (increasing K_p). In this interval, both joint error and end-effector error increased because of the voluntary relaxation of the subject. As soon as relaxation was over, the subjects were again contributing to the performance, the errors were drastically decreasing, and thus the robot compliance increased again.

Trials 36-40: correcting a different coordination For the second part of the experiment, in the interval of trials 36-40, we asked the subjects to try to perform the same end-effector task while adopting a different inter-joint coordination. The task was performed by increasing both the abduction and the internal rotation of the shoulder with respect to the desired joint trajectories, exploiting the ABLE/human system redundancy (figure 3.9). Figure 3.12 shows the resulting behaviour of the robot, for a typical subject. In particular, the joint

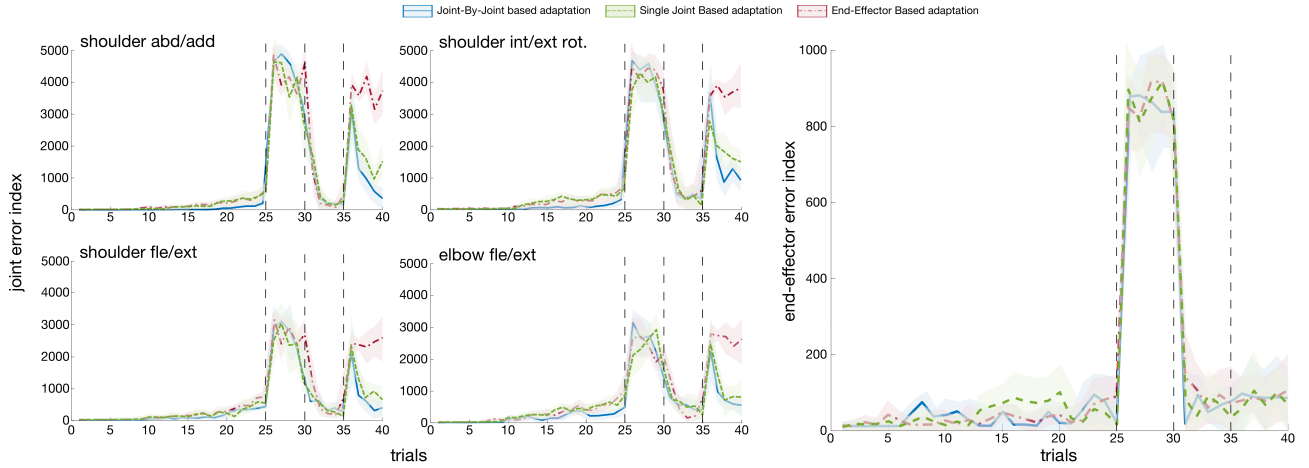


Figure 3.11: Average error indexes. On the left, average joint errors (sum of position and velocity error) and, on the right, average end-effector error (sum of position and velocity error), for the five subjects and the three adaptive processes. For each condition, the shaded coloured area represents the standard error.

trajectory of trial 36 (dashed line) and 40 (solid line) are shown for each choice of error signal.

As we can see, the different inter-joint coordination was “allowed” by the EEB adaptation, in which clearly the performance index (the end-effector error, which remained small) was not influenced by joint level performances. In fact, in this case, K_p did not increase (it remained almost null, providing transparency to the exoskeleton), and different joint trajectories with respect to the desired ones were performed. On the contrary, JBJ adaptation quickly brought the operator back to the desired coordination. K_p , with this strategy, increased fast to decrease joints errors. Finally, an in-between solution was provided by SJB adaptation, in which the K_p increased but larger differences in the joint coordination were allowed. Figure 3.11 shows clearly that all the controllers allowed for similar end-effector error scores, thus the different inter-joint coordination did not affect the tracking task.

Discussion

We determined three different adaptation strategies for our AAN controller, respectively based on the local error of each joint of the exoskeleton (JBJ), on the error of the end-effector (EEB), and on the error of a single joint (SJB), in particular the α_{HF} usually impaired in post-stroke survivors.

These three adaptation paradigms performed as expected in a typical tracking task, with variable voluntary behaviour of the human operators. All the protocols were able to react either to increased (trials 1-25, and 31-35) or to decreased activity (trials 25-30) by the subjects, showing the overall efficiency of the AAN control. Nonetheless it seems possible to suggest that a local adaptation strategy, as in JBJ, could better fit for early rehabilitation, when mostly targeting motor recovery. For example in this phase, as said, stroke survivors show decreased capacities to extend their elbow [152], having difficulties in achieving most of the motion tasks; a JBJ solution could provide better control along a desired reference coordination, performing better tracking of desired joint trajectories, while a global adaptation strategy (like in EEB or SJB) could determine larger joint errors.

When considering instead the second part of the experiment (from trial 36), we targeted stroke survivors who are more capable of acting alone (late rehabilitation), a situation in which the controller should allow the patients to train intensively, with a minimal assistance to avoid negative behaviour.

End-effector based solution, due to its architecture, allowed any motion the subject wanted to perform (control gains remained almost null, keeping the robot in transparency, figure 3.10), as long as the end-effector task was achieved (small end-effector error in figure 3.11), and indeed it did not assist anymore the patient along the desired motion coordinations (large joint error in figure 3.11). Unfortunately it is clear that perfect perfor-

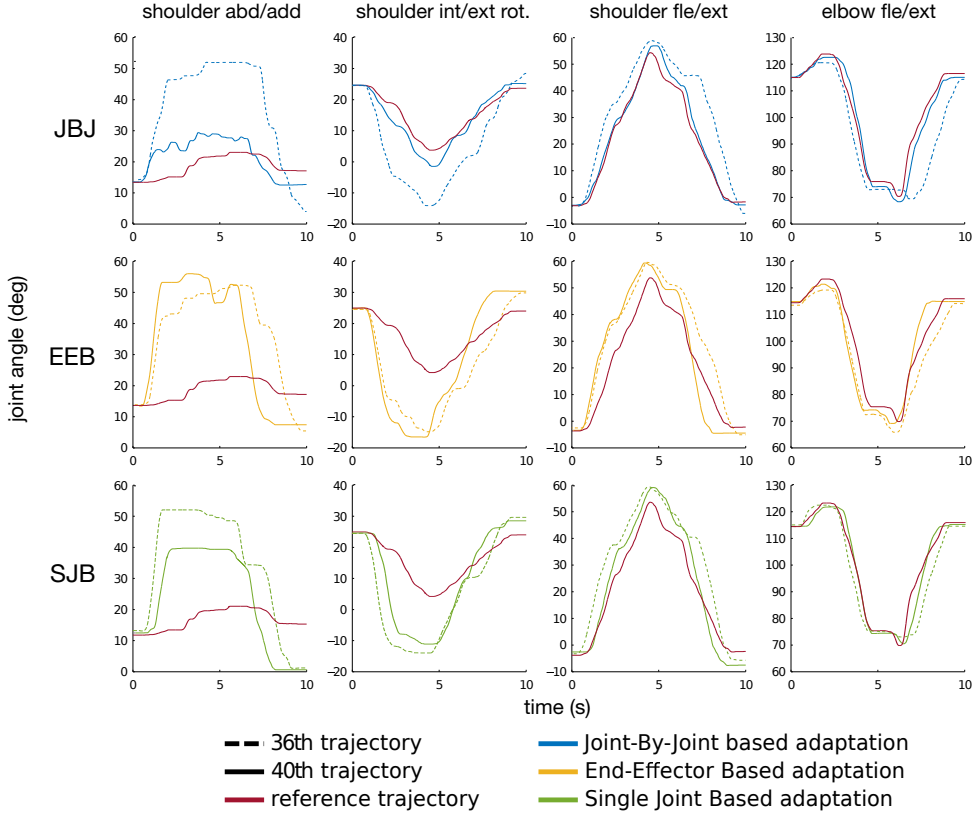


Figure 3.12: Joint trajectories for the three strategies. Each column is one of the four joints of the ABLE exoskeleton. For each plot, three trajectories are shown: in red, the desired joint trajectory, dashed line the 36th motion (the first with a different inter-joint coordination), and in solid line the last motion (always with a different coordination, trial 40). First row is the JBJ adaptation, second EEB adaptation, third SJB adaptation.

mance at the end-effector may happen together with negative compensation at the shoulder level, producing potentially inadequate therapy [127]. We believe that adapting and basing the rehabilitation performance on a single parameter, as the end-effector score, could therefore in some case mislead the therapy and the robotic assistance.

Joint-by-joint assistance, on the contrary, once determined the desired joint trajectory, almost did not allow any different coordination. This paradigm, for later stages of stroke recovery, could be too strict. In fact, thanks to human arm redundancy, there may be slightly different coordination to complete the same task, without involving unnatural and pathological behaviour at the joint level or at the shoulder. Therefore the JBJ approach would also necessitate of highly customized references, since different patients may require different coordinations. One possible solution to use JBJ, even with chronic patients, would be to develop a simultaneous adaptation of the desired trajectories, in order to allow feasible and safe multiple strategies. But obviously these would increase the complexity of the controller and would require a difficult online evaluation of the feasibility of a coordination strategy.

Finally, the SJB adaptation seems to be promising. It better performed during the last trials, showing capabilities to assist the subject while leaving some freedom in slightly changing of the arm coordination. A weakness of this strategy is the global adaptation of the joint stiffness which generally produced larger joint errors during trials 1-25 with respect to local adaptation. A possible solution could be obtained by tuning the values of the adaptive parameters (β and γ) differently for each joint, thus creating distinct joint adaptations to the same error signal. Of course, a drawback would be to determine the metrics to perform the mentioned tuning.

Therefore it seems clear that there is no a single optimal strategy to drive the adaptation in AAN controllers,

Paradigm	Adaptation	Joint Control	Scope
End-Effector Based	Global	Rigid on the end-effector and on the intermediate joints while gains are large. If more compliant, it loses control on the inter-joint coordination as long as the end-effector respects the reference.	Functional training
Single Joint Based	Global	Rigid on the chosen joint and on the other joints while gains are large. The inter-joint coordination is constrained, above all if the selected joint is not distal, but it allows for some compliances.	Hybrid training
Joint-By-Joint Based	Local	Rigid on each joint for which a reference is provided. The inter-joint coordination is always constrained to the one inferred by the references.	Strength training

Table 3.2: The characteristics of the three different adaptive paradigms.

above all without considering the specificity of the involved patients. However, this not trivial parameter must be carefully kept in consideration and tuned for improving the efficiency of any robot-led therapy. A summary of the effects of each adaptive paradigm analysed is given in table 3.2.

3.5 Conclusions and perspectives

An *assist-as-needed* solution controlling the ABLE exoskeleton has been developed in order to study the capability of the robot to adapt to different human level of involvements in the action. In particular, the adaptive strategy aimed at maximizing the involvement of the subjects and better following the unstable recovery progress of potential patients, during post-stroke therapy. Interestingly, this strategy has in its simplicity a fundamental property: the same adaptive paradigm could be applied to most of the existing non-adaptive solutions currently implemented on rehabilitation exoskeletons. Indeed, it is based on an impedance control mode, which is yet the most common control strategy available on these specific devices, see chapter 2.

Our adaptive solutions performed well in tracking the performance of several healthy human operators, exhibiting a range of different dynamical behaviour. We focused on the possibility to build a customizable controller, which could adapt based both on short-term performance (within session, *fast adaptation*) or on long-term ones (within therapy, *slow adaptation*). The manual tuning of the adaptive parameter β and γ (which could be simplified) could allow the physiotherapist to control these strategies, based on the necessities of each patient. We also tested the possibility to drive the adaptation on different error signals (a classical end-effector based strategy, a more localized joint-by-joint based solution, and finally an in-between single-joint based strategy), a parameter of the therapy that should be kept into consideration by the supervisor of the rehabilitation.

The JBJ strategy rigidly forces one specific coordination, the one inferred by the reference trajectories: despite it could be a good solution for early assistance, it could become clearly too rigid with the motor recovery of the patient. On the other side, an EEB strategy loses quickly the control over the inter-joint coordination, focusing only on the end-effector kinematics. An hybrid strategy with control over a proximal joint of the upper-limb could provide an interesting in-between solution, despite none of the three would be able to correctly follow alone the whole recovery of the patient.

The performance of the controller was analysed with respect to the characteristics of a tracking trajectory problem, which is one of the most common requirements for rehabilitation exoskeleton exercises. However the proposed solution is not constrained to this specific problem and could be easily generalized to different variables of interests, like motor synergies [43], or not necessarily kinematics as, for example, subject force and muscular activity, or even an hybrid solution taking care of multiple indexes simultaneously.

Yet, this study on the adaptive controller lacks of testing with patients with sensorymotor impairments. We are currently working with the rehabilitation department of the *Hôpital Universitaire Pitié-Salpêtrière*, in Paris, in order to program a preliminary experiment on stroke survivors, in order to test the applicability of the adaptive paradigm in a real clinical environment, with the adaptation of the robotic behaviour to the less regular impaired motor capabilities of real stroke patients. Therefore the main objective of this preliminary evaluation will be the study of the dynamics of the process of adaptation when dealing with impaired subjects, to analyse the applicability (is the robot adaptation able to converge quickly to assist-as-needed the patient?) and efficacy of a trial-by-trial paradigm, as the one adopted with healthy participants, rather than a slower within-session or within-days solution (which adaptation paradigm better follows the patient improvements?).

Chapter 4

Human adaptation to the robot action

Contents

4.1	Introduction	55
4.1.1	Results on motor adaptation with planar robots	56
4.1.2	Exoskeletons potentialities	57
4.2	Modifying the inter-joint coordination: the experimental setup	58
4.2.1	The exoskeleton controllers	58
4.2.2	Experimental protocol	59
4.2.3	Quantification of the human spontaneous variability within the exoskeleton	62
4.3	Data processing	62
4.3.1	Data gathering	62
4.3.2	Joint kinematics	62
4.3.3	End-effector kinematics	63
4.3.4	Principal Component Analysis	63
4.3.5	Statistics	63
4.4	Results	64
4.4.1	Individual results	64
4.4.2	Movements towards ET: adaptation to KSC	67
4.4.3	Movements towards GT: catch-trials unexposed to KSC	71
4.5	Discussion	74
4.5.1	Adapting to new upper-limb synergies	74
4.5.2	Application to rehabilitation / Limits	75
4.5.3	Assessing learning effects with an exoskeleton	76
4.6	Transferring of post-effects outside the robot	76
4.7	Conclusions and perspectives	81

4.1 Introduction

Dealing with physical human-robot interaction, it is fundamental to understand the effects of this interaction on the human natural behaviour. Indeed, it is reasonable to imagine that any robotic device, even the most backdriveable, modifies the natural upper-limb movements [86]. We can imagine to exploit this property to potentially induce learning of new healthy imposed motor control strategies in post-stroke survivors. The characterization of this human natural adaptation to the robot action could be interesting to boost neuromotor

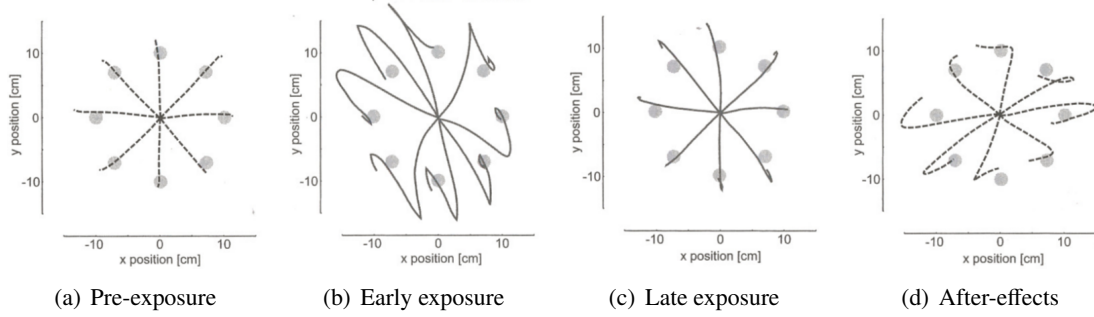


Figure 4.1: The four typical consecutive phases of human motor adaptation and after-effects on 2D experiments. Reproduced from Shadmehr and Mussa-Ivaldi [161].

rehabilitation. In fact, as seen in section 1.2.2, post-stroke hemiparetic patients normally exhibit pathological synergies in their upper-limb movements, resulting in global and stereotyped unnatural patterns of coordination of their arm joints. These impaired synergies can induce in the stroke survivors harmful compensations at the shoulder and trunk levels, having a negative impact on the quality of movement performance and potentially limiting the long term prognosis [101, 171].

Therefore, a central question in neurorehabilitation is whether it is possible to modify the patients impaired upper-limb synergy in order to regain a more natural and healthier control of the arm [43]. In particular, we are interested in understanding if this is also possible by exploiting the adaptation to the exoskeleton control and action. Despite the large number of robotic devices, current studies on adaptation and learning, when performing the exercises within a robotic setup, mostly concern planar robots [196], thus addressing end-effector-based 2D movements with no control and interaction with the other upper-limb joints.

4.1.1 Results on motor adaptation with planar robots

Learning is a complex process involving several phenomena such as motor adaptation, post-effects of this adaptation, generalization over workspace and movements, and retention. In particular, what is crucial for modern neurorehabilitation is the aptitude of the impaired patients to transfer the post-effects of rehabilitative exercises to different activities of daily living (*generalization*), and to maintain these effects during the weeks after the training (*retention*).

A landmark result on motor learning was given by Shadmehr and Mussa-Ivaldi in 1994 [161]. In an experiment, several healthy subjects were asked to perform point-to-point arm motions, under the effect of a velocity-dependent deviating force field produced by a planar robot. After an initial failure phase, due to the force field, the users were able to learn how to complete the required task by adapting to these disturbances. The term *adaptation* describes the progressive reduction of the effects of the perturbation performed on the human upper-limb movements by the presence of the force field. Once the force field was removed, participants temporarily showed an over-shoot on the opposite direction of the field, as an *after-effects* or *post-effects*, see figure 4.1. Authors explained this phenomenon as the formation, by the human Central Nervous System (CNS), of an *internal model* of the disturbances produced by the field. As a consequence, the internal model was utilized to compensate the deviating forces in a feedforward manner. Such motor adaptation had also been shown earlier by Lackner and Dizio [97] with an experiment on the adaptation to the Coriolis force perturbation, due to body rotation, during forward reaching movements.

Many researches were carried out to study the characteristics of motor adaptation by adopting a similar experimental setup as in [161]. In particular, in [158] the authors examined the post-effects exhibited after removing a lateral force-field when the lateral kinematic error was prevented by confining the movements along the straight-line to the target through using a “haptic channel”. Wash-out of motor adaptation in the channel resulted in a much slower rate of disadaptation, providing evidence that motor adaptation is influenced

simultaneously by dynamic and kinematic factors, with the latter strongly central in the rapid loss of adaptation after restoring the original dynamics. Similarly, in [131] Patton and Mussa-Ivaldi showed how, by suppressing to the participants the vision of the hand location and thus the visual feedback on the error, the post-effects persisted longer in the wash-out phase. Later the same research team observed the fundamental presence of after-effects in eighteen stroke survivors [132], even if these effects were not correlated with classical clinical scores for monitoring motor impairments. At the same time, they compared error augmentation strategy (when the training forces increased the original error) with an assistive strategy (when either no fields were applied or the robot was actively reducing the error) demonstrating the more effectiveness of the error-amplifying therapy. A further experimentation on twenty-six participants with chronic hemiparesis, during two weeks of training, resulted in small but significant improvements in Fugl-Meyer motor score and in Wolf Motor Function Test, with respect to a control group without error augmentation practice [3]. In [81], the authors used negative viscosity to amplify movement error by generating assistive forces in the direction of the motion, combined with an assistive acceleration-dependent force field. They found that the combined training resulted in lower error, a broader range of speeds, and broader exploration when comparing to training with only acceleration dependent force field, although the potential of muscle co-contraction was not examined. Testing on thirty chronic stroke survivors confirmed the capability of negative viscosity to induce improvements in motor exploration, above all along the sagittal axis of motion [80].

As said, the crucial aspect of motor learning for rehabilitation is the ability of transferring the learnt skills from a context to another. Yet this is a critical issue for rehabilitation robotics, since important results on generalization are still missing. This may be related to the fact that robots are seen as external tools by the patients, meaning that they associate the learnt strategies to the context of “*being inside the robot*”, and thus, positive effects decay when the orthosis are detached from the impaired limb [82]. This is possibly the biggest challenge of rehabilitation robotics. Nonetheless, some of the above-mentioned publications [161, 131, 80] found that the participants were able to transfer after-effects in regions of the workspace where no exposure to the force fields took place; however these transfer effects were only spatial generalizations, limited by the necessary presence of the planar robotic devices.

4.1.2 Exoskeletons potentialities

The studies presented so far were all limited to movements in a plane, due to the architectural properties of the utilized devices. The limitations of the planar devices did not allow to directly address intermediate joint movements analysis. Dipietro *et al.* [43], for example, showed how the shoulder-elbow impaired independence was improved in a circle drawing task for 117 chronic stroke survivors, after training with a planar robot on a therapy of assisted point-to-point movements. However, the shoulder and elbow joint angles were only deducted from the measured hand path, through a simplified non-redundant two-link model of the human arm.

As mentioned in section 1, modern robotic exoskeletons, on the contrary, thanks to a larger number of DOF with respect to planar robots, are able to impose forces at each joint of the upper-limb separately and to collect reliable measures of the intermediate joints movements, providing a promising framework to test adaptation and learning on 3D activities. Clearly an interesting aspect of working with exoskeletons is the possibility to investigate the way the human CNS deals with the natural upper-limb redundancy for common activities like pointing or tracking tasks.

Therefore, we are interested in better understanding the possibility of former results on manipulanda to be generalized to inter-joint coordination in such a redundant system, *i.e.* the 7-DOF of the human arm. In fact, beyond performing therapy for upper-limb movements and functional recovery, there is a growing need for rehabilitating synergies of patients towards more normal patterns of motion, but yet fundamental studies and experimental results are lacking on how humans, even healthy, adapt to imposed constraints on the inter-joint coordination.

To the authors’ knowledge, only Mistry *et al.* [121] investigated human force field adaptation using an exoskeleton with multiple coupled parts and joint level interactions (in particular a 7-DOF *Sarcos Master Arm* robotic exoskeleton). However, the authors of this experiment limited the application of the force fields to a

single joint; in particular, they used the exoskeleton to perturb the elbow flexion/extension, during point-to-point reaching tasks, by driving a disturbing force field based on the shoulder velocity (respectively the sum of the shoulder flexion/extension and the shoulder abduction/adduction). The authors found that the human nervous system exploited the redundancy of the upper-limb to minimize the effects of the force field on the realization of the endpoint trajectory. In fact, when the force field was turned on and after a period of adaptation (about 100 movements), while the trajectories at the joint level remained changed, the hand trajectories returned to baseline as before the application of the field. Moreover, they observed after-effects when suddenly removing the perturbation but this result consisted of only 3 catch-trial movements, with no consequent analysis on the wash-out.

The goal of this chapter is therefore to try to answer to some of the following questions by utilizing a robotic exoskeleton.

- Can we modify upper-limb synergies and teach a specific inter-joint coordination?
- If we apply some viscous distributed inter-joint constraints through an exoskeleton, without constraining the end-effector movements, how would subjects react?
- Do the participants adapt as in the case of constraints applied at the end-effector only?

We hypothesize that the awareness of motor performance is certainly higher when dealing with task completion (like reaching an object) than the awareness of the motor coordination to perform the task (which is autonomously and implicitly solved by the CNS, exploiting the upper-limb redundancy). Therefore would participants, exploiting this redundancy in the perturbing environment, adapt their motor coordination and show similar after-effects as the ones appearing on the end-effector in state-of-the-art studies, in which, however, the effects on the inter-joint coordination were not taken into consideration?

Such knowledge could be fundamental to exploit the main characteristics of modern robotic exoskeletons – the possibility to control multiple joints separately, by imposing distributed coordination control – and could lead to the opportunity, in a near future, to rehabilitate pathological synergies with robots.

4.2 Modifying the inter-joint coordination: the experimental setup

We set up an experiment to test the possibility to modify upper-limb synergies in healthy participants, by inducing adaptation and learning of joint coordination through the exposition to viscous force fields. For this experiment, we used the ABLE exoskeleton and a 7-DOF WAM robotic manipulator, as shown in figure 4.2. In the following part of the section, the protocol is described.

4.2.1 The exoskeleton controllers

We utilized two different control modes on the ABLE exoskeleton: the Kinematic Synergy Control, to expose subjects to viscous force field that may modify the joints coordination during movement, and the *Gravity Compensation* mode allowing unconstrained upper-limb motion.

A reactive controller based on viscous corrective force field

The Kinematic Synergy Control (KSC) is a controller developed by Crocher *et. al* [29], which generates reactive viscous joint torques to impose specific patterns of inter-joint coordination without constraining the hand motion in space. By exploiting the human natural upper-limb redundancy when performing reaching tasks, this controller corrects the free arm movement if the operator is not respecting a desired synergy – a desired ratio among the upper-limb joint velocities – thus encouraging the user to modify his inter-joint coordination. In this case, the KSC generates dissipative velocity dependent forces to constrain the undesired upper-limb coordination directly at the joint level, without directly affecting the end-point motion. Otherwise,

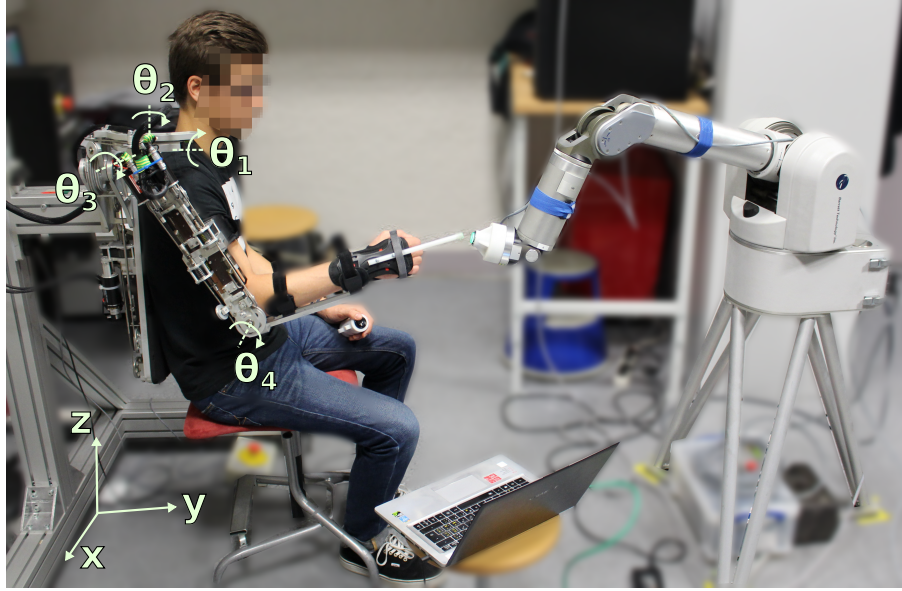


Figure 4.2: Experimental setup. On the left, a participant of the experiment within the ABLE exoskeleton. On the right, the WAM manipulator with the push button on top. $\theta_1 \dots \theta_4$ are the angles defining the four different joints orientation.

if the given pattern of joint coordination is followed, the controller produces a null torque. More details on this controller are given in Appendix B.

For our experiment we used the following version of the KSC:

$$\tau = -k\mathbf{C}^T \mathbf{C}\dot{\mathbf{q}} \quad (4.1)$$

where τ is the vector of the output torque to the exoskeleton joints $\tau = [\tau_1 \ \tau_2 \ \tau_3 \ \tau_4]^T$, $k \in \mathbb{R}^4$ is a vector of viscous gains, $\dot{\mathbf{q}} \in \mathbb{R}^4$ is the vector of joints velocity, and $\mathbf{C} \in \mathbb{R}^4$ is an arbitrary imposed vector of constraints, which we set for the experiment as

$$\mathbf{C} = [0.667 \ 0 \ -0.667 \ 0.333]. \quad (4.2)$$

The chosen values of \mathbf{C} provided a generic perturbing behaviour pushing towards unnatural inter-joint coordination, as, for example in our experiment, over abduction while flexing the shoulder during forward hand movement, instead of the natural synergy (shoulder flexion and elbow extension). Furthermore, the resulting constraints, imposing a ratio among the different joint velocities, were complex for the participants to be understood, providing a not easily predictable exoskeleton behaviour for the users.

Gravity compensation mode

This control mode consisted in a feedforward gravity compensation of the exoskeleton. With this mode, the robot produces minimal resistance to the human motion, giving freedom of movement to the user [87]. Actually, the gravity compensation was always active as a feedforward compensation, even simultaneously to the KSC, thus this control mode can be seen as the situation in which the corrective force fields were inactive.

4.2.2 Experimental protocol

The experimental protocol has been validated by the ethics committee of the Paris Descartes University (see end of the thesis for the CERES certificate).



Figure 4.3: Example of goal-directed pointing task (GDM). The four pictures show the motion from the starting position to the WAM button, while performing GDM task. In this case the subjects were not asked to follow any specific endpoint trajectory.



Figure 4.4: Example of path-constrained tracking task (PCT). The four pictures show the motion from the starting position to the WAM button, while performing PCT exercise. The participants were asked to follow the specific endpoint path shown by the rubber band going from the starting position of the ABLE exoskeleton to the WAM end-effector.

Participants

Twenty healthy individuals participated in this study (12 male and 8 female, aged 24.5 ± 4.8), giving informed consent before participation. They were members of the laboratory or relatives, naive to the experiment. We measured subjects size and their maximum grip force with a dynamometer.

Tasks

The participants were asked to perform several pointing tasks with the ABLE exoskeleton while sitting comfortably on a stool. The exoskeleton was connected to the right arm of the operator through three velcro cuffs, one on the upper-arm and two on the forearm. Besides, the subjects wore a commercial wrist splint to limit wrist motion and prono-supination (not controlled nor measured by the robot).

A 7-DOF WAM manipulator (© *Barrett Technology*), with a press button at its extremity, was placed in front of the participants for presenting the pointing targets. Starting from a resting position (the upper-arm along the body, with the elbow bent about 90 degrees and the forearm along the leg), the participants were asked to push the button on the WAM through a plastic rod, screwed on the splint. Once the target button was pressed, the ABLE exoskeleton was actively bringing back the upper-limb to the starting position, through a position control mode, while the subjects were remaining passive. For each pointing trial, participants manually triggered the record of the motion by pushing on a secondary button with the free left hand and they had 4s to complete the movement.

We chose two different testing tasks:

- *Goal-Directed Mode* (GDM), a simple pointing task, the participants were free to move from the starting position to the button, *i.e.* they were not asked to follow any specific trajectory or arm coordination, see figure 4.3.
- *Path-Constrained Tracking mode* (PCT), a path following task, the subjects were asked to follow a specific straight end-point path from the initial position to the WAM push-button, see figure 4.4. The end-point path was shown by an elastic rubber band connecting the starting position to the WAM button.

The average total times for each reaching task were about 90 minutes for GDM and 105 minutes for PCT.

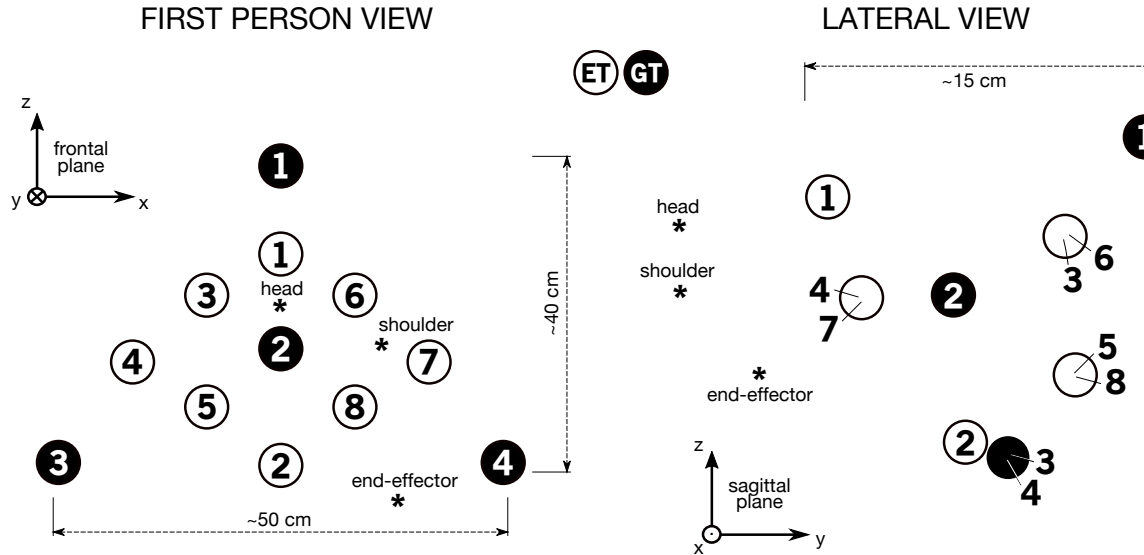


Figure 4.5: WAM positions. The eight Experimental Target positions (ET) and the four Generalization Target positions (GT). The asterisks * show the mean position of head and shoulder, and the projection of the starting position of the elbow/end-effector. On the left, x - z frontal plane, on the right, y - z sagittal plane (some targets are coincident on this plane). The frames are consistent with the reference frame of figure 4.3.

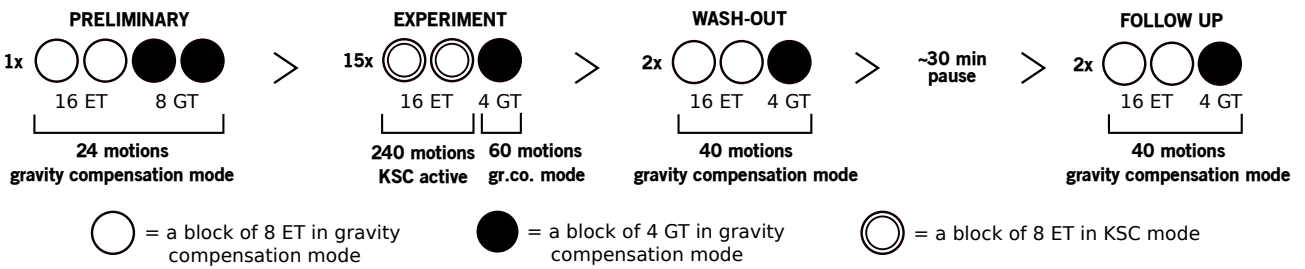


Figure 4.6: Phases of the experiment. Experimental protocol, showing the four consecutive phases, respectively *preliminary*, *experiment*, *wash-out* and *follow up*. Before the follow up, the subject was resting, detached from the exoskeleton, for about 30 minutes. The number in front of each phase stands for the number of repetition of each pattern (1 repetition for PRE, 15 for EXP, and 2 for WAS and FOL).

Reaching targets

The protocol consisted in 12 different final positions presented by the WAM robot, grouped in *Experimental Targets* (ET, 8 positions) and in *Generalization Targets* (GT, 4 positions), shown in figure 4.5. While the ET were periodically exposed to the perturbation of the corrective fields, the GT positions were never exposed to any field. These positions were fixed for all the subjects. The targets ET 1 and GT 2 were placed in the sagittal plane of the participant, the ET targets 6-8 and ET 7 were placed in a para-sagittal plane respectively more internal and external to the plane of the participant's upper-arm. The targets were placed at different depths (about 15cm of range between the closest position to the subject and the furthest one, figure 4.5). The distance WAM-ABLE was fixed for all the participants, but selected such that every participant could reach any target position with the exoskeleton.

Procedure

Ten participants carried out the GDM, and ten the PCT. Initially, every subject was given the possibility to practice free movements with gravity compensation mode for few minutes. After this initial training, the subject was asked to point to the different targets with the robotic exoskeleton. All the sequences of pointing tasks were performed by blocks of 8 ET or 4 GT trials presented in the same randomized order for each subject.

The experiment consisted of 4 phases: *preliminary* (PRE), *experiment* (EXP), *wash-out* (WAS), and *follow up* (FOL).

In particular we had:

- **PRE** (24 total pointing task) was 2x8 ET followed by 2x4 GT;
- **EXP** (300 total pointing task) was 15 repetitions of 2x8 ET plus 4 GT, that is every repetition consisted of 20 pointing tasks;
- **WAS** (40 total pointing task) was two repetitions of 2x8 ET plus 4 GT;
- **FOL** (40 total pointing task) was two repetitions of 2x8 ET plus 4 GT.

Figure 4.6 shows a scheme of the patterns and the phases.

PRE, EXP, and WAS were performed in sequence, while before FOL there was a pause of about 30 minutes, during which the participants rested, detached from the exoskeleton. It is important to underline that the KSC was active only during EXP and only during the pointing tasks towards ET. Otherwise, the robot was controlled in gravity compensation mode. Therefore, as shown in figure 4.6, the KSC was perturbing and correcting the subject free motion only during 240 movements over the 404 total movements of each experiment. GT movements were always unconstrained.

4.2.3 Quantification of the human spontaneous variability within the exoskeleton

A specific experiment was performed in order to quantify the spontaneous variability of human subjects performing reaching tasks with the exoskeleton in gravity compensation mode. We performed this experiment with 10 healthy subjects – participants of the KSC experiment but naive at the moment of the variability test – performing pointing task to GT targets. Five subjects practised with each exercise (GDM and PCT). They performed four sequences of five repetitions of pointing tasks, towards the 4 GT positions (thus a total of 20 motions per sequence) for a total of 80 reaching tasks for each subject. The sequences were separated each other by one hour of resting time, during which the participants were detached from the exoskeleton. In this way, we aimed at measuring the spontaneous human variability and, additionally, at capturing the variability due to the different arrangement of the device on the human arm, consequence of detaching and attaching the participants to the exoskeleton. The outcome of this preliminary experiment showed a small and stable variability among subjects, providing a reference value to compare with the results of the training with the exoskeleton.

4.3 Data processing

4.3.1 Data gathering

Kinematics data were collected through the four differential encoders of the ABLE exoskeleton. For the end-point kinematics (the tip of the rod) a direct kinematic model of the robotic upper-limb was used together with a measure of the subject forearm length. Post-processing was done using Matlab environment (© *The MathWorks, Inc.*). All the recorded data were low-pass filtered using a 4th order Butterworth filter, with cut-off frequency of 5Hz.

4.3.2 Joint kinematics

We analysed the final arm-robot configuration at the time when the subjects were pushing the WAM button. The final posture joint angles q_i , with $i = 1, 2, 3, 4$, were expressed relatively to their values at the end of the first movement in the preliminary phase, thus before any force fields exposition.

4.3.3 End-effector kinematics

We computed the speed profile (norm of velocity) of the endpoint motion and considered the following temporal parameters

- motion duration T , for which we defined the beginning and end of each movement as 10% of its peak velocity;
- end-point motion smoothness η , as the spectral arc-length metric defined by [6], for which large negative values mean reduced smoothness;
- maximum end-point velocity v_{max} .

The spatial characteristics of the trajectory were studied thanks to the *curvature* parameter Φ , defined by [87] as the maximum deflection of the hand path from a straight line joining the initial and final positions, showing if the hand is deviated from its natural path:

$$\Phi = \frac{1}{l} \max(d_p(t)) \quad (4.3)$$

where $l = \left\| \overrightarrow{P(t_{end})} - \overrightarrow{P(t_{in})} \right\|$ is the length of the vector from the start to the final positions, and

$$d_p(t) = \frac{1}{l} \left\| \left(\overrightarrow{P(t)} - \overrightarrow{P(t_{in})} \right) \times \left(\overrightarrow{P(t_{end})} - \overrightarrow{P(t_{in})} \right) \right\| \quad (4.4)$$

is the instantaneous distance of the vector position of the pointer, $\overrightarrow{P(t)}$, from the straight line joining $\overrightarrow{P(t_{in})}$ and $\overrightarrow{P(t_{end})}$.

4.3.4 Principal Component Analysis

A Principal Component Analysis (PCA) was performed on the simultaneous coordination of the four joints, *i.e.* a test to spot potential resulting *joint synergy*. Each PCA was performed on the joint velocities of a single repetition of reaching tasks, therefore on four reaching movements for the GT (one PCA for each black circle in figure 4.6) and on sixteen reaching movements for the ET (one PCA for each couple of white circles in figure 4.6).

In order to determine if two motions were similarly coordinated, we applied the metrics previously developed in [16] that is a distance metrics between subspaces:

$$\psi(\mathbf{U}, \mathbf{V}) = \sqrt{1 - S_{min}^2(\mathbf{U}^T \mathbf{V})} \quad (4.5)$$

where S_{min} is the minimal singular value of the matrix $\mathbf{U}^T \mathbf{V}$, with \mathbf{U} and \mathbf{V} the two subspaces defined by the first three Principal Components (PCs). This function represents the sine of the minimal angle of rotation between the two subspaces, where $\psi = 0$ stands for no rotation and $\psi = 1$ for orthogonality. Thus, a small distance between subspaces, representing different motions, would mean that these motions were performed by using similar joint synergies, while a large distance would indicate that the subject has changed his coordination while performing the same task.

4.3.5 Statistics

For the statistical analysis on the whole group of participants, the analyses were performed separately for the ET and GT trials. The values of the end-point and the joint variables were averaged during five phases of the procedure, for each target. In particular we considered 2 blocks of PRE trials, the two first and two last blocks of the EXP trials, respectively Early and Late exposition to KSC (E-EXP and L-EXP), the first two blocks of

wash-out WAS, and the first two of follow up FOL. Non-parametric statistics were performed on these five different phases. A Mann-Whitney U test was used to compare the effect of mode (GDM versus PCT) in every different phase-target combinations (5 phases, 5x8 cases for ET targets, and 5x4 cases for GT targets). A Friedman ANOVA test was used to detect the effect of phase (PRE, E-EXP, L-EXP, WAS, and FOL) and target (ET versus GT) separately for the two modes. If these effects were statistically significant, further two-by-two comparisons were performed with the Wilcoxon test.

To analyse individual results, we focused on the shoulder abduction/adduction movements. For each subject we compared data from PRE and WAS (the mean final posture of the two movements in PRE with respect to the first two movements in WAS, therefore only during the first repetition of WAS), to determine the presence of after-effects, and data from early EXP and late EXP (the mean final posture of the first two movements in EXP with respect to the last two movements in EXP), to determine the presence of adaptation. On these two intervals, we therefore computed a Student's t-test.

For the PCA analysis, we computed the distance metric (section 4.3.4) between the subspaces describing the PRE trial and all the subsequent blocks in the same mode. These distances were then compared to subspaces describing the spontaneous variability observed during the spontaneous variability experiment (4 blocks of 5 repetitions). To this purpose, for each mode, we calculated the mean of the permutation of the distance between PCs subspaces and used this value as hypothesized value for a non parametric one-sample sign test.

Finally, correlation analyses were also performed between morphological and kinematic data. All the statistical computation were performed using Statistica (© Dell Inc.).

4.4 Results

First the results of two illustrative participants are presented in order to show the effect of KSC and the consequent inter-individual difference. Then, separately, the results of the experiment are analysed with respect to the whole group of participants and the three different tasks, considering successively the effect of the direct exposition to the corrective force fields (movements towards ET), and the consequences over targets and movements which were never exposed to these fields (towards GT).

4.4.1 Individual results

Two illustrative cases

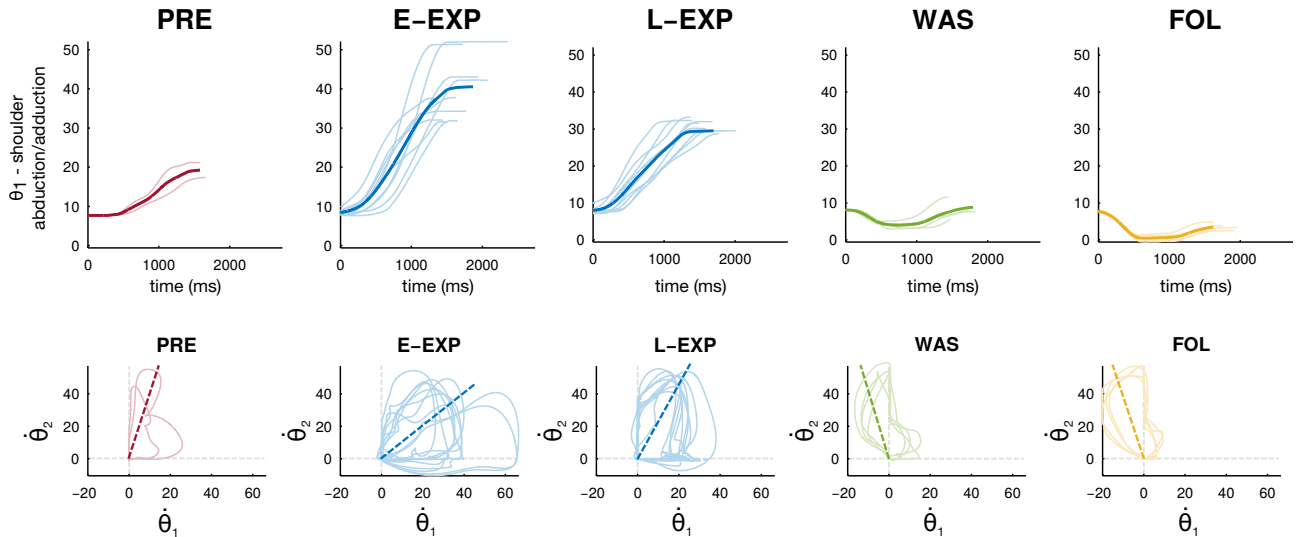
Figure 4.7 is composed of four figures showing the results of two typical scenarios, representing the different behaviours observable during the experiment. For both cases, the task was the goal-directed mode. The top figure, for each case, represents the trajectories of the first angle (the shoulder abduction/adduction) on motions towards the ET number 4 (placed on the left of the plane including the shoulder, thus producing internal shoulder rotation), for 5 phases of the experiment, respectively preliminary, early exposition (first five repetitions of EXP), late exposition (last five repetitions of EXP), wash-out, and follow up.

As we can see, the effect of the KSC (E-EXP) was, in one situation (case 1) to increase the value of abduction above the initial level (PRE). Then during the continuous exposition to the KSC (L-EXP) the level of abduction tended to return to the original one. After the removal of KSC (WAS), the subject showed an over-shoot of the shoulder angle in the opposite direction of the constraints (in this case, a stronger adduction) which persisted during follow-up. Similar results were observed mainly for the first two angles, on most of the ET positions.

In the other situation (case 2), clearly the post-effect after the exposition of the force fields is rather a coordination in between the one imposed by the KSC and the natural one. In addition we did not see any type of adaptation during the L-EXP phase.

Another way to illustrate these phenomena is by looking at the velocity cycloids *i.e.* graphs showing the velocity of a joint according to the velocity of another joint, thus showing joint velocity synergies. The bottom graph of figure 4.7, for each case, shows the cycloids for movement towards target number 4 and, in

case 1: over-shoot (30% of movements)



case 2: persistent perturbation (55% of movements)

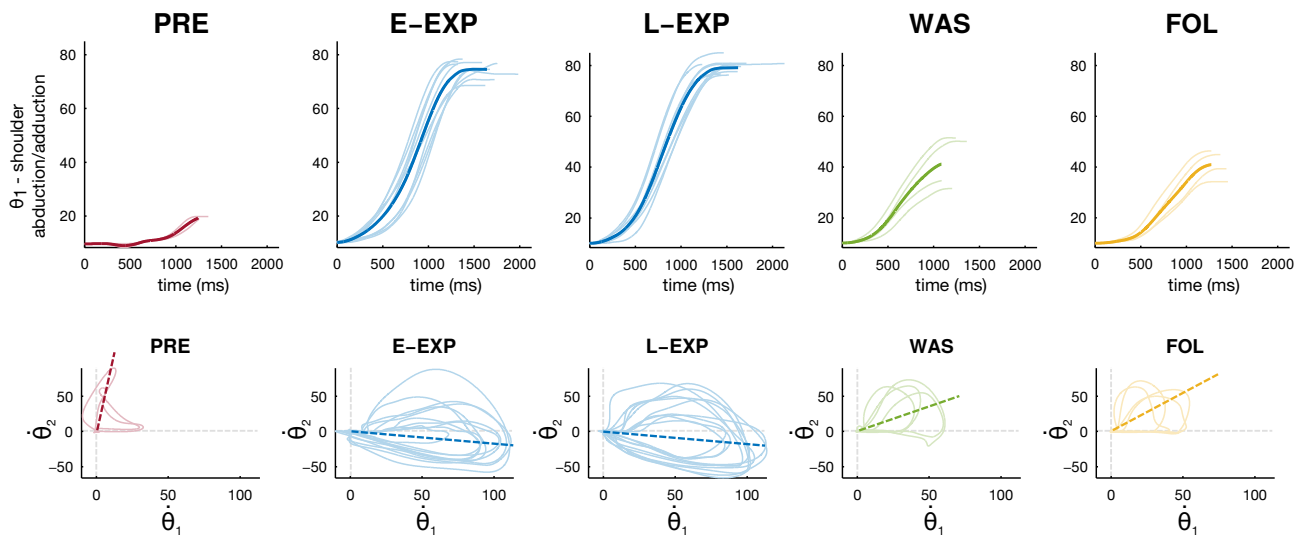


Figure 4.7: Two illustrative cases. For two subjects, during GDM task, we show two different figures: on top, the averaged trajectory of the shoulder abduction/adduction (dark plots) and the single trajectories (lighter plots), when moving towards ET 4; on bottom, for the same target, the resulting cycloids when considering the ratio between the first two joint velocities (shoulder abduction/adduction versus internal/external rotation). In this case the light plots are the cycloids, while the dark dashed lines are the mean ratio. For the four graphs, data refer to the 5 phases of the experiment, preliminary (PRE), early exposition (E-EXP, first five repetitions of EXP), late exposition (L-EXP, last five repetitions of EXP), wash-out (WAS), and follow up (FOL).

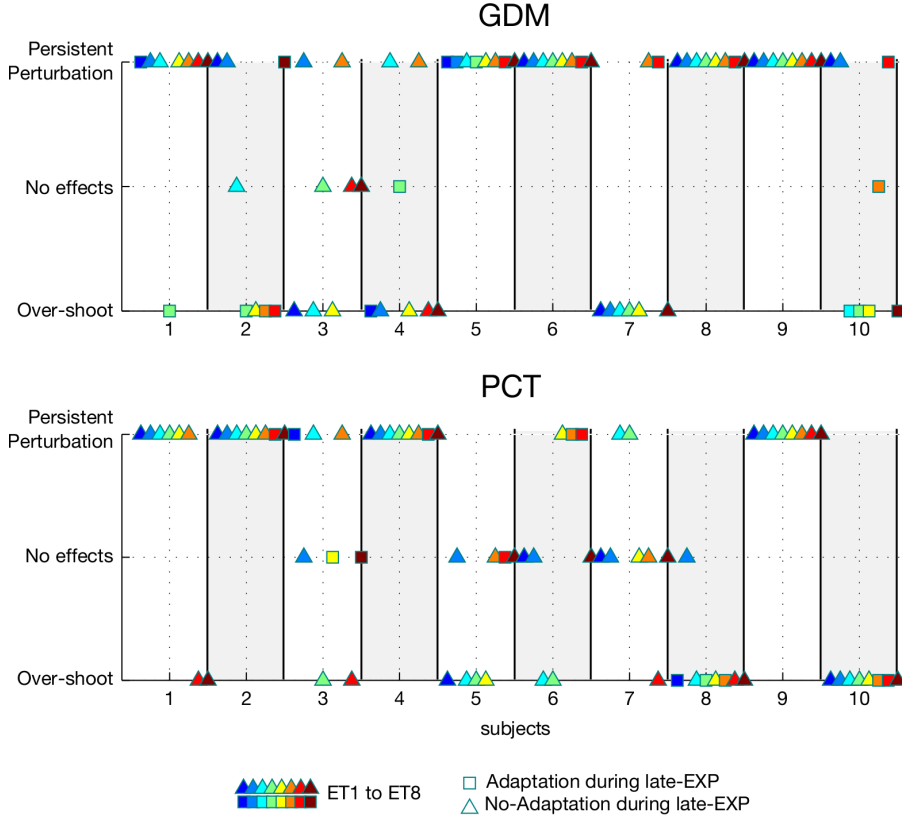


Figure 4.8: Inter-individual differences on the effect of the KSC exposition, for the first joint, during WAS. Each symbol corresponds to one movement, performed by one subject, towards one ET. The three possible effects during the WAS are: persistent perturbation, over-shoot, and no-effect. To the same color corresponds the same ET. Additionally, the presence or not of the adaptation during the exposition to the force fields (during EXP) is shown respectively by a square or a triangle.

particular, the velocity of the first joint (shoulder abduction/adduction) with respect to the second joint (shoulder internal/external rotation), during the 5 phases of the experiment. The results are consistent with the two phenomena of either late-exposition adaptation towards the original movement, with a strong over-shoot as post-effect during both WAS and FOL, or absence of adaptation in L-EXP, followed by persistent perturbation as post-effect during both WAS and FOL. These are also underlined by the dashed lines representing the mean ratio between the two joint velocities.

Inter-individual differences

During WAS and FOL, most of the movements resulted in either a persistent perturbation or in an overshoot. In a smaller number of movements, no effects were observed when the KSC was removed. At the same time, generally either adaptation occurred during late-EXP, or participants did not change their coordination while moving within the force fields. The behaviour of each subject, during and after the exposition to KSC, was identified thanks to the analysis described in section 4.3.5, is shown in figure 4.8. Based on these, the persistent perturbation was the most common effect (55% of the movements), while one third of the tasks were followed by over-shoot. No effects were observed only on 22 movements out of 160 (14% of cases), and these were almost equally distributed on the two tasks. GDM resulted mostly in persistent perturbation during WAS (63% of the movements), while during PCT we observed a slight increase of over-shoot effects (48% of persistent perturbation versus 33% of over-shoot). Finally late exposition adaptation occurred only in the 21% of the movements, more frequently during pointing tasks (GDM) than in tracking (PCT).

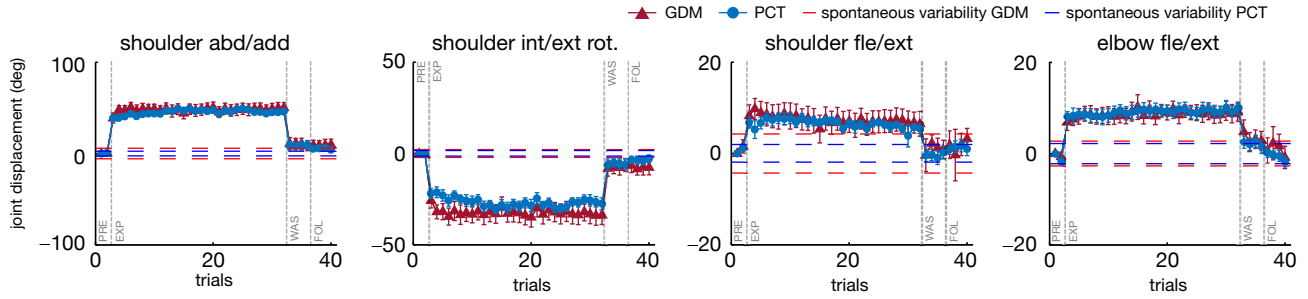


Figure 4.9: Mean joint final displacement on movement towards ET 3. Mean joint final displacement and standard error with respect to the final posture of first movement in PRE, in the two different modes, over the 10 subjects. The target position is ET number 3. Columns are the four joint of the exoskeleton. Horizontal dashed lines represent the joint maximum standard deviation σ for the spontaneous variability experiment.

4.4.2 Movements towards ET: adaptation to KSC

Joint kinematics

The mean final upper-limb posture, for ET 3 over the whole experiment and for both tasks, is presented in figure 4.9. The illustrated target was chosen since its height and internal position, with respect to the right arm of the participants, involved large rotations on which the effects of the KSC are more observable.

Mann-Whitney U test performed separately for the 160 cases (4 joints, 5 phases, 8 targets combinations) showed that the final angle in the different joints did not vary significantly with the mode except in 4/160 cases (3 times for joint 2, once for joint 4).¹ Friedman ANOVA, performed separately for each mode, showed that the posture, for all the joints, varied significantly with the targets and the phases ($p < 0.001$). Paired comparisons, through the Wilcoxon test, were used to analyze the differences between phases separately for each mode and each target.

The first joint angle (shoulder abduction/adduction) increased significantly between PRE and E-EXP, for both GDM and PCT modes, for all the targets ($p < 0.01$), indicating the direct effect of the KSC. It remained increased by reference to PRE during L-EXP ($p < 0.01$). There were no significant differences between E-EXP and L-EXP phases, except for a slight increase of the deviation for target 4 ($p < 0.01$), and a decrease for target 7 in PCT mode ($p < 0.05$). The angle returned close to PRE values during WAS for all the targets but for targets 6 in GDM mode, for which the deviation persisted ($p < 0.01$). During FOL the joint postures were mostly similar to PRE values, except for targets 6 in both modes ($p < 0.05$).

The second joint angle (shoulder internal/external rotation) decreased significantly between PRE and E-EXP (for targets 1 and 3-6, whatever the mode $p < 0.01$, for target 8 in GDM and target 7 in PCT $p < 0.05$). This deviation lasted during the exposition to the KSC and remained different to PRE values during L-EXP ($p < 0.01$), except for targets 2 and 7. There were significant differences between E-EXP and L-EXP phases only for target 5 in GDM ($p < 0.05$) and targets 4, 5, and 8 in PCT ($p < 0.05$). During WAS, the joint angles remained decreased by reference to PRE values for target 6 in GDM ($p < 0.01$) and targets 2 and 5 for PCT. During FOL, the values were decreased by reference to PRE values for targets 3, 5 ($p < 0.05$) and 6 ($p < 0.01$) in GDM.

The third joint angle (shoulder flexion/extension) was significantly modified by the KSC as shown by significant differences between PRE and E-EXP, except for target 1 ($p < 0.01$ for targets 3-7, $p < 0.05$ for targets 2,8 in GDM mode and $p < 0.01$ for targets 3-8 in PCT mode). The direction of the modification depended on the target: the angle was increased for targets 2-5 and decreased for targets 6-8. During L-EXP, the angle remained deviated in the same direction ($p < 0.05$ for targets 3 and 4, $p < 0.01$ for targets 5-8 in GDM, $p < 0.01$ in PCT). There were only slightly differences between E-EXP and L-EXP depending on the

¹Joint 2, during PRE, for target 6 ($p < 0.02$) and, during E-EXP, for targets 1 and 4 ($p < 0.05$). Joint 4, during E-EXP, for target 1 ($p < 0.01$).

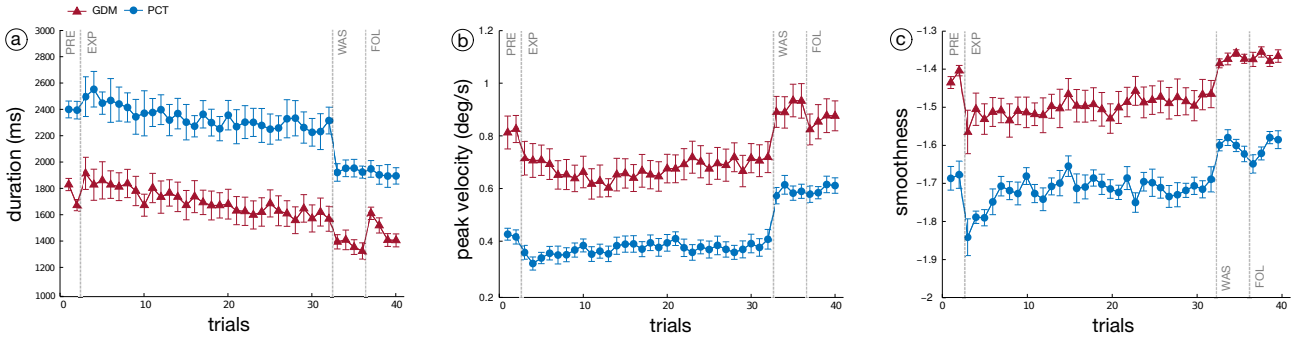


Figure 4.10: Mean motion duration T (a), mean peak velocity v_{max} (b), and mean smoothness η (c). Averaged data over the ten participants and standard error for the pointing tasks towards ET positions for the two different modes. Smoothness, through spectral arc-length, is higher when η is closer to zero.

mode and the target.² The amount of the deviation decreased during WAS (without changing direction) but remained significant for targets 6-8 in GDM ($p < 0.01$) and for targets 1, 5 ($p < 0.05$) and 6, 8 ($p < 0.01$) in PCT. During FOL, the values were not significantly different with respect to the PRE phase.

The fourth joint angle (elbow flexion/extension) significantly increased between PRE and E-EXP ($p < 0.01$ whatever the mode and the target). This deviation remained during L-EXP, as shown by significant differences between PRE and L-EXP, except for target 7 ($p < 0.01$ for targets 2-6, 8 and $p < 0.05$ for target 1 in GDM, $p < 0.01$ for targets 3-6, 8 and $p < 0.05$ for target 1 and 2 in PCT). There were no differences between E-EXP and L-EXP in GDM and only a decrease of the deviation for target 1 in PCT ($p < 0.05$). During WAS, the values were not significantly different from the ones in PRE, for the GDM, except for a persisting deviation for target 5 ($p < 0.05$). In PCT, there was a persistent deviation for targets 3 ($p < 0.05$) and 5 ($p < 0.01$), and a reversal of the effect with decreased values, by reference to the PRE values, for targets 1 and 7 ($p < 0.05$). During FOL, the values were not different to those in PRE, in GDM, but they remained decreased w.r.t. PRE for targets 1 and 7 in PCT ($p < 0.01$).

In conclusion, the KSC consistently modified the final joint postures and its effect lasted as long as the exposition to the perturbation with small differences between the early and late periods. After the removal of the KSC, participants were often performing differently from their natural coordination, depending on the mode and the target. The after-effect were mostly characterized by the persistence (in the same direction but with a reduced amount) of the deviation observed during the exposition to KSC. A significant overshoot was only observed for joint 4, during reaching for two targets in PCT.

End-point kinematics

Motion duration and peak velocity for ET motions are shown in figure 4.10.a and figure 4.10.b. Mann-Whitney U test, performed separately for the 40 cases, confirmed that the velocity of the movements was slower in PCT than GDM mode (significant in 36/40 cases, the exceptions were during WAS or FOL) with a longer duration (significant in 29/40 cases, the exceptions were mostly during FOL). Friedman ANOVA performed separately for each mode showed that the velocity and duration varied significantly with the target and the phase ($p < 0.001$). Post-hoc paired comparison, through the Wilcoxon test, confirmed that the peak velocity decreased during the early exposition to KSC (significant decrease between PRE and E-EXP for 2 targets in GDM mode and 4 in PCT mode), then it remained stable during the exposition to KSC between E-EXP and L-EXP (except a significant increase for one target in PCT). The peak velocity increased after the removal of KSC (significant difference between L-EXP and WAS for six targets in GDM and for every target in PCT, and between L-EXP and FOL, for seven targets in GDM and for every target in PCT). The velocity was slightly

²A decrease of the angle for target 1 ($p < 0.05$ in GDM, $p < 0.01$ in PCT), a lessening of the initial deviation for target 3 ($p < 0.05$ in GDM and PCT) or an increase of the initial deviation (for targets 7 and 8, in GDM $p < 0.05$, and for targets 6-8 in PCT mode $p < 0.01$).

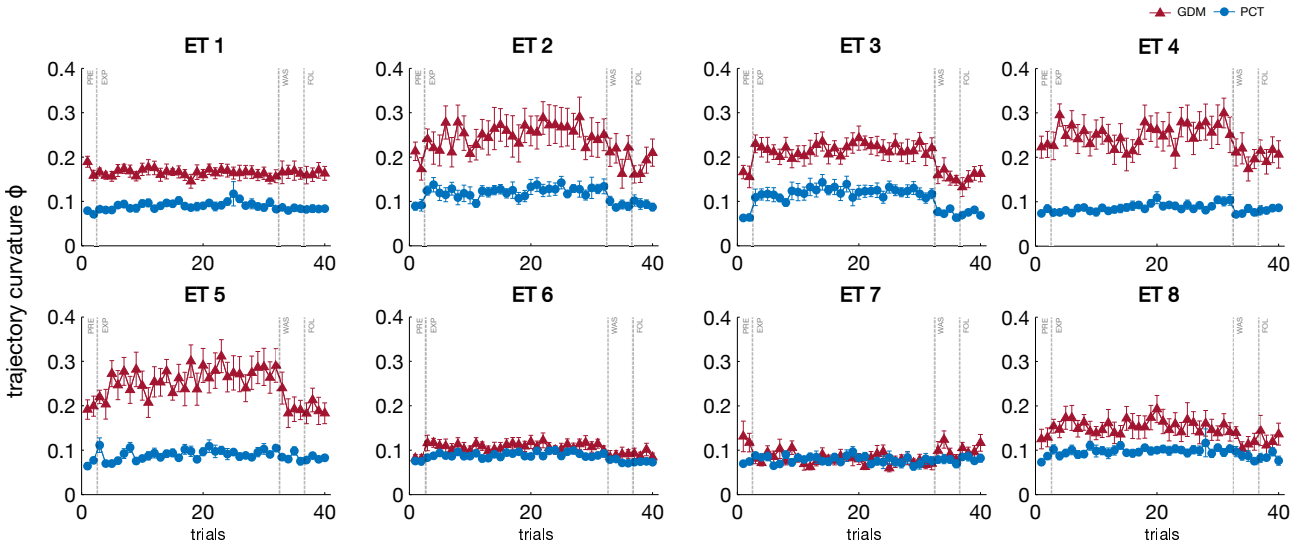


Figure 4.11: Mean trajectory curvature Φ . Mean trajectory curvature and standard error for the ten subjects, over the 8 ET positions, for the two tasks.

higher during FOL than PRE in PCT mode (significant for seven targets). The duration of the movement was slightly increased at the beginning of KSC (significant difference between PRE and E-EXP for two targets for GDM and PCT) then decreased during exposition to KSC (significant difference between E-EXP and L-EXP for four targets in GDM and PCT). The duration decreased further after the removal of KSC (significant difference between L-EXP and WAS for four targets in GDM and five in PCT, and between L-EXP and FOL for one target in GDM and for five in PCT). During WAS and FOL the movements were shorter than before exposition to KSC (significant difference PRE-WAS for five targets in GDM and for all target in PCT, significant difference PRE-FOL for three targets in GDM and six targets in PCT).

As expected (figure 4.10.c), the movements were less smooth in PCT than in GDM. This was confirmed by Mann-Whitney U test showing a significant difference in 32/40 cases. Friedman ANOVA performed, separately for each mode, showed that the smoothness varied significantly with the target and the phase ($p < 0.001$). The exposition to the KSC immediately decreased the smoothness of the movement (Wilcoxon: significant difference between PRE and E-EXP for six targets in GDM and two in PCT) and this effect lasted during the KSC exposition (no difference between E-EXP and L-EXP; except one target in PCT). When the KSC was off, the smoothness was slightly improved during WAS by reference to L-EXP (significant difference in four targets in GDM and three in PCT).

The variation of the trajectory curvature Φ as a function of ET target position for the different modes is shown on figure 4.11. Mann-Whitney U test confirmed that the curvature was usually greater in GDM than in PCT (significant in 27/40 cases). The increase of curvature was observed for the more distant targets (target 1-5 during all the phases and target 8 for phases PRE and E-EXP) but not the closest ones (targets 6 and 7). Friedman ANOVA, performed separately for each mode, showed that the curvature varied significantly with the target and the phase ($p < 0.001$). The curvature increased at the beginning of exposition to KSC (significant difference between PRE and E-EXP for targets 3 and 6 in GDM, and targets 2, 3, 6, 8 in PCT) then remained at a similar level during the exposition to KSC (no significant difference between E-EXP and L-EXP, except target 4 in PCT). The curvature regained PRE level during WAS and FOL.

Summarizing, the results from velocity and duration parameters are consistent: the subjects slowed down their movements as soon as the KSC became active. Once the KSC was removed, the movements became faster and shorter. The smoothness of the trajectories reduced and their curvature increased during the application of the KSC without clear after effects.

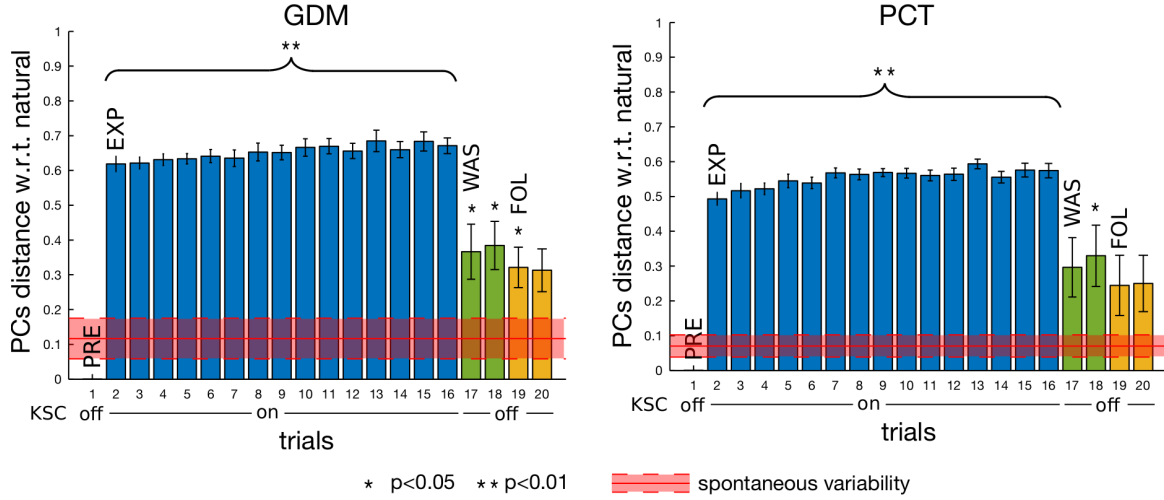


Figure 4.12: PCs distance from PRE, on ET pointing task, for the two tasks GDM and PCT. PC subspaces mean distance and standard error with respect to first repetition in PRE phase (trial 1) over the 10 participants when pointing toward ET. In red, mean values and standard deviation of spontaneous variability experiment with 5 healthy subjects of section 4.2.3. Asterisks * mean significant difference w.r.t. spontaneous variability after non parametric one-sample sign test

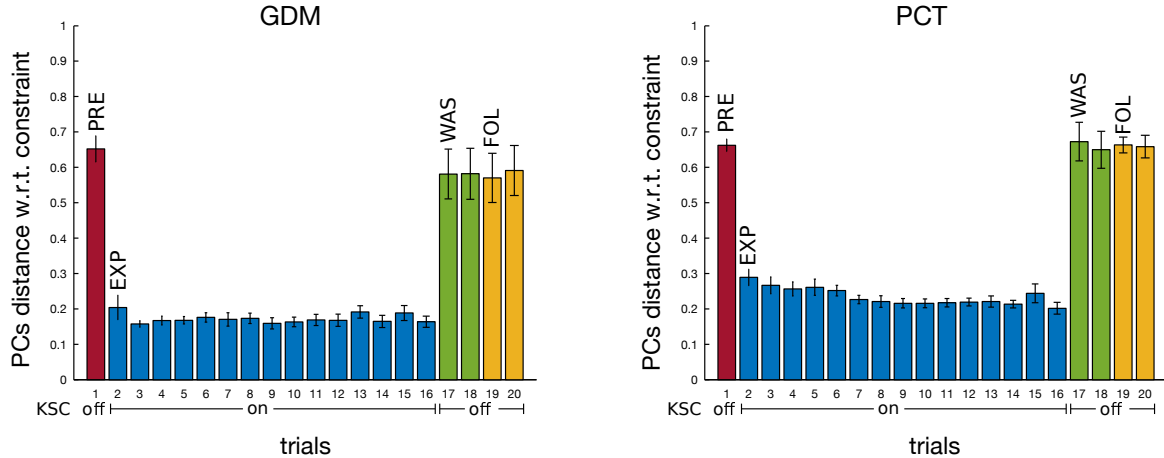


Figure 4.13: PCs distance from constraining vector, on ET pointing task, for the two tasks GDM and PCT. PC subspaces mean distance and standard error from constraining vector (equation 4.2) over the 10 subjects during pointing task towards ET.

Inter-joint coordination

PCA analysis and the above-mentioned subspace-distance based metrics were used to analyse the effect of KSC on inter-joint coordination. By construction, the KSC should increase the distance of the EXP PCs from the natural PCs (the one computed during the PRE phase) and decrease the distance from the space defined by the KSC constraining vector of equation 4.2. Figure 4.12 shows the distance between PCs subspaces from the motions in the preliminary phase, thus motions before the exposition to any force fields (the first value of the distance is null, since it represents the distance of the first synergy from itself). For the two tasks, we can clearly see the consistent effect of the presence of the KSC during the experiment phase (bars in blue). In fact these distances are large and almost constant for all the subjects in all the cases (GDM and PCT). Horizontally, in red, we plotted the value of the spontaneous variability experiment showing a visual representation of natural synergy variability of healthy humans performing pointing tasks, see section 4.2.3.

The last four bars, respectively two for WAS and two for FOL, represent the post-effects of the force fields exposition. During these phases, participants were no longer under the constraints by the KSC, but were instead performing with a gravity compensated robot, similarly to the PRE phase. Wash-out synergies, both

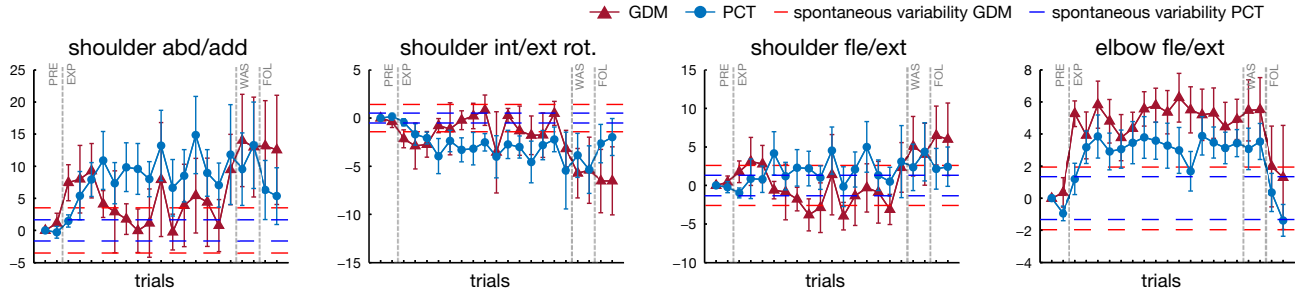


Figure 4.14: Mean joint final displacement on movement towards GT 3. Mean joint displacement and standard error with respect to final posture in PRE, in the two different modes, over the 10 subjects. The target position is GT number 3. Columns are the four joint of the exoskeleton. Horizontal dashed lines represent the joint maximum standard deviation σ for the spontaneous variability experiment.

in GDM and PCT exercises, show statistically significant difference to the spontaneous variability value (after non parametric one-sample sign test). In path-constrained tracking task, this difference is also kept during the FOL phase, meaning that a different inter-joint coordination was still present, on most of the participants, even 30 minutes after having performed the last movements under the perturbation by the KSC.

Figure 4.13 shows the distance between each PCs subspace with respect to the subspace computed from the constraining vector of equation 4.2. Mainly a small distance indicates that the subject is performing the movement following the imposed constraints, while a large distance stands for different upper-limb patterns of coordination. Therefore the KSC was able to correctly constrain the participants to perform the desired synergy (EXP phase) for each mode. On the other side, the post-effect of WAS and FOL phases does not seem to correspond to the effective constraints on the joint coordination.

4.4.3 Movements towards GT: catch-trials unexposed to KSC

Joint kinematics

Catch-trials to GT were performed with the exoskeleton in gravity compensation mode and the reaching movements towards GT targets have never been exposed to KSC-generated force fields.

Mann-Whitney U test, performed separately for the 80 cases (4 joints, 5 phases, 4 targets combinations), showed that the final angle in the different joints did not vary significantly with the mode except in 7/80 cases (3 times for joint 1, once for joint 2 and 4, and 2 times for joint 3). Friedman ANOVA, performed separately for each mode, showed that in GDM the posture for all the joints varied significantly with the target and the phase ($p < 0.05$ for joint 1, $p < 0.001$ for the other joints), while, in PCT, it varied significantly with the target and the phase for joint 1 ($p < 0.01$), joint 2-4 ($p < 0.001$), but not for joint 3.

The first joint angle (shoulder abduction/adduction) increased significantly between PRE and E-EXP for targets 1, 2, and 4 ($p < 0.05$) in GDM, and for target 3 in PCT. It remained increased, by reference to PRE, during L-EXP for target 1 in GDM ($p < 0.05$). The angle returned close to PRE values during WAS and FOL.

The second joint angle (shoulder internal/external rotation) decreased significantly in GDM between PRE and E-EXP for target 2 ($p < 0.05$), and between PRE and L-EXP for target 1 ($p < 0.05$). A decrease also appeared for target 3 during WAS and FOL by reference to PRE. There were no significant differences in PCT.

The third joint angle (shoulder flexion/extension), during GDM, was significantly decreased for target 4 between PRE and E-EXP ($p < 0.05$) and for targets 1 and 4 between PRE and L-EXP (respectively $p < 0.05$ and $p < 0.01$). It remained decreased during WAS for target 1 ($p < 0.05$). It was also increased for target 3 but not significantly due to large variability (figure 4.14).

The fourth joint angle (elbow flexion/extension) significantly increased between PRE and E-EXP (in GDM: $p < 0.05$ for target 1, $p < 0.01$ for targets 2-4, and in PCT $p < 0.05$ for targets 1, 3, 4). This deviation remained during L-EXP (in GDM for target 3, $p < 0.05$, and in PCT for targets 1, 3, $p < 0.05$ and 4, $p < 0.01$). During

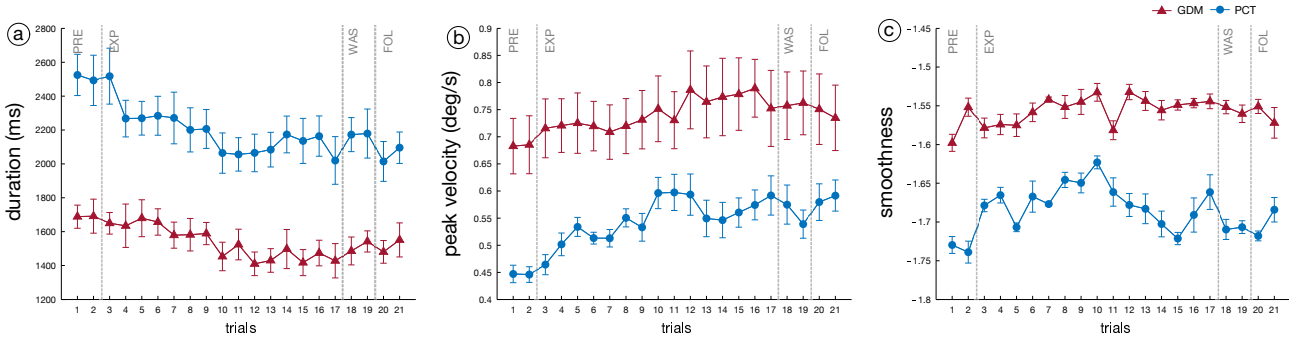


Figure 4.15: Mean motion duration T (a), mean peak velocity v_{max} (b), and mean smoothness η (c). Averaged data over the ten participants and standard error for the pointing tasks towards GT positions for the two different modes. Smoothness, through spectral arc-length, is higher when η is closer to zero.

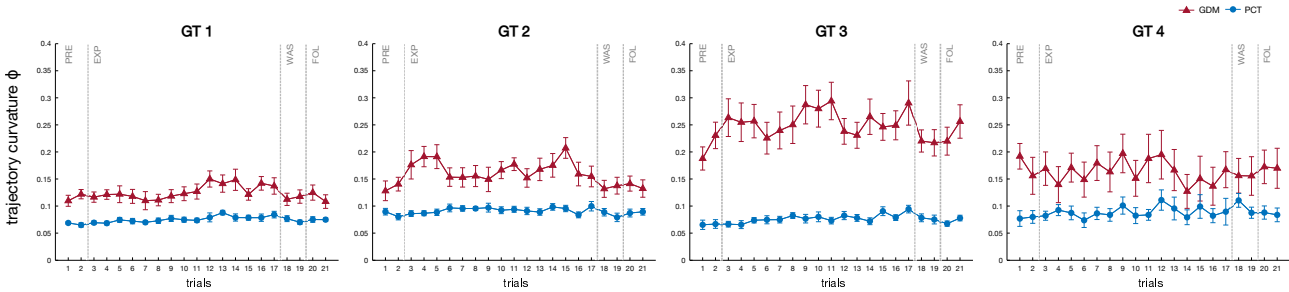


Figure 4.16: Mean trajectory curvature Φ . Mean trajectory curvature and standard error for the ten subjects, over the 4 GT positions, for the two tasks.

WAS, the increase remained significant for target 3 in GDM and for targets 1 and 3 for the PCT. During FOL, the values were not different than in PRE, except a decrease in PCT for target 2 ($p < 0.05$).

In brief, during the experimental period when the KSC was active, it also consistently modified the final posture during catch-trials to targets that have never been directly exposed to KSC, suggesting both spatial and temporal generalization of the effect of KSC. This effect depended of the target but lasted as long as the exposition to the force fields. When significant, the after-effects were characterized by the persistence of the deviation observed during the exposition to KSC.

End-point kinematics

Motion duration and peak velocity for movements toward generalization targets are shown in figure 4.15.a and 4.15.b. Mann-Whitney U test confirmed that the velocity of the movements was slower in PCT than in GDM, with a smaller velocity peak (significant in 14/15 cases for targets 1-3 and 1/5 case for the closest target 4) and a longer duration (significant in 17/20 phase-targets conditions). Friedman ANOVA, performed separately for each mode, showed that the velocity and duration varied significantly with the target and the phase ($p < 0.001$). Post-hoc paired comparison with the Wilcoxon test confirmed that the peak velocity did not change during the early exposition to KSC (no significant difference between PRE and E-EXP), but it increased progressively during exposition to KSC (significant difference between PRE and L-EXP for target 3 in GDM and targets 1, 3, and 4 in PCT). The peak velocity did not change after the removal of KSC (no significant difference between L-EXP and WAS). In PCT, the peak velocity remained higher during WAS and FOL than during PRE (significant for 4 targets).

The duration of the movement was slightly decreased at the beginning of KSC (significant difference between PRE and E-EXP for target 3 in GDM and target 2 in PCT) then decreased during exposition to KSC (significant difference between E-EXP and L-EXP for target 3 in GDM and 1, 3, 4 in PCT). The duration remained stable after the removal of KSC (no significant difference between L-EXP and WAS, nor between

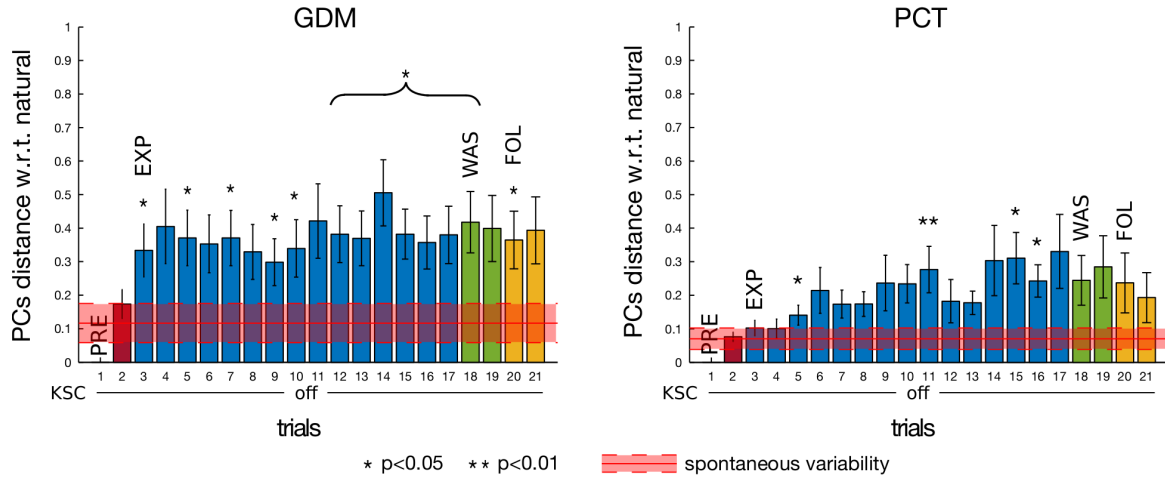


Figure 4.17: PCs distance from PRE, on GT pointing task, for the red two tasks GDM and PCT. PC subspaces mean distance and standard error with respect to first repetition in PRE phase (trial 1) over the 10 participants when pointing toward GT. In red, spontaneous variability mean values and standard deviation of spontaneous variability experiment with 5 healthy subjects of section 4.2.3. Asterisks * mean significant difference w.r.t. spontaneous variability after non parametric one-sample sign test.

L-EXP and FOL). In PCT, the duration was shorter after than before exposition to KSC (significant difference PRE-WAS and PRE-FOL for 3 targets).

As expected, the movements were less smooth in PCT than in GDM (figure 4.15.c). This was confirmed by Mann-Whitney U test: the differences were significant in 14/15 cases for targets 1, 2, 4 and 1/5 case for target 3. Friedman ANOVA showed that the smoothness varied significantly with the target and the phase in PCT ($p < 0.05$), but not in GDM. In PCT, the smoothness was improved during the period of exposition to KSC (Wilcoxon: significant difference between PRE and E-EXP for targets 1, 2 and between PRE and L-EXP for target 1).

The variation of the trajectory curvature as a function of CT target position for the different modes is shown on figure 4.16. Mann-Whitney U test confirmed that the curvature was greater in GDM than in PCT for the more distant GTs but less for the closest target 4 (significant difference in 14/15 cases for targets 1-3 and in 1/5 cases for target 4). Friedman ANOVA performed separately for each mode showed that the curvature varied significantly with the target and the phase ($p < 0.001$ in GDM, $p < 0.01$ in PCT). In GDM, the curvature increased at the beginning of the exposition to KSC (significant difference between PRE and E-EXP for targets 2, 3) and remained at the same level (no significant difference between E-EXP and L-EXP). In PCT, the curvature was significantly increased during the late period (significant difference between E-EXP and L-EXP for targets 1, 3). Then it did not change during the exposition to KSC (no significant difference between E-EXP and L-EXP, except target 4 in PCT) then regained PRE level during WAS and FOL.

Summarizing, in contrast to the direct slowing effect of the KSC, the movements performed during the catch-trials toward generalization targets had a tendency to be performed faster with an improved smoothness. This effect was progressively built up and maximized during the L-EXP period. The effect of KSC on the curvature, observed for the experimental targets, was generalized for the GT targets.

Inter-joint coordination

PCA analysis showed that the distance between spaces, defined by the 3 main PCs, during the catch-trials progressively increased with respect to the initial coordination, during the EXP phase, and it lasted afterwards, during WAS and FOL, as shown by figure 4.17. A non parametric one-sample sign test performed with respect the spontaneous variability experiment, showed that most of the resulting different synergies, above all in GDM, were statistically significant. The distance between the actual coordination and the constraining vector was not significantly modified (figure 4.18) as previously observed for the movements exposed to KSC.

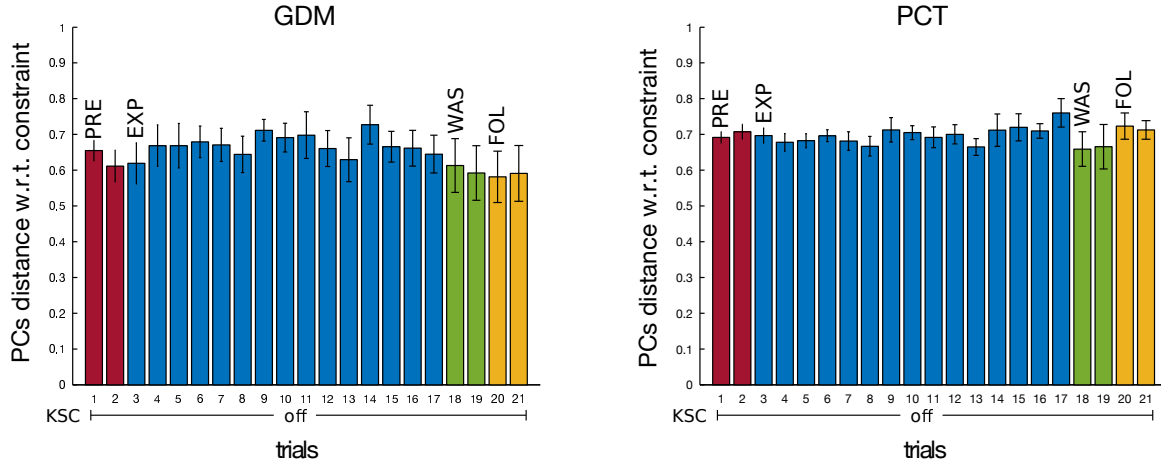


Figure 4.18: PCs distance from constraining vector, on GT pointing task, for the two tasks GDM and PCT. PC subspaces mean distance and standard error from constraining vector (equation 4.2) over the 10 subjects during pointing task towards GT.

4.5 Discussion

It is important to underline that, in the next discussion we will refer to the term *motor adaptation* as “the recovery of performance within the changed mechanical environment”, as in the original Shadmehr and Mussa-Ivaldi study [161]. On the other hand, *post-effect* will be used to analyse the motor behaviour resulting at the end of the perturbations caused by the force fields.

4.5.1 Adapting to new upper-limb synergies

Results overview Twenty participants of our experiment performed a total of 404 pointing/tracking tasks, 240 of which under the effect of inter-joint corrective viscous force fields. Subjects were all healthy, naive, without any known pathology to the upper-limb.

The peculiarity of our experimental protocol allowed us to analyse different aspects of learning. First, we were able to study the direct effect of the presence of multiple viscous force fields, perturbing the arm kinematics at the joint level and therefore at the end-point. Second, we analysed human adaptation to the KSC correction, looking for progressive decrease of the perturbations during the force fields exposition (experimental phase of the practice). Third, we evaluated the presence of post-effects when, at the end of the experimental phase, the force fields were removed. Fourth, finally, thanks to the subgroup of targets GT, which were never exposed to any fields, we observed temporal and spatial generalization of the imposed upper-limb coordination.

The results showed that most of the subjects could learn from this unknown and unnatural environment, meaning that their natural upper-limb coordination was exhibiting effects of the force fields exposition in terms of adaptation, post-effects, and generalization. The presence of after-effects was still observable after 30 minutes from the last constrained movements, during which time subjects were detached from the exoskeleton and rested. These results extended the conclusions found on experiments with planar robots [161] or, preliminary, with an exoskeleton [121].

Poor adaptation during the exposition We observed adaptation to the original coordination, during late-EXP phase, meaning a reduction of the effect of the perturbation induced by the fields, only on 21% of the testing population. In most of the subjects, we did not observe changes neither in their coordination, nor at the end-effector kinematics, between E-EXP and L-EXP, *i.e.* they did not adapt by compensating for the external perturbation, as usual in state of the art experiments with planar robot. The absence of joint space adaptation was observed also in the results by Mistry *et al.* [121], but differently from their experiment, since in our case no adaptation of the end-point movements occurred.

Post-effects: two observable distinct behaviours At the same time, distinct post-effects were observed after the removal of the KSC: they consisted, in some cases (30%), in over-shoot on the opposite direction of the natural original coordination – thus similarly to Shadmehr and Mussa-Ivaldi original experiment, but at the joint level, rather than at the end-effector – but the main pattern (55%) consisted of a persistence of the perturbation during the wash-out and even the follow up period. This persistence of the perturbation could be the direct consequence of the CNS not globally optimizing the motor behaviour, but rather tending to repeat suboptimal task-satisfying solutions, because of influenced by motor memory, as described by Ganesh et al. [57]. In the remaining 15% of the movements, we did not observe any post-effect.

Different dynamics, similar results: comparing the two testing modes When considering the constraint of following a path with the end-effector (thus in PCT), PCA results – meaning the existence of larger PCs deviation from the preliminary motion with respect to the spontaneous variability experiment – are weaker than in GDM, but we can still see, almost always, persistent post-effects in movements towards both ET and GT. At the same time, during wash-out and follow up phases, in both cases most of the participants produced an upper-limb coordination strategy modified with respect to their natural preliminary one (respectively 63% persistent perturbation and 29% over-shoot in GDM, versus 48% and 33% in PCT). These results are interesting considering the different dynamics of the two tasks (PCT generally required slower movements and longer duration). Indeed generally GDM task corresponded to ballistic movements, thus probably mostly driven by feedforward control and offline adaptation, while PCT requested stronger visual feedback to correct online the trajectory, as demonstrated by longer duration, slower velocity, and poorer smoothness.

4.5.2 Application to rehabilitation / Limits

Differences from existing studies A clear difference from Shadmehr and Mussa-Ivaldi original experiments and most of the results described in the introduction of this chapter of the thesis, is linked to the nature of the requested task to the participants. In fact, while in 2D experiments, participants were asked to perform point-to-point reaching task, thus explicitly requiring to contrast the deviating force fields, in our experiment we never asked the participants to follow any specific behaviour in terms of coordination. Thus, subjects were voluntarily deciding to resist the effects of the robot, to follow the constraints imposed by the KSC, or, of course, any possible strategy in between. Additionally, in 2D experiments, the perturbations were applied in the task space, as velocity dependant fields on the end-effector, whilst in this case, applying the velocity dependant force fields at the joint space, the subjects were implicitly constrained while moving and while being focused on the reaching tasks.

Ability to impose a specific synergy The main purpose of utilizing a KSC-like strategy with post-stroke patients would be the possibility for the exoskeleton to teach a healthy natural upper-limb coordination, in order to correct common negative and pathological compensations in impaired subjects. Our results did not perform as expected, since after the KSC practice, we did not observe the desired coordination imposed by the force fields. This result, observable in the distance from the constraints of graph 4.13 and 4.18, could be related to the only dissipative nature of the version of the kinematic synergy controlled that we adopted for this experiment. The original KSC [28] presents also a non-dissipative viscous torque, developed to avoid energy waste by the exoskeleton and to encourage motions which satisfy the desired constraints. In the future we will need to verify if, by adding this assistive term to the control law, we could obtain better performance on the post-practice resulting coordination. Furthermore, it is reasonable to consider that imposing and retaining a non-optimal synergy in healthy subjects is highly challenging. Probably the effects of the exposition to the natural correction by the exoskeleton would achieve better outcomes when modifying impaired pathological synergies in post-stroke survivors.

Subjects awareness We observed learning in participants who were not aware – at least at the beginning of the training – of the effects of the control law imposed by the exoskeleton, who were only told to focus on the achievement of the task (pushing the button) rather than on the performance of the motion itself (*i.e.* the inter-joint coordination). The idea of *implicit learning* of motor control was already analysed by Patton *et al.* [131] in an experiment with a planar robot, observing a detectable reduction in the washout of the after-effects. Indeed, this phenomenon of long lasting effects seems confirmed in our case. This “unawareness” of the participants could have also interesting application for neurorehabilitation: we can imagine to train patients on rehabilitative exercises for the upper-limb inter-joint coordination while asking them to play video games, involving end-effector movements, on ad-hoc virtual environments. Post-stroke participants could then focus their attention only on the video games controlled by the end-effector, rather than being involved in performing particular upper-limb motions and therefore being forced to consider multiple goals for the movement of the joints of the arm. Meanwhile the exoskeleton could impose healthy rehabilitative constraints at the joints of the arm, decreasing the cognitive load on the impaired subjects. Moreover, computing performances for inter-joint coordination could be more complex to judge and qualify in order to produce the rewards-metric, mostly due to the human upper-limb redundancy. Thus considering the feedback to the user from the end-point only, while leaving the robot taking care of the correct joint synergy, could simplify the overall rehabilitative therapy.

Behind no-adaptation and distinct post-effects An important inter-individual difference was observed, both at the level of presence of adaptation during the exposition, and at the level of consequent post-effects. At the same time, a smaller but not negligible variability within subjects of these parameters was also found. Personal participants data as weight, height, and grasp force were collected and correlations analysis were performed between these data and the results of the experiment. Learning generally happened when subjects were stronger, taller, heavier, and moving faster, but the difference between any two groups of participants (by either defining the group in which we observed post-effects, and the one in which these effects did not happen, or by taking the group which adapted versus the one which did not adapt, or again, the group which resulted in persistent perturbation versus the one which resulted in over-shoot) were not statistically significant for any of these parameters. The fact that our exoskeleton has fixed-length joint, thus not adjustable to the user physical characteristics, and that the distance between the exoskeleton and the WAM manipulator was not changed with respect to the different height of the participants, may have affected the results.

4.5.3 Assessing learning effects with an exoskeleton

A central issue for this experiment was clearly the definition of parameters to assess adaptation, post-effects and generalization occurring during the robotic-aided training. Most of the usual adopted indexes to qualify the presence of these phenomena – in literature it is often shown a sufficient number of kinematic parameters as joint trajectory, end-point trajectory, speed profiles of one or more representative subjects – have been mostly developed for analysing 2D tasks, for which the requested behaviour of the participants was clear (point-to-point movements by following a straight-line). We believe that utilizing PCA analysis helped us to quantify phenomena happening during the motion and not only resulting in different configuration at the end of the movements. However the PCs distance metric was often not sufficient to describe the adaptation: for example, being an unsigned index, it could not discern the observable different post-effects of section 4.4.1. Cycloids seemed to be a fine tool when compared to PCs distance, but their computation produced complex reports to analyse (six cycloids per motion for a 4-DOF robot as ABLE).

4.6 Transferring of post-effects outside the robot

Given these promising results, an interesting investigation should be performed on the effects on the participants when the upper-limb is detached from the robotic exoskeleton. Could we still observe any effect on their arm synergy with respect to their natural unperturbed strategy before the experiment? This fundamental question



Figure 4.19: Setup of the transferring experiment with the Codamotion system. The seven markers are circled in orange (1 on the end-point of the plastic rod, 1 on the hand, 1 on the forearm, 1 on the upper-arm, 1 on each shoulder, and 1 on the trunk. On the left two of the three cameras of the Codamotion (the third is hidden on the right of the photo).

affects directly the transferring to ADLs, outside the clinical environment and without the assistance of the robot, and thus deeply concerns corrective strategies potentiality on the rehabilitation efficacy. In fact, due to the

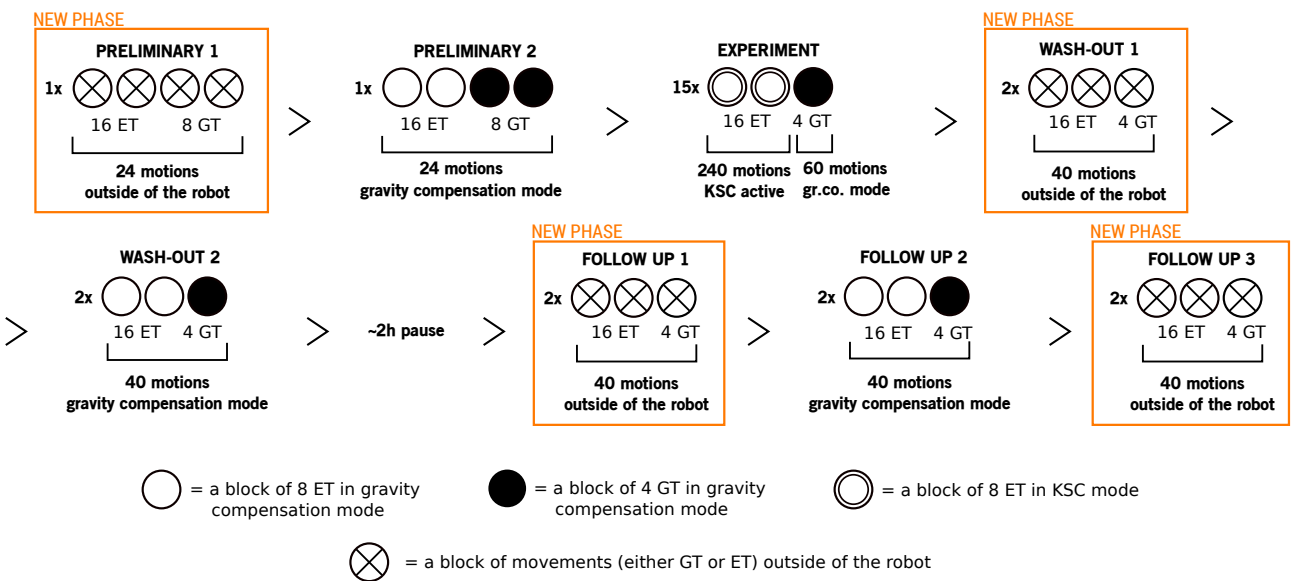


Figure 4.20: Phases of the transferring experiment with the Codamotion system. To the original phases, four intermediate phases, consisting of movements outside of the robot, were added.

internal model hypothesis, the two different contexts (being or not in physical interaction with the exoskeleton) would rely on different internal models: this fact could limit the effects of the exposition to the robot constraints on the movements performed outside of the exoskeleton, reducing the robot-led therapy efficacy.

For this reason, we preliminary tested potential generalizations and post-effects outside of the robot, by performing the same experimental protocol with a naive subject. We used a camera-based motion capture system (the Codamotion, © Charnwood Dynamics Ltd.) that uses infra-red cameras to locate infra-red emitting markers, placed on the participant; 3 cameras were used in the setup and 7 markers were placed on the subject's body, as depicted in figure 4.19. The motion capture system acquisition frequency was 100Hz. We asked the participant to replicate the same exercise as in the goal-directed mode, moving from a given external start-

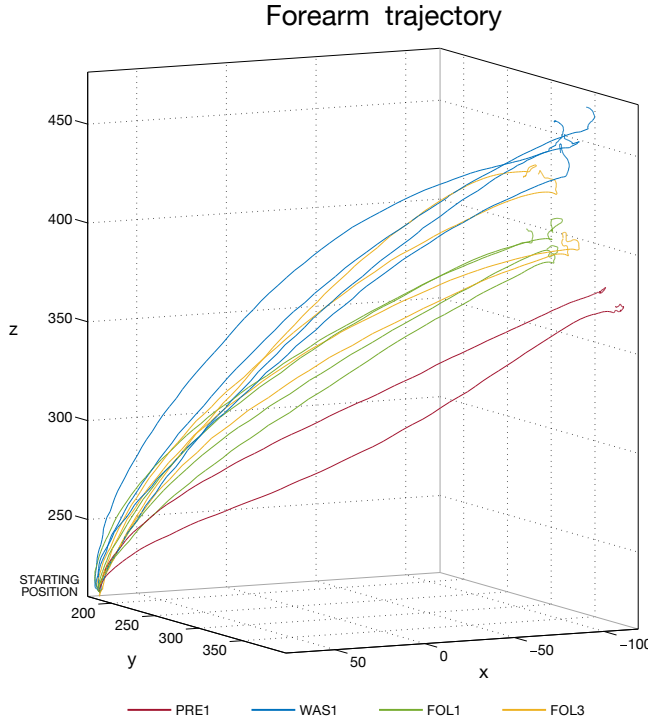


Figure 4.21: 3D view of the movements of a point of the forearm, recorded through the MOCAP system. The target shown is experimental 4 (ET4). Values are in mm. The marker was placed on the forearm of the participant. The axes are coincident with the one of figure 4.19.

ing position (indicated by a wood stick placed vertically on the floor) to reach the push-button on the WAM. Concerning the experimental protocol and the data processing, we kept the same structure described in section 4.2.2. The only relevant difference between the two experiments, consisted in the presence of four intermediate phases, with respect to the pattern of figure 4.6, in which the participant was asked to perform the pointing exercise, but detached from the exoskeleton, thus without any possible effects due to the robotic device presence. Therefore, in these intermediate phases, the motion capture system recorded the subject movements. The new pattern of phases is shown in figure 4.20.

In the following results section, we show the movements towards an experimental target (in particular the ET4): due to the nature of the constraining vector of equation 4.2, the effect of the movements towards this particular target were evident in the previous work. Nonetheless, at the end of the section, we also show how similar effects were observed on the entire set of experimental targets. The graphs present movements only performed outside of the exoskeleton, thus in a unperturbed, unconstrained, natural context for the participant. These movements are shown in figure 4.21 (3D view of the movements) and figure 4.22 (the same movements, projected in the three different 2D planes xy , xz , and yz), for marker number 3 (the one placed on the participant's forearm).

The result of this generalization experiment seems promising. Indeed, it is possible to observe different phenomena, occurring at the successive phases of repetition of the exercise. In particular:

- An important modification of the motion trajectories occurred generally among the phases but largely during the wash-out: here the trajectories were strongly modified by the exposition to the KSC force fields (up to a maximum deviation of about 15cm of the elbow position along the z -axis), even if the robot perturbation was null at that time.
- By looking at the trajectories performed during the first follow up (thus about 2 hours after the exposition and before being reattached to the exoskeleton), even if they converged back towards the original preliminary shape – thus showing the process of recovery of the natural inter-joint coordination – still, it

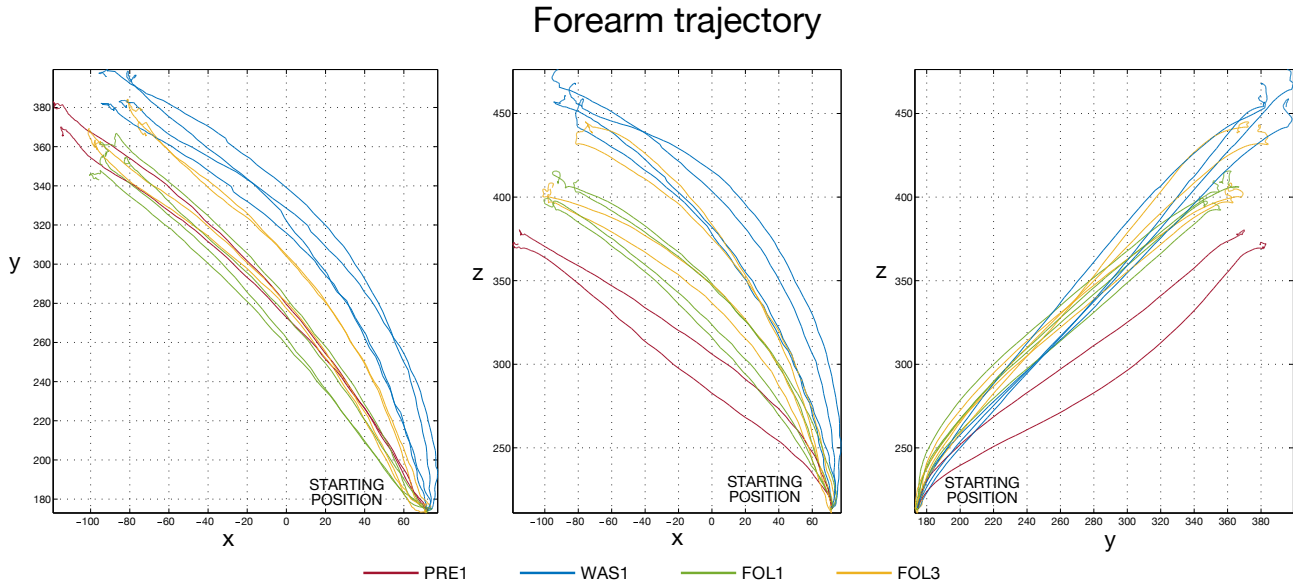


Figure 4.22: 2D views of the movements, recorded through the MOCAP system. From left to right, respectively planes xy , xz , and yz . The target shown is experimental 4 (ET4). Values are in mm. The marker was placed on the forearm of the participant. The axes are coincident with the one of figure 4.19.

is possible to observe non-negligible deviations of the elbow position, for a maximum of about 7cm on the z -axis from the trajectory performed in the preliminary phase.

- An interesting phenomenon is observable in the final repetition – the third follow up – just after having performed a classical follow up pointing exercise within the exoskeleton (not applying any constraint). Indeed, having the participant reattached to the ABLE exoskeleton for a short period of time and detached again, caused an important deviation of the forearm trajectories – maximum deviation of the elbow position along the z -axis of more than 5cm with respect to the last movement in the first follow up outside of the robot – which could be the results of motor memory due to the re-exposition to the presence of the gravity-compensated exoskeleton.

Therefore, although preliminary, the results show 1) a process of transfer to movements without the robot (*i.e.* in a different context), and 2) an access to motor memory. The 2D planes of figure 4.22 confirm that the KSC correction was mainly affecting the elbow elevation, thus along the z -axis, as an expected consequence of the chosen constraining vector for the KSC controller.

Considering the same movements but different body parts, figure 4.23 shows the trajectories for marker 1 (end-point of the plastic rod) and for marker 4 (upper-arm of the participant). The upper-arm follows the same general analysis of the forearm one, confirming the interesting preliminary results on the modification of the inter-joint coordination (in particular the elbow elevation while pointing at the target). On the contrary, for the movements of the end-point, the paths were not largely affected by the exposition to the KSC fields (maximum deviation always less than 5cm on the z -axis). This is a direct consequence of the redundancy of the system with respect to the task and of the paradigm behind this controller, which affects as much as possible the upper-limb inter-joint coordination, without deeply impacting the end-effector movements. The same result, but extended to all the other experimental targets, is presented in figure 4.24, which represents the mean final elevation, thus the final position along the z -axis, for the 8 experimental targets, along with the relative standard error, respectively for the end-point and for the upper-arm. This graphs generalizes the former analysis performed on the ET4 to the other targets, underlying the efficacy of the KSC approach to movements even outside of the robotic device. Moreover, we can again observe the role of motor memory by looking at the increase of elevation during the third follow up phase, for the upper-arm.

The last result of this experiment is shown in figure 4.25. We performed principal component analysis on the

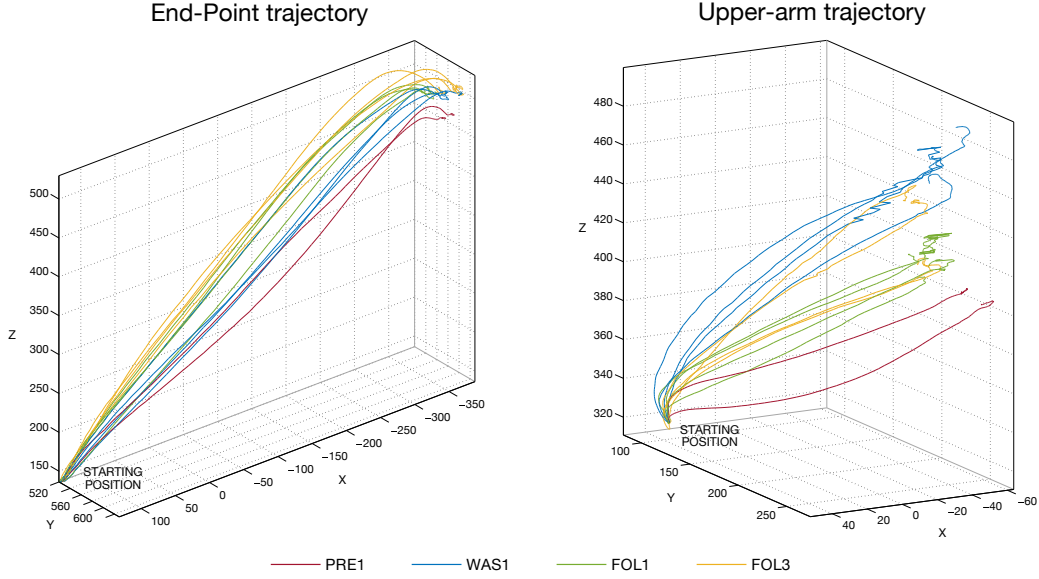


Figure 4.23: 3D views of the movements, recorded through the MOCAP system. From left to right, respectively movements of marker 1 (end-point of the plastic rod) and marker 4 (upper-arm of the participant). The target shown is experimental 4 (ET4). Values are in mm. The axes are coincident with the one of figure 4.19.

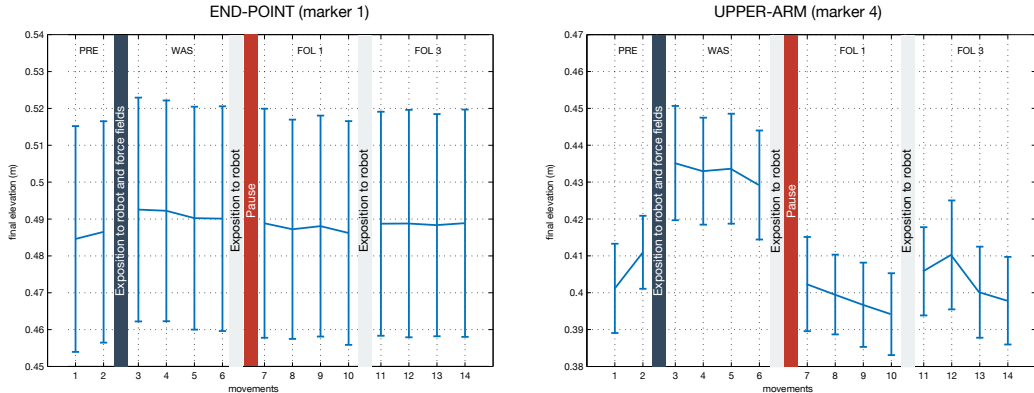


Figure 4.24: Mean final position along the z-axis and standard error, over the 8ET. Final elevation, averaged over the 8ET, respectively for marker 1 (end-point of the plastic rod) and marker 4 (upper-arm of the participant). Values are in m.

movements outside of the robot, thus using the data obtained through the motion capture system. Successively, by following the subspace distance metrics of equation 4.5, we calculated the distance between the preliminary inter-joint coordination (the subject natural one, before being attached to the exoskeleton) and the other ones, evaluated after the exposition to the fields, but always measured outside of the robotic arm. This bar plot confirms how the inter-joint coordination was modified, when detaching the participant from the exoskeleton, by showing an increased distance from the natural coordination, larger than the reference of the spontaneous variability (recorded and computed within the exoskeleton, thus larger than the healthy synergy variability performing pointing task in the free space, with no constraints). As expected, this modified coordination washed out in the first follow up; however the effect of the perturbation significantly reappeared in the second follow up, as said before, probably as a consequence of the motor memory activated by the second exposition to the robotic device (even if it was not applying any constraint).

Although very preliminary, these are the first results of transfer of motor adaptation outside of a controlled environment, after being exposed to distributed corrective force fields produced by an exoskeleton. The shown behaviour appeared on all the targets, both the experimental one (*i.e.* the one on which there has been a training phase with the presence of the force fields) and the generalization one (the target never exposed to any

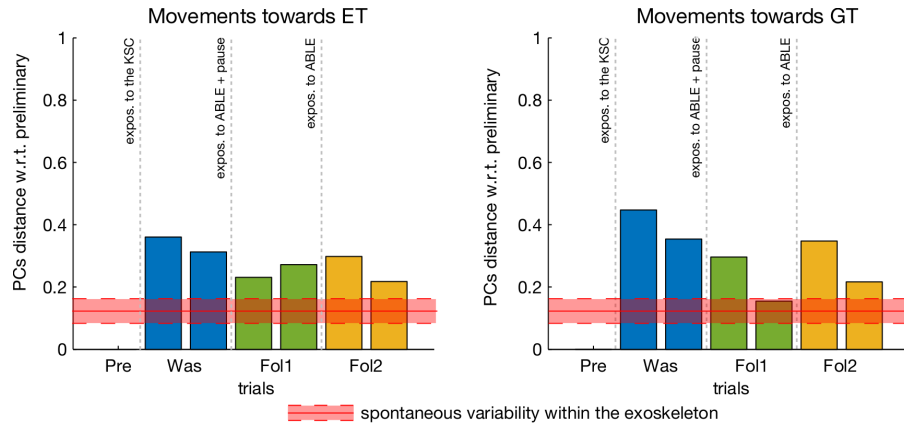


Figure 4.25: PCs distance with respect to the coordination in the preliminary phase. On the left, PCA on movements towards experimental targets, on the right, towards generalization targets. The principal component analysis was performed only on the movements outside of the robot. In red, the spontaneous variability measure from the former KSC experiment.

constraint). Clearly, the preliminary nature of the study, which above all concerned only one subject, does not allow to derive any conclusion. However, if the results were confirmed in the future, they could be fundamental to rehabilitation robotics and could open new opportunities for using exoskeletons for neurorehabilitation.

4.7 Conclusions and perspectives

By using a 4-DOF robotic exoskeleton, we were able to modify more than to teach new upper-limb synergies on twenty healthy subjects, performing pointing and tracking tasks. The peculiarity of our experimental protocol allowed us to observe and analyse different effects of learning – *adaptation* to force field, presence of post-effects, and *generalization* of the adaptation – separately on two sets of pointing targets. Although adaptation (during the exposition to the force fields) did not occur in the majority of the cases, the presence of different after-effects was persistent and observable even after 30 minutes from the last constrained movements, which represents a new result with respect to classical motor adaptation experiments with robots.

One reason of this long lasting effects could be linked to the unexplicit nature of the constraints imposed by the exoskeleton and consequently a decreased involvement of the participants in the process of synergy modification. This result, if confirmed, could have interesting effects on the rehabilitation of post-stroke patients and the creation of intensive therapy. Unfortunately, the chosen number of repetitions for observing a complete wash-out was not always sufficient, thus, in future, an effort will be done to study the effective duration of these effects.

An interesting but preliminary investigation was also performed on the effects on the participants when the upper-limb was detached from the robotic exoskeleton. This is a fundamental issue which affects directly the transfer of robot-led therapy to ADLs outside the clinical environment and without the assistance of the robot, and thus deeply concerns corrective strategies potentiality on the rehabilitation efficacy. We observed the possibility to modify the upper-limb coordination even on movements outside of the robotic device, providing a new and promising result for rehabilitation robotics with exoskeletons. Data from this investigation were obtained by using an external motion capture system and the study was performed on a single healthy participant. Clearly, although very promising, these results necessitate deeper analysis, confirmed on a larger population and tested while performing different tasks. Above all, a similar approach must be carried out to study the potential effects on a group of impaired patients, in order to provide conclusions on the therapy.

Many questions are still unanswered, above all concerning the subset of participants who did not adapt and did show post-effects during the training with the exoskeleton, and the presence of two distinct adaptive behaviours, not necessarily correlated with any measurement performed or with the requested tasks. Additionally, one of this two behaviours seems not to follow the well-established internal model hypothesis, due to the

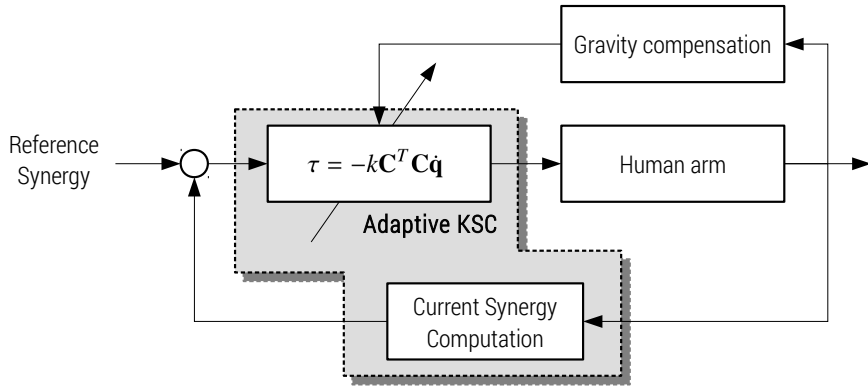


Figure 4.26: The Adaptive KSC control scheme Possible future implementation of an adaptive corrective strategy for the ABLE exoskeleton.

absence of over-shoot in the post-effects phase, and we will need to investigate if they could follow other recent paradigms (as for example the *use-dependent learning* [40] or the *model-free learning* [71]). In particular, the use-dependent learning is the idea of a secondary mechanism of learning, with respect to the classical error-based paradigm, leading to persistent behavioural changes induced through simple repetition of movements in the absence of systematic errors. These changes are obviously allowed when the perturbations are applied along redundant dimensions of the movements, that is, without preventing successful task performance. Model-free learning, instead, is a third alternative model of human learning related to a slow mechanism of adaptation which relies only on the degree of success of a movement and not on the directionality or magnitude of errors. Therefore it is a learning mechanism driven directly by reinforcement of successful actions, without update of an internal model. Clearly, all these theories have to be considered as complementary rather than in contrast to describe the complexity of the architecture of learning of the human CNS.

In the future, we could verify the reaction of the participants when testing the same protocol on multiple sessions, during successive days, to understand if possibly the post-effects are reinforced and/or anticipated in order to provide a better insight on the property of the human CNS and the role of motor memory, as preliminary observed in section 4.6.

Moreover, it could be interesting to adopt different techniques to analyse the experimental data, in order to better characterize the obtained results. For example, an interesting study would be the use of the *uncontrolled manifolds* principle, as made by Scholz *et al.* in [159], which could give better insights on the role of inter-joint synergies and determine relevant task variables.

Concerning the observed inter-individual variability and the absence of effects in few participants, one hypothesis could arise about the magnitude of the distributed force fields, which was constant among subjects, and therefore could have been not enough for some of them to be noticed, to generate a reaction and thus an adaptation to the perturbation. One possibility, which will be studied in the near future, is then the development of an adaptive corrective approach, *i.e.* an Adaptive KSC. A scheme of this approach is depicted in figure 4.26. This new solution should modify the magnitude of the corrective constraints accordingly to the resulting inter-joint coordination, following therefore the same paradigm of the adaptive control of chapter 3. In particular, the gain k of equation 4.1 would be the adaptive parameter to account for the differences among participants reactions and the discrepancy between the desired synergy and the current one, parameters which are not adjusted by the current control architecture. By increasing or decreasing the strength of the applied corrective force fields, it would be possible to obtain a more customized controller, which could stimulate more efficaciously the adaptation of the participants to the constraints and generally better perform with respect to the original KSC.

Chapter 5

Conclusions and perspectives

Despite the large number of robotic exoskeletons for neurorehabilitation and the potentialities of this technology, modern robotics has not yet pushed further the achievements reached by the standard therapy. We hypothesize that a fundamental property which could improve exoskeletons results would be the use of adaptive techniques in order to maximize the subject involvement, to evolve the therapy with the patient recovery, and to challenge the patient current physical capabilities. These actions are naturally performed by any physiotherapist, when leading the rehabilitation. However, if correctly implemented on modern exoskeletons, adaptation could exploit the large amount of data feedback that these devices can measure throughout the training, to produce a finer control of the recovery process.

For this reason we studied the simultaneous adaptation occurring when a subject performs any action within a robotic exoskeleton, *i.e.* the adaptation of the human motor control to the new environment and to the presence of the robot control action, and the possible concurrent adaptation of the robotic assistance to the human behaviour and performance.

We developed a new adaptive control strategy, which shapes the robotic assistance, and in particular the exoskeleton compliance, based on the motor performance of the human subject, on a trial-by-trial basis. This strategy has in its simplicity a fundamental property: the same paradigm could indeed be applied to most of the existing non-adaptive solutions currently implemented on rehabilitation exoskeletons. This controller was then preliminary tested on healthy subjects, showing the feasibility of the paradigm and its capability to react to different human motor dynamics. Furthermore, we tested different approaches to guide the robotic adaptation, by comparing multiple error signals to feedback and compute the human operator performance. The results of this analysis showed interesting characteristics for each strategy, suggesting distinctive use depending on the patient recovery stage. Future works will certainly concern the possibility to test this controller on patients with sensorimotor impairments, as post-stroke survivors, within a clinical environment, in order to analyse the adaptability to the motor peculiarities of these impaired subjects and the potential benefits of using this approach in a context of neurorehabilitation.

In parallel, we were interested in studying the human adaptation to distributed force fields, acting at the joint level, as in the case of interaction with a robotic exoskeleton. We observed, analysed, and, for the first time quantified the effects of the prolonged exposition to corrective distributed force fields, at the joint level, in particular by showing their post-effects and the results of the generalization, both spatial and temporal. For this experiment we engaged more than 20 healthy people, obtaining an interesting inter-individual variability, which still leaves many open fundamental questions on the underlying phenomenon of motor adaptation and learning. Additionally, we were also able to preliminary observe the motor control adaptation even outside of the robotic device, obtaining a very promising result for rehabilitation and the applicability of robotic exoskeleton-led therapy. However, even in this case (the general case study of human adaptation to the robot action), we will still need to confirm our results by testing the experimental setup with impaired subjects, since all our analysis were carried out exclusively by working with healthy participants.

We are currently working with the rehabilitation department of the *Hôpital Universitaire Pitié-Salpêtrière*,

in Paris, in order to program preliminary experiments on stroke survivors, in order to test the applicability of the adaptive paradigm in a real clinical environment, and to study the possibility to modify the upper-limb inter-joint coordination even in impaired subjects.

The perspective of this work of thesis, centred on the study of the mutual adaptation when physical human-robot interaction occurs, is therefore the development of an innovative control strategy for rehabilitation robotics, especially for multi-DOF exoskeletons, able to address the inter-joint coordination issue, to adapt to the current stage of recovery of the patients, personalized to their real abilities, and capable of truly exploiting the huge amount of collectable data that modern devices can produce.

Appendix A

Elements of Anatomy

A simplified overview of the anatomy of human upper limb is provided in this appendix in order to facilitate the understanding of the thesis work.

The human *upper limb* or *upper extremity* is the part of the human body extending from the deltoid region to the hand, figure A.1. It includes, respectively from the deltoid region to the hand, the shoulder (girdle and joint), the arm, the forearm, the wrist, and the hand.

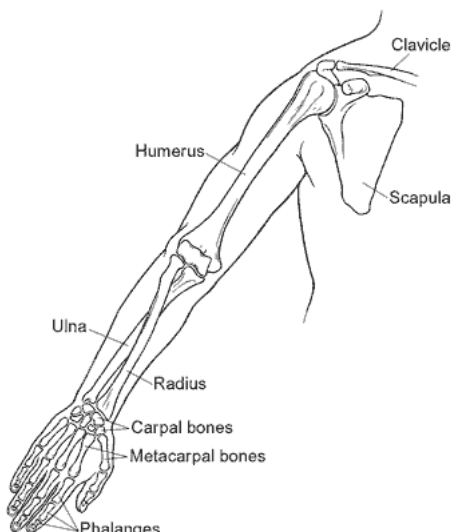


Figure A.1: Principal bones of the human arm.

- The **shoulder girdle** or *pectoral girdle*, composed of the clavicle and the scapula, connects the upper limb to the axial skeleton through the sternoclavicular joint (the only joint in the upper limb that directly articulates with the trunk), a ball and socket joint supported by the subclavius muscle which acts as a dynamic ligament. The girdle is supported by a large number of muscles, among which the trapezius, the sternocleidomastoideus, the pectoralis minor, the two rhomboideus, and the muscles of the scapula. The girdle provides 3-DOF to the upper limb, in particular those motions related to the scapula elevation/depression, retraction/protraction (also known as adduction/abduction), and the upward/downward rotation, see figure A.2.
- The *glenohumeral* joint (colloquially called the **shoulder**) is the highly mobile ball and socket joint between the glenoid cavity of the scapula and the head of the humerus. Lacking the passive stabilisation offered by ligaments in other joints, the glenohumeral joint is actively stabilised by the rotator cuff, a

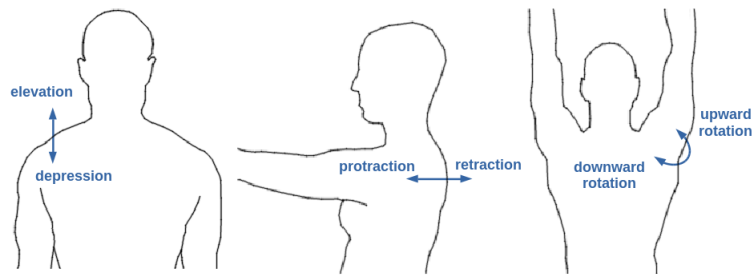


Figure A.2: Shoulder girdle degrees of freedom. Scapula elevation/depression, scapula protraction/retraction, and girdle upward/downward rotation.

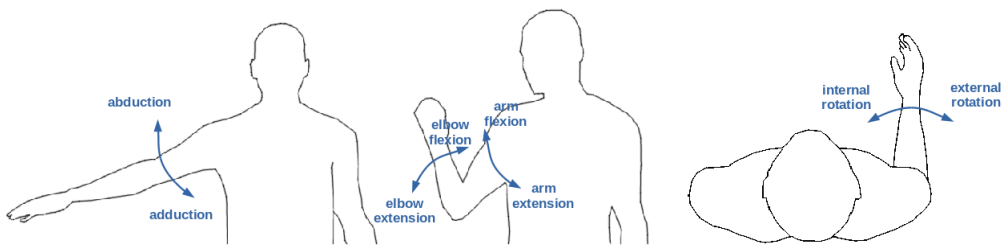
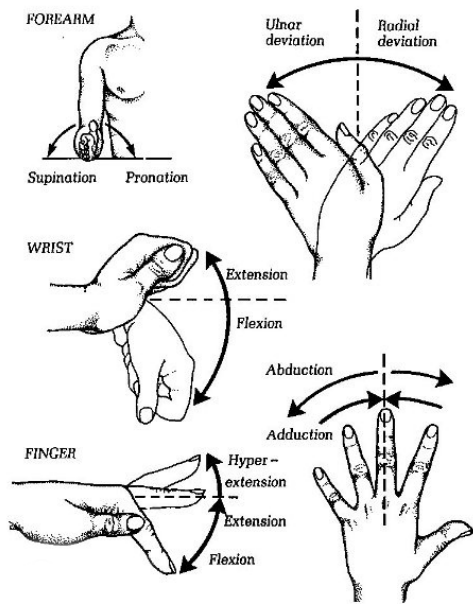


Figure A.3: Shoulder joint and arm movements. Shoulder abduction/adduction, shoulder internal/external rotation, shoulder flexion/extension, and elbow flexion/extension.

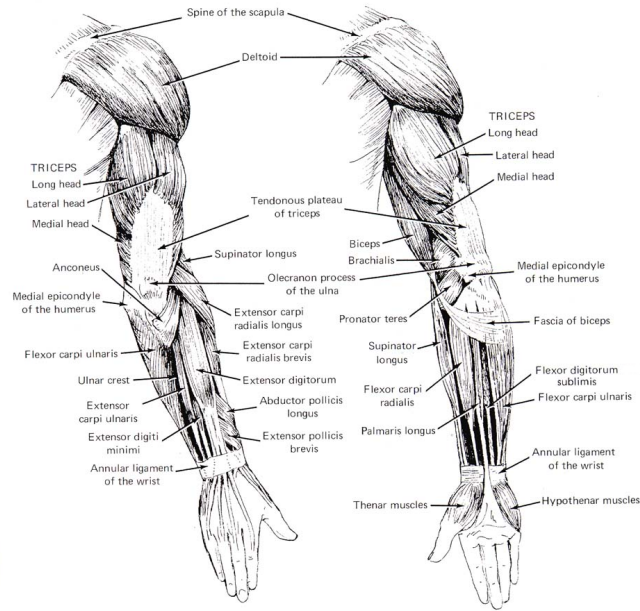
group of short muscles stretching from the scapula to the humerus. Among the muscles of interest for this joint, we can cite the supraspinatus, the infraspinatus, the deltoideus, and the pectoralis major. The glenohumeral joint provides other 3-DOF to the human limb: shoulder abduction/adduction, flexion/extension, and internal/external rotation, see figure A.3.

- The **arm**, sometimes called the *upper arm*, the region between the shoulder and the elbow, is composed of the humerus with the elbow joint at its distal end. Biceps and triceps are the main muscles involved in producing 1-DOF motion: the elbow flexion/extension.
- The **forearm** is composed of the radius and ulna: the latter is the main distal part of the elbow joint, while the former composes the main proximal part of the wrist joint. The most of the muscles in the forearm are used to control the motion of wrist, hand and fingers. We can consider the forearm controlling the rotation/pronosupination of the wrist, see figure A.4(a).
- The **wrist** is a 2-DOF (3-DOF taking into account the pronosupination) joint, made of the carpal bones and connecting the hand to the upper limb. Many muscles are involved in controlling and moving the wrist, and it is quite complex to describe. The 2-DOF produced are the wrist flexion/extension and the ulna/radial deviation, figure A.4(a).
- Finally, the **hand** is composed of 5 classes of bones (carpals, metacarpals, proximal phalanges, intermediate phalanges, and distal phalanges) for a total of 27 bones, not including the sesamoid bone, the number of which varies between people. In the hand there are a total of 34 muscles which move the fingers and thumb: 17 are in the palm of the hand, and the remaining 18 in the forearm. An interesting fact about the human hand is that about a quarter of the motor cortex in the human brain is devoted to the muscles of the hands. The human hand has 21 degrees of freedom: 4 in each finger, 3 for extension and flexion and one for abduction/adduction; the thumb is more complicated and has 5-DOF. For a reference of the hand movements, see figure A.4(a).

Wrapping up, not considering the hand, the human upper limb is a 10-DOF system, usually divided into the 3-DOF of the scapula and the 7-DOF of the arm. A trivial consequence is the redundancy of our arm to carry out



(a) Forearm, wrist, and hand movements



(b) Muscles of the human arm

Figure A.4: Wrist movements and arm muscles.

most of the tasks in the 3D space (for example, all the pointing tasks require 3-DOF, 6 if we consider also the orientation of the finger), meaning that we can achieve the same task by adopting different arm configurations or poses, by exploiting the so-called *self-motion*, motions which involve the unconstrained DOFs. The exact number of muscles is difficult to determine, but we can consider about 23 teamed muscle groups controlling the whole upper limb, excluding the hand. Some of these muscles are shown in figure A.4(b).

Appendix B

The Kinematic Synergy Control

The Kinematic Synergy Control is a controller, developed by Crocher *et. al* [29], which aimed at affecting the natural synergy of the human arm. Given the number of available joints n and the number of degrees of freedom required to achieve the task m , this controller worked when $n > m$, that is in the case of redundancy, by imposing $l \leq n - m$ scalar constraints to the robot joint velocity vector $\dot{q} \in R^n$. More precisely, the different constraints are defined as a set of C^1 scalar constraints $f_i(\dot{q}) = 0$ that can be grouped in a vector function $\mathbf{F} : R^n \rightarrow R^l$:

$$\mathbf{F}(\dot{q}) = \begin{bmatrix} f_1(\dot{q}) \\ \vdots \\ f_i(\dot{q}) \\ \vdots \\ f_l(\dot{q}) \end{bmatrix} = 0.$$

The controller is a reactive controller, working without any *a priori* knowledge on the motion intended by the patient. It has the form of a viscous impedance control law

$$\tau = -\mathbf{K}\dot{q}$$

where $\mathbf{K} \in R^{n \times n}$ is a viscosity matrix, not necessarily constant nor diagonal. Assuming the exoskeleton moved by the subject, if $\mathbf{F}(\dot{q}) = 0$ the resistive torque should be null, because the subject's motion satisfies the constraints. In any other case the velocity should be corrected. Namely, the velocity correction $\delta\dot{q}$ is such that

$$\mathbf{F}(\dot{q} + \delta\dot{q}) = 0. \quad (\text{B.1})$$

Considering small correction we obtain

$$\mathbf{F}(\dot{q} + \delta\dot{q}) - \mathbf{F}(\dot{q}) \approx \mathbf{J}\delta\dot{q}$$

and to satisfy (B.1) we need

$$-\mathbf{F}(\dot{q}) = \mathbf{J}\delta\dot{q}$$

and so

$$\delta\dot{q} = -\mathbf{J}^+\mathbf{F}(\dot{q})$$

where \mathbf{J}^+ is the pseudo-inverse of the jacobian matrix

$$\mathbf{J}^+ = \mathbf{J}^T(\mathbf{J}\mathbf{J}^T)^{-1}.$$

Finally, the torques applied by the controller are

$$\tau = k\delta\dot{q} = -k\mathbf{J}^+\mathbf{F}(\dot{q}) \quad (\text{B.2})$$

where k is a scalar viscosity factor. Obviously this torque will be null when $\mathbf{F}(\dot{\mathbf{q}}) = 0$. In the particular case of linear constraints

$$\mathbf{F}(\dot{\mathbf{q}}) = \mathbf{C}\dot{\mathbf{q}} = 0$$

with $\mathbf{C} \in R^{l \times m}$, and therefore, since $\mathbf{J} = \mathbf{C}$, we have

$$\tau = -k\mathbf{C}^+\mathbf{C}\dot{\mathbf{q}}.$$

To define the correct vector of constraints \mathbf{C} , Crocher *et. al* analysed human motions during 3D pointing tasks. In this case, the task dimension is $m = 3$. By performing Principal Component Analysis (PCA) on the joint velocities $\dot{\mathbf{q}}(t)$, they expressed these in terms of Principal Components (PC) \mathbf{p}_i and their respective weight $c_i(t)$

$$\dot{\mathbf{q}}(t) = \sum_{i=0}^4 c_i(t)\mathbf{p}_i. \quad (\text{B.3})$$

Classically, however, upper-limb synergies are characterized, within the PCA framework, by the fact that less than four principal components are sufficient to *explain* most of the movement, that is

$$\dot{\mathbf{q}}(t) \approx \sum_{i=0}^d c_i(t)\mathbf{p}_i. \quad (\text{B.4})$$

where $d < 4$. Indeed, they verified that 3 PCs are sufficient to describe more than 90% of the movement within the exoskeleton. This means that the fourth component \mathbf{p}_4 can be viewed as a constraint that characterizes pointing movements for a given human being. In particular, the *natural constraint* \mathbf{C}_n

$$\mathbf{C}_n = \mathbf{p}_4 \quad (\text{B.5})$$

is supposed to impose a constraint that corresponds to the one naturally employed by the subject. Therefore, with this choice, the exoskeleton does not modify the subject upper-limb synergy. On the contrary, when $\mathbf{C} \neq \mathbf{C}_n$, a modification of the joint synchronization is performed.

Appendix C

Upper-limb rehabilitation assessment methods

The most common methods for assessing upper-limb rehabilitation recovery are presented in this appendix, divided into *functional assessment methods* and *recovery from impairments assessment methods*.

Functional assessment methods

Functional assessment deals with the capacity of motor control recovery in functional activities like ADLs. Functional tests assess task-specific improvements, for example, grasping a wooden block or pouring water. Because these tests do not consider possible compensatory strategies, frequently adopted by stroke survivors during activities of daily living, these assessments do not necessarily reflect true recovery [185]. The most common tests are:

Wolf Motor Function Test (WMFT)

Quantitative measure of upper extremity motor ability through timed and functional tasks. The widely used version of the WMFT consists of 17 items. Composed of 3 parts: Time, Functional ability, and Strength. Examiner should test the less affected upper extremity followed by the most affected side. Uses a 6-point ordinal scale: 0 = “does not attempt with the involved arm to 5 = “arm does participate; movement appears to be normal. Maximum score is 75.

Length: 6 to 30 minutes.

Equipment: can, pencil, paper clip, lock and key, face towel, ...

Arm Mobility Arm Test (AMAT)

The test consists of 13 ADL (cutting and eating meat, drinking from a mug, opening a jar, tying shoelace, use telephone, wiping up spilled water, putting on t-shirt and sweater, ...) activities involving one to three component tasks or movement segments.

Length: 30 minutes.

Equipment: about 30 objects.

Jebson Hand Function Test

To assess a broad range of uni-manual hand functions required for activities of daily living (ADLs). Lower score corresponds to greater function. It assesses speed, not quality of performance.

Length: 15 minutes.

Equipment: 7 items.

Action Research Arm Test (ARAT)

The ARAT's is a 19 item measure divided into 4 sub-tests (grasp, grip, pinch, and gross arm movement).

Performance on each item is rated on a 4-point ordinal scale (possible range 0 to 57).

Length: 10 minutes.

Equipment: various sized wood blocks, cricket ball, stone, jug and glass, ...

Nine-Hole Peg Test (NHPT)

Measures finger dexterity Administered by asking the client to take the pegs from a container, one by one, and place them into the holes on the board, as quickly as possible. Participants must then remove the pegs from the holes, one by one, and replace them back into the container. Scores are based on the time taken to complete the test activity, recorded in seconds.

Length: less than 1 minute.

Equipment: 1 wood block and 9 pegs.

Box and Block Test (BBT)

Assesses unilateral gross manual dexterity Individuals are seated at a table, facing a rectangular box that is divided into two square compartments of equal dimension by means of a partition. One hundred and fifty, 2.5 cm, colored, wooden cubes or blocks are placed in one compartment or the other. The individual is instructed to move as many blocks as possible, one at a time, from one compartment to the other for a period of 60 seconds. The BBT is scored by counting the number of blocks carried over the partition from one compartment to the other during the one-minute trial period.

Length: less than 5 minutes.

Equipment: a box with two compartments and 150 wooden cubes.

Stroke Impact Scale (SIS)

Assesses health status following stroke A 59 item measure, 8 domains assessed: 1. Strength 2. Hand function 3. ADL/IADL 4. Mobility 5. Communication 6. Emotion 7. Memory and thinking 8. Participation/Role function. Each item is rated in a 5-point Likert scale in terms of the difficulty the patient has experienced in completing each item. Summative scores are generated for each domain, scores range from 0-100.

Length: 30 minutes.

Equipment: a questionnaire with 59 questions.

Motor Assessment Scale (MAS)

Assesses everyday motor function in stroke patients 8 items that assess 8 areas of motor function. Patients perform each task 3 times, only the best performance is recorded. Items are assessed using a 7-point scale (0 to 6). A score of 6 indicates optimal motor behavior. Item scores are summed to provide an overall score (out of 48 points).

Length: 30 minutes.

Equipment: 8 objects (stopwatch, jellybeans, cup, rubber ball, spoon, pen, ...).

Barthel Index (BI)

Assesses the ability of an individual with a neuromuscular or musculoskeletal disorder to care for him/herself. 10 ADL/mobility activities including feeding, bathing, grooming, dressing, ambulation, stair climbing,

...

Length: 30 minutes.

Equipment: a questionnaire with 10 questions.

Functional Independence Measure (FIM)

Contains 18 items composed of 13 motor tasks and 5 cognitive tasks (considered basic activities of daily living). Tasks are rated on a 7 point ordinal scale that ranges from total assistance (or complete dependence) to complete independence. Scores range from 18 (lowest) to 126 (highest) indicating level of function. Activities include feeding, bathing, grooming, dressing, ambulation, stair climbing, ...

Length: 30-45 minutes.

Equipment: a questionnaire with 18 questions.

Recovery from impairments assessment methods

These methods provides measurements of the impairment by, for example, measuring pain level during stretching, range of motion of single joints, arm strength, ...

The most common method is the **Fugl-Meyer Assessment (FMA)**, one of the most widely used quantitative measures of motor impairment [62]. It evaluates and measures recovery in post-stroke hemiplegic patients, and it is used in both clinical and research settings. For FMA, items are scored on a 3-point ordinal scale: 0 = cannot perform, 1 = performs partially, 2 = performs fully. The maximum Score is 226 points. The five domains assessed include: motor function, sensory function, balance, joint range of motion, joint pain. Modified (abbreviated) versions have been developed. It lasts about 30 minutes.

Another common test is the **Ashworth Scale** or **Modified Ashworth Scale**, originally developed to assess the effects of antispasticity drugs on spasticity in Multiple Sclerosis, it measures spasticity in patients with lesions of the Central Nervous System. The original Ashworth Scale tests resistance to passive movement about a joint with varying degrees of velocity. Scores range from 0-4, with 5 choices. A score of 1 indicates no resistance and 5 indicates rigidity. For the Modified Ashworth Scale, the test is similar to Ashworth, but adds a 1+ scoring category to indicate resistance through less than half of the movement. Thus scores range from 0-4, with 6 choices. Score: 0 = No increase in tone, 4/5 = Limb rigid in flexion or extension. Both test last less than 5 minutes, depending on the number of muscles/joints tested.

Finally, other assessment methods are the **MRC Scale** and **Frenchay Arm Test**, which are less used but with similar approaches.

Comité d'éthique de la recherche en santé (CERES)

Président : Denis Berthiau

ceres_parisdescartes@services.cnrs.fr

N° 2016/20

PROTOCOLE

Optimizing relearning of motor coordination in post-stroke neurorehabilitation with an upper-limb robotic exoskeleton

Noms du/ des chercheur(s) :

Tommaso Proietti

Nathanaël Jarrassé

Agnès Roby-Brami

Labo/ Service: ISIR, UPMC

Email pour la correspondance : proietti@isir.upmc.fr

Evalué à la séance du : 16 Février 2016

AVIS : Favorable

Commentaires :

N°IRB : 20162000001072



Bibliography

- [1] National stroke association website. <http://www.stroke.org/>. Accessed: 2015-05-01. [cited on pp. 12]
- [2] World health organization website. <http://www.who.int>. Accessed: 2013-03-01. [cited on pp. 12]
- [3] F. Abdollahi, E. D. C. Lazarro, M. Listenberger, R. V. Kenyon, M. Kovic, R. A. Bogey, D. Hedeker, B. D. Jovanovic, and J. L. Patton. Error augmentation enhancing arm recovery in individuals with chronic stroke a randomized crossover design. *Neurorehabilitation and Neural Repair*, page 1545968313498649, 2013. [cited on pp. 57]
- [4] W. Abend, E. Bizzi, and P. Morasso. Human arm trajectory formation. *Brain*, 105(Pt 2):331–348, 1982. [cited on pp. 11]
- [5] A. Alwan et al. *Global status report on noncommunicable diseases 2010*. World Health Organization, 2011. [cited on pp. 12]
- [6] S. Balasubramanian, A. Melendez-Calderon, and E. Burdet. A robust and sensitive metric for quantifying movement smoothness. *IEEE Transactions on Biomedical Engineering*, 59(8):2126–2136, 2012. [cited on pp. 39, 63]
- [7] S. Balasubramanian, R. Wei, and J. He. RUPERT closed loop control design. In *IEEE International Conference of the Engineering in Medicine and Biology Society, EMBC*, pages 3467–3470, Aug. 2008. [cited on pp. 27]
- [8] S. Balasubramanian, R. Wei, M. Perez, B. Shepard, E. Koeneman, J. Koeneman, and J. He. RUPERT: An exoskeleton robot for assisting rehabilitation of arm functions. In *Virtual Rehabilitation*, pages 163–167. IEEE, 2008. [cited on pp. 26, 28, 31]
- [9] S. J. Ball, I. E. Brown, and S. H. Scott. MEDARM: a rehabilitation robot with 5-DOF at the shoulder complex. In *IEEE/ASME International Conference on Advanced Intelligent Mechatronics*, pages 1–6. IEEE, 2007. [cited on pp. 26]
- [10] M. Barsotti, D. Leonardis, C. Loconsole, M. Solazzi, E. Sotgiu, C. Procopio, C. Chisari, M. Bergamasco, and A. Frisoli. A full upper limb robotic exoskeleton for reaching and grasping rehabilitation triggered by MI-BCI. In *IEEE International Conference on Rehabilitation Robotics, ICORR*, pages 49–54. IEEE, 2015. [cited on pp. 29]
- [11] A. Basteris, S. M. Nijenhuis, A. H. Stienen, J. H. Buurke, G. B. Prange, and F. Amirabdollahian. Training modalities in robot-mediated upper limb rehabilitation in stroke: a framework for classification based on a systematic review. *Journal of Neuroengineering and Rehabilitation*, 11(1):111, 2014. [cited on pp. 23, 24, 25]

- [12] R. F. Beer, J. P. Dewald, M. L. Dawson, and W. Z. Rymer. Target-dependent differences between free and constrained arm movements in chronic hemiparesis. *Experimental Brain Research*, 156(4):458–70, 2004. [cited on pp. 15]
- [13] R. F. Beer, J. P. Dewald, and W. Z. Rymer. Deficits in the coordination of multijoint arm movements in patients with hemiparesis: evidence for disturbed control of limb dynamics. *Experimental Brain Research*, 131(3):305–319, 2000. [cited on pp. 15]
- [14] N. Bernstein. *The coordination and regulation of movement*. 1967. [cited on pp. 11, 33]
- [15] E. Bizzi, V. Cheung, A. d’Avella, P. Saltiel, and M. Tresch. Combining modules for movement. *Brain Research Reviews*, 57(1):125–133, 2008. [cited on pp. 11]
- [16] T. Bockemühl, N. F. Troje, and V. Dürr. Inter-joint coupling and joint angle synergies of human catching movements. *Human Movement Science*, 29(1):73–93, 2010. [cited on pp. 63]
- [17] D. Brauchle, M. Vukelić, R. Bauer, and A. Gharabaghi. Brain-state dependent robotic reaching movement with a multi-joint arm exoskeleton: combining brain-machine interfacing and robotic rehabilitation. *Frontiers in Human Neuroscience*, 9:564, 2015. [cited on pp. 29]
- [18] E. B. Brokaw, T. Murray, T. Nef, and P. S. Lum. Retraining of interjoint arm coordination after stroke using robot-assisted time-independent functional training. *Journal of Rehabilitation Research and Development*, 48(4):299–316, 2011. [cited on pp. 33, 35]
- [19] E. B. Brokaw, D. Nichols, R. J. Holley, and P. S. Lum. Robotic therapy provides a stimulus for upper limb motor recovery after stroke that is complementary to and distinct from conventional therapy. *Neurorehabilitation and Neural Repair*, page 1545968313510974, 2013. [cited on pp. 33]
- [20] S. Brunnstrom. *Movement therapy in hemiplegia: a neurophysiological approach*. Harper & Row, New York, 1970. [cited on pp. 14]
- [21] E. Burdet, D. W. Franklin, and T. E. Milner. *Human robotics: neuromechanics and motor control*. MIT Press, 2013. [cited on pp. 12, 39]
- [22] C. G. Burgar, P. S. Lum, P. C. Shor, and H. M. Van der Loos. Development of robots for rehabilitation therapy: the palo alto VA/Stanford experience. *Journal of Rehabilitation Research and Development*, 37(6):663–674, 2000. [cited on pp. 18]
- [23] D. G. Caldwell, N. G. Tsagarakis, S. Kousidou, N. Costa, and I. Sarakoglou. Soft exoskeleton for upper and lower body rehabilitation - desing, control and testing. *International Journal of Humanoid Robotics*, 4(03):549–573, 2007. [cited on pp. 26]
- [24] C. Carignan, J. Tang, and S. Roderick. Development of an exoskeleton haptic interface for virtual task training. In *IEEE/RSJ International Conference on Intelligent Robots and Systems, IROS*, pages 3697–3702. IEEE, 2009. [cited on pp. 26, 28, 30]
- [25] W. H. Chang and Y.-H. Kim. Robot-assisted therapy in stroke rehabilitation. *Journal of Stroke*, 15(3):174–181, 2013. [cited on pp. 23]
- [26] M. Cirstea and M. F. Levin. Compensatory strategies for reaching in stroke. *Brain*, 123(5):940–953, 2000. [cited on pp. 14, 15]
- [27] M. C. Cirstea, A. B. Mitnitski, A. G. Feldman, and M. F. Levin. Interjoint coordination dynamics during reaching in stroke. *Experimental Brain Research*, 151(3):289–300, 2003. [cited on pp. 15]

- [28] V. Crocher, N. Jarrassé, A. Sahbani, A. Roby-Brami, and G. Morel. Changing human upper-limb synergies with an exoskeleton using viscous fields. In *IEEE International Conference on Robotics and Automation, ICRA*, pages 4657–4663. IEEE, 2011. [cited on pp. 75]
- [29] V. Crocher, A. Sahbani, J. Robertson, A. Roby-Brami, and G. Morel. Constraining upper limb synergies of hemiparetic patients using a robotic exoskeleton in the perspective of neuro-rehabilitation. *IEEE Transactions on Neural Systems and Rehabilitation Engineering*, 20(3):247–257, 2012. [cited on pp. 26, 33, 35, 36, 58, 88]
- [30] P. Culmer, A. Jackson, S. Makower, R. Richardson, J. Cozens, M. Levesley, and B. Bhakta. A control strategy for upper limb robotic rehabilitation with a dual robot system. *IEEE/ASME Transactions on Mechatronics*, 15(4):575–585, Aug. 2010. [cited on pp. 30]
- [31] P. R. Culmer, A. E. Jackson, S. G. Makower, J. A. Cozens, M. C. Levesley, M. Mon-Williams, and B. Bhakta. A novel robotic system for quantifying arm kinematics and kinetics: Description and evaluation in therapist-assisted passive arm movements post-stroke. *Journal of Neuroscience Methods*, 197(2):259–269, Apr. 2011. [cited on pp. 26]
- [32] A. d’Avella, L. Fernandez, A. Portone, and F. Lacquaniti. Modulation of phasic and tonic muscle synergies with reaching direction and speed. *Journal of Neurophysiology*, 100(3):1433–1454, 2008. [cited on pp. 11]
- [33] A. d’Avella, A. Portone, L. Fernandez, and F. Lacquaniti. Control of fast-reaching movements by muscle synergy combinations. *The Journal of Neuroscience*, 26(30):7791–7810, 2006. [cited on pp. 11]
- [34] A. Dawson, J. Knox, A. McClure, N. Foley, and R. Teasell. On behalf of the stroke rehabilitation writing group. *Chapter 5: Stroke Rehabilitation*, 2013. [cited on pp. 15]
- [35] G. De Lee, W.-W. Wang, K.-W. Lee, S.-Y. Lin, L.-C. Fu, J.-S. Lai, W.-S. Chen, and J.-J. Luh. Arm exoskeleton rehabilitation robot with assistive system for patient after stroke. In *IEEE International Conference on Control, Automation and Systems, ICCAS*, pages 1943–1948. IEEE, 2012. [cited on pp. 26]
- [36] M. Desmurget, H. Gréa, and C. Prablanc. Final posture of the upper limb depends on the initial position of the hand during prehension movements. *Experimental Brain Research*, 119(4):511–516, 1998. [cited on pp. 11]
- [37] M. Desmurget and C. Prablanc. Postural control of three-dimensional prehension movements. *Journal of Neurophysiology*, 77(1):452–464, 1997. [cited on pp. 11]
- [38] J. P. Dewald and R. F. Beer. Abnormal joint torque patterns in the paretic upper limb of subjects with hemiparesis. *Muscle & Nerve*, 24(2):273–83, 2001. [cited on pp. 14]
- [39] J. P. Dewald, P. S. Pope, J. D. Given, T. S. Buchanan, and W. Z. Rymer. Abnormal muscle coactivation patterns during isometric torque generation at the elbow and shoulder in hemiparetic subjects. *Brain*, 118 (Pt 2):495–510, 1995. [cited on pp. 14]
- [40] J. Diedrichsen, O. White, D. Newman, and N. Lally. Use-dependent and error-based learning of motor behaviors. *Journal of Neuroscience*, 30(15):5159–5166, 2010. [cited on pp. 82]
- [41] M. Ding, K. Hirasawa, Y. Kurita, H. Takemura, J. Takamatsu, H. Mizoguchi, and T. Ogasawara. Pin-pointed muscle force control in consideration of human motion and external force. In *IEEE International Conference on Robotics and Biomimetics, ROBIO*, pages 739–744. IEEE, 2010. [cited on pp. 31]

- [42] M. Ding, J. Ueda, and T. Ogasawara. Pinpointed muscle force control using a power-assisting device: system configuration and experiment. In *IEEE RAS & EMBS International Conference on Biomedical Robotics and Biomechatronics, BioRob*, pages 181–186. IEEE, 2008. [cited on pp. 26, 31]
- [43] L. Dipietro, H. I. Krebs, S. E. Fasoli, B. T. Volpe, J. Stein, C. Bever, and N. Hogan. Changing motor synergies in chronic stroke. *Journal of neurophysiology*, 98(2):757–768, 2007. [cited on pp. 53, 56, 57]
- [44] M. D. Ellis, T. Sukal, T. DeMott, and J. P. Dewald. Augmenting clinical evaluation of hemiparetic arm movement with a laboratory-based quantitative measurement of kinematics as a function of limb loading. *Neurorehabilitation & Neural Repair*, 22(4):321–9, 2008. [cited on pp. 15]
- [45] M. A. Ergin and V. Patoglu. ASSISTON-SE: A self-aligning shoulder-elbow exoskeleton. In *IEEE International Conference on Robotics and Automation, ICRA*, pages 2479–2485. IEEE, 2012. [cited on pp. 26]
- [46] G. Fazekas, M. Horvath, T. Troznai, and A. Toth. Robot-mediated upper limb physiotherapy for patients with spastic hemiparesis: A preliminary study. *Journal of Rehabilitation Medicine*, 39(7):580–582, 2007. [cited on pp. 26]
- [47] A. G. Feldman and M. F. Levin. The origin and use of positional frames of reference in motor control. *Behavioral and Brain Sciences*, 18(04):723–744, 1995. [cited on pp. 11]
- [48] P. M. Fitts. The information capacity of the human motor system in controlling the amplitude of movement. *Journal of Experimental Psychology*, 47(6):381, 1954. [cited on pp. 12]
- [49] M. Flanders and U. Herrmann. Two components of muscle activation: scaling with the speed of arm movement. *Journal of Neurophysiology*, 67(4):931–943, 1992. [cited on pp. 11]
- [50] J. Fong, V. Crocher, D. Oetomo, and Y. Tan. An investigation into the reliability of upper-limb robotic exoskeleton measurements for clinical evaluation in neurorehabilitation. In *IEEE EMBS Conference on Neural Engineering, NER*, 2015. [cited on pp. 34]
- [51] D. W. Franklin, E. Burdet, K. P. Tee, R. Osu, C.-M. Chew, T. E. Milner, and M. Kawato. Cns learns stable, accurate, and efficient movements using a simple algorithm. *The Journal of Neuroscience*, 28(44):11165–11173, 2008. [cited on pp. 12, 36, 38]
- [52] A. Frisoli, L. Borelli, A. Montagner, S. Marcheschi, C. Procopio, F. Salsedo, M. Bergamasco, M. Carboncini, M. Tolaini, and B. Rossi. Arm rehabilitation with a robotic exoskeleton in virtual reality. In *IEEE International Conference on Rehabilitation Robotics, ICORR*, pages 631–642. IEEE, 2007. [cited on pp. 26]
- [53] A. Frisoli, C. Loconsole, R. Bartalucci, and M. Bergamasco. A new bounded jerk on-line trajectory planning for mimicking human movements in robot-aided neurorehabilitation. *Robotics and Autonomous Systems*, 61(4):404–415, 2013. [cited on pp. 28]
- [54] A. Frisoli, C. Loconsole, D. Leonardi, F. Banno, M. Barsotti, C. Chisari, and M. Bergamasco. A new gaze-BCI-driven control of an upper limb exoskeleton for rehabilitation in real-world tasks. *IEEE Transactions on Systems, Man, and Cybernetics, Part C: Applications and Reviews*, 42(6):1169–1179, 2012. [cited on pp. 29, 34]
- [55] A. Frisoli, C. Procopio, C. Chisari, I. Creatini, L. Bonfiglio, M. Bergamasco, B. Rossi, M. C. Carboncini, et al. Positive effects of robotic exoskeleton training of upper limb reaching movements after stroke. *Journal of Neuroengineering and Rehabilitation*, 9(1):36, 2012. [cited on pp. 26, 30, 36]

- [56] A. Frisoli, F. Salsedo, M. Bergamasco, B. Rossi, and M. C. Carboncini. A force-feedback exoskeleton for upper-limb rehabilitation in virtual reality. *Applied Bionics and Biomechanics*, 6(2):115–126, 2009. [cited on pp. 30]
- [57] G. Ganesh and E. Burdet. Motor planning explains human behaviour in tasks with multiple solutions. *Robotics and Autonomous Systems*, 61(4):362–368, 2013. [cited on pp. 75]
- [58] G. Ganesh, A. Takagi, R. Osu, T. Yoshioka, M. Kawato, and E. Burdet. Two is better than one: physical interactions improve motor performance in humans. *Scientific Reports*, 4, 2014. [cited on pp. 37]
- [59] P. Garrec. Screw, nut and cable transmission, 2008. US Patent 7,389,974. [cited on pp. 20]
- [60] P. Garrec, J. P. Friconneau, Y. Measson, and Y. Perrot. ABLE an innovative transparent exoskeleton for the upper-limb. In *IEEE/RSJ International Conference on Intelligent Robots and Systems, IROS*, pages 1483–1488. IEEE, 2008. [cited on pp. 20, 26]
- [61] J. Garrido, W. Yu, and A. Soria. Modular design and modeling of an upper limb exoskeleton. In *IEEE/RAS-EMBS International Conference on Biomedical Robotics and Biomechatronics, BioRob*, pages 508–513. IEEE, 2014. [cited on pp. 26, 28]
- [62] D. J. Gladstone, C. J. Danells, and S. E. Black. The Fugl-Meyer assessment of motor recovery after stroke: a critical review of its measurement properties. *Neurorehabilitation and Neural Repair*, 16(3):232–240, 2002. [cited on pp. 92]
- [63] R. A. R. C. Gopura, K. Kiguchi, and Y. Li. SUEFUL-7: A 7-DOF upper-limb exoskeleton robot with muscle-model-oriented EMG-based control. In *IEEE/RSJ International Conference on Intelligent Robots and Systems, IROS*, pages 1126–1131. IEEE, 2009. [cited on pp. 26, 30, 34]
- [64] M. Guidali, A. Duschau-Wicke, S. Broggi, V. Klamroth-Marganska, T. Nef, and R. Riener. A robotic system to train activities of daily living in a virtual environment. *Medical & Biological Engineering & Computing*, 49(10):1213–1223, July 2011. [cited on pp. 26, 32]
- [65] M. Guidali, M. Schmiedeskamp, V. Klamroth, and R. Riener. Assessment and training of synergies with an arm rehabilitation robot. In *IEEE International Conference on Rehabilitation Robotics, ICORR*, pages 772–776. IEEE, 2009. [cited on pp. 33, 35]
- [66] E. Guigon, P. Baraduc, and M. Desmurget. Computational motor control: redundancy and invariance. *Journal of Neurophysiology*, 97(1):331–347, 2007. [cited on pp. 11]
- [67] E. Guigon, P. Baraduc, and M. Desmurget. Computational motor control: redundancy and invariance. *Journal of Neurophysiology*, 97(1):331–347, 2007. [cited on pp. 28]
- [68] M. Gunasekara, R. Gopura, and S. Jayawardena. 6-REXOS: upper limb exoskeleton robot with improved pHRI. *International Journal of Advanced Robotic Systems*, pages 12–47, 2015. [cited on pp. 26]
- [69] S. Guo, W. Zhang, W. Wei, J. Guo, Y. Ji, and Y. Wang. A kinematic model of an upper limb rehabilitation robot system. In *IEEE International Conference on Mechatronics and Automation, ICMA*, pages 968–973. IEEE, 2013. [cited on pp. 29]
- [70] A. Gupta and M. O’Malley. Design of a haptic arm exoskeleton for training and rehabilitation. *IEEE/ASME Transactions on Mechatronics*, 11(3):280–289, June 2006. [cited on pp. 26, 30]
- [71] A. M. Haith and J. W. Krakauer. Model-based and model-free mechanisms of human motor learning. In *Progress in Motor Control*, pages 1–21. Springer, 2013. [cited on pp. 82]

- [72] A. Heller, D. Wade, V. A. Wood, A. Sunderland, R. L. Hewer, and E. Ward. Arm function after stroke: measurement and recovery over the first three months. *Journal of Neurology, Neurosurgery & Psychiatry*, 50(6):714–719, 1987. [cited on pp. 16]
- [73] A. Henry and A. Barrett. Wii-habilitation and robotic exoskeletons: technology in physiotherapy. *Royal College of Surgeons in Ireland Student Medical Journal*, 3:70–4, 2010. [cited on pp. 37]
- [74] Y. Hidaka, C. E. Han, S. L. Wolf, C. J. Winstein, and N. Schweighofer. Use it and improve it or lose it: interactions between arm function and use in humans post-stroke. *PLOS Computational Biology*, 8(2):e1002343, 2012. [cited on pp. 15]
- [75] J. Hidler, W. Wisman, and N. Neckel. Kinematic trajectories while walking within the Lokomat robotic gait-orthosis. *Clinical Biomechanics*, 23(10):1251–1259, 2008. [cited on pp. 37]
- [76] N. Hogan. Impedance control: An approach to manipulation. In *American Control Conference*, pages 304–313, 1984. [cited on pp. 30]
- [77] N. Hogan and H. I. Krebs. Interactive robots for neuro-rehabilitation. *Restorative neurology and neuroscience*, 22(3):349–358, 2004. [cited on pp. 30]
- [78] N. Hogan, H. I. Krebs, J. Charnnarong, P. Srikrishna, and A. Sharon. MIT-MANUS: a workstation for manual therapy and training ii. In *Applications in Optical Science and Engineering*, pages 28–34. International Society for Optics and Photonics, 1993. [cited on pp. 17]
- [79] N. Hogan, H. I. Krebs, B. Rohrer, J. J. Palazzolo, L. Dipietro, S. E. Fasoli, J. Stein, R. Hughes, W. R. Frontera, D. Lynch, et al. Motions or muscles? some behavioral factors underlying robotic assistance of motor recovery. *Journal of Rehabilitation Research and Development*, 43(5):605, 2006. [cited on pp. 30]
- [80] F. C. Huang and J. L. Patton. Augmented dynamics and motor exploration as training for stroke. *IEEE Transactions on Biomedical Engineering*, 60(3):838–844, 2013. [cited on pp. 57]
- [81] F. C. Huang, J. L. Patton, and F. A. Mussa-Ivaldi. Manual skill generalization enhanced by negative viscosity. *Journal of Neurophysiology*, 104(4):2008–2019, 2010. [cited on pp. 57]
- [82] V. S. Huang and J. W. Krakauer. Robotic neurorehabilitation: a computational motor learning perspective. *Journal of Neuroengineering and Rehabilitation*, 6(1):5, 2009. [cited on pp. 18, 22, 23, 25, 35, 36, 57]
- [83] A. E. Jackson, R. J. Holt, P. R. Culmer, S. G. Makower, M. C. Levesley, R. C. Richardson, J. A. Cozens, M. M. Williams, and B. B. Bhakta. Dual robot system for upper limb rehabilitation after stroke: The design process. *Proceedings of the Institution of Mechanical Engineers, Part C: Journal of Mechanical Engineering Science*, 221(7):845–857, July 2007. [cited on pp. 24, 26]
- [84] N. Jarrassé, J. Paik, V. Pasqui, and G. Morel. How can human motion prediction increase transparency? In *IEEE International Conference on Robotics and Automation, ICRA*, pages 2134–2139. IEEE, 2008. [cited on pp. 19]
- [85] N. Jarrassé, T. Proietti, V. Crocher, J. Robertson, A. Sahbani, G. Morel, and A. Roby-Brami. Robotic exoskeletons: a perspective for the rehabilitation of arm coordination in stroke patients. *Frontiers in Human Neuroscience*, 8:947, 2014. [cited on pp. 35]
- [86] N. Jarrasse, M. Tagliabue, J. V. Robertson, A. Maiza, V. Crocher, A. Roby-Brami, and G. Morel. A methodology to quantify alterations in human upper limb movement during co-manipulation with an exoskeleton. *IEEE Transactions on Neural Systems and Rehabilitation Engineering*, 18(4):389–397, 2010. [cited on pp. 33, 55]

- [87] N. Jarrassé, M. Tagliabue, J. V. Robertson, A. Maiza, V. Crocher, A. Roby-Brami, and G. Morel. A methodology to quantify alterations in human upper limb movement during co-manipulation with an exoskeleton. *IEEE Transactions on Neural Systems and Rehabilitation Engineering*, 18(4):389–397, 2010. [cited on pp. 59, 63]
- [88] G. R. Johnson, D. A. Carus, G. Parrini, S. Marchese, and R. Valeggi. The design of a five-degree-of-freedom powered orthosis for the upper limb. *Proceedings of the Institution of Mechanical Engineers, Part H: Journal of Engineering in Medicine*, 215(3):275–284, Mar. 2001. [cited on pp. 26]
- [89] D. G. Kamper, A. N. McKenna-Cole, L. E. Kahn, and D. J. Reinkensmeyer. Alterations in reaching after stroke and their relation to movement direction and impairment severity. *Archives of Physical Medicine and Rehabilitation*, 83(5):702–707, 2002. [cited on pp. 15]
- [90] H. Kim, Z. Li, D. Milutinovic, and J. Rosen. Resolving the redundancy of a seven DOF wearable robotic system based on kinematic and dynamic constraint. In *IEEE International Conference on Robotics and Automation, ICRA*, pages 305–310. IEEE, 2012. [cited on pp. 31]
- [91] H. Kim, L. M. Miller, I. Fedulow, M. Simkins, G. M. Abrams, N. Byl, and J. Rosen. Kinematic data analysis for post-stroke patients following bilateral versus unilateral rehabilitation with an upper limb wearable robotic system. *IEEE Transactions on Neural Systems and Rehabilitation Engineering*, 21(2):153–164, 2013. [cited on pp. 31, 36]
- [92] T. Kitago and J. W. Krakauer. Motor learning principles for neurorehabilitation. *Handbook of Clinical Neurology*, 110:93–103, 2013. [cited on pp. 12]
- [93] V. Klamroth-Marganska, J. Blanco, K. Campen, A. Curt, V. Dietz, T. Ettlin, M. Felder, B. Fellinghauer, M. Guidali, and A. Kollmar. Three-dimensional, task-specific robot therapy of the arm after stroke: a multicentre, parallel-group randomised trial. *The Lancet Neurology*, 13(2):159–166, 2014. [cited on pp. 18, 21, 26, 32, 35, 36]
- [94] J. Klein, S. Spencer, J. Allington, K. Minakata, E. Wolbrecht, R. Smith, J. Bobrow, and D. Reinkensmeyer. Biomimetic orthosis for the neurorehabilitation of the elbow and shoulder (BONES). In *IEEE RAS & EMBS International Conference on Biomedical Robotics and Biomechatronics, BioRob*, pages 535–541. IEEE, 2008. [cited on pp. 24, 26]
- [95] S. Kousidou, N. G. Tsagarakis, C. Smith, and D. G. Caldwell. Task-orientated biofeedback system for the rehabilitation of the upper limb. In *IEEE International Conference on Rehabilitation Robotics, ICORR*, pages 376–384. IEEE, 2007. [cited on pp. 28, 30]
- [96] G. Kwakkel, B. J. Kollen, and H. I. Krebs. Effects of robot-assisted therapy on upper limb recovery after stroke: a systematic review. *Neurorehabilitation and Neural Repair*, 2007. [cited on pp. 18]
- [97] J. R. Lackner and P. Dizio. Rapid adaptation to Coriolis force perturbations of arm trajectory. *Journal of Neurophysiology*, 72(1):299–313, 1994. [cited on pp. 56]
- [98] P. Langhorne, J. Bernhardt, and G. Kwakkel. Stroke rehabilitation. *Lancet*, 377(9778):1693–702, 2011. [cited on pp. 16]
- [99] M. L. Latash and J. G. Anson. Synergies in health and disease: relations to adaptive changes in motor coordination. *Physical therapy*, 86(8):1151–1160, 2006. [cited on pp. 11]
- [100] M. F. Levin. Interjoint coordination during pointing movements is disrupted in spastic hemiparesis. *Brain*, 119 (Pt 1):281–93, 1996. [cited on pp. 15]

- [101] M. F. Levin, J. A. Kleim, and S. L. Wolf. What do motor “recovery” and “compensation” mean in patients following stroke? *Neurorehabilitation & Neural Repair*, 23(4):313–9, 2009. [cited on pp. 15, 56]
- [102] Z. Li, C. Su, G. Li, and H. Su. Fuzzy approximation-based adaptive backstepping control of an exoskeleton for human upper limbs. *IEEE Transactions on Fuzzy Systems*, 2015. [cited on pp. 28]
- [103] A. C. Lo, P. D. Guarino, L. G. Richards, J. K. Haselkorn, G. F. Wittenberg, D. G. Federman, R. J. Ringer, T. H. Wagner, H. I. Krebs, B. T. Volpe, et al. Robot-assisted therapy for long-term upper-limb impairment after stroke. *New England Journal of Medicine*, 362(19):1772–1783, 2010. [cited on pp. 18]
- [104] H. S. Lo and S. Q. Xie. Exoskeleton robots for upper-limb rehabilitation: State of the art and future prospects. *Medical Engineering & Physics*, 34(3):261–268, Apr. 2012. [cited on pp. 23]
- [105] H. S. Lo and S. S. Xie. An upper limb exoskeleton with an optimized 4r spherical wrist mechanism for the shoulder joint. In *IEEE/ASME International Conference on Advanced Intelligent Mechatronics, AIM*, pages 269–274. IEEE, 2014. [cited on pp. 26]
- [106] C. Loconsole, S. Dettori, A. Frisoli, C. A. Avizzano, and M. Bergamasco. An EMG-based approach for on-line predicted torque control in robotic-assisted rehabilitation. In *IEEE Haptics Symposium*, pages 181–186. IEEE, 2014. [cited on pp. 28, 34]
- [107] B. J. Lutz, M. E. Young, K. J. Cox, C. Martz, and K. R. Creasy. The crisis of stroke: experiences of patients and their family caregivers. *Topics in Stroke Rehabilitation*, 2015. [cited on pp. 16]
- [108] D. Lynch, M. Ferraro, J. Krol, C. M. Trudell, P. Christos, and B. T. Volpe. Continuous passive motion improves shoulder joint integrity following stroke. *Clinical Rehabilitation*, 19(6):594–599, 2005. [cited on pp. 25, 29]
- [109] P. Maciejasz, J. Eschweiler, K. Gerlach-Hahn, A. Jansen-Troy, and S. Leonhardt. A survey on robotic devices for upper limb rehabilitation. *Journal of Neuroengineering and Rehabilitation*, 11(1):3, Jan. 2014. [cited on pp. 23]
- [110] Y. Mao and S. Agrawal. Design of a cable-driven arm exoskeleton (carex) for neural rehabilitation. *IEEE Transactions on Robotics*, 28(4):922–931, Aug. 2012. [cited on pp. 24, 26, 28]
- [111] Y. Mao and S. K. Agrawal. A cable driven upper arm exoskeleton for upper extremity rehabilitation. In *IEEE International Conference on Robotics and Automation, ICRA*, pages 4163–4168. IEEE, 2011. [cited on pp. 32]
- [112] Y. Mao, X. Jin, G. G. Dutta, J. P. Scholz, and S. K. Agrawal. Human movement training with a cable driven arm exoskeleton (CAREX). *IEEE Transactions on Neural Systems and Rehabilitation Engineering*, 2014. [cited on pp. 32, 36]
- [113] L. Marchal-Crespo and D. J. Reinkensmeyer. Review of control strategies for robotic movement training after neurologic injury. *Journal of Neuroengineering and Rehabilitation*, 6(1):20, 2009. [cited on pp. 23]
- [114] J. A. Martinez, P. Ng, S. Lu, M. S. Campagna, and O. Celik. Design of wrist gimbal: A forearm and wrist exoskeleton for stroke rehabilitation. In *IEEE International Conference on Rehabilitation Robotics, ICORR*, pages 1–6. IEEE, 2013. [cited on pp. 26, 28]
- [115] S. Masiero, M. Armani, G. Ferlini, G. Rosati, and A. Rossi. Randomized trial of a robotic assistive device for the upper extremity during early inpatient stroke rehabilitation. *Neurorehabilitation and Neural Repair*, Dec. 2013. [cited on pp. 26]

- [116] A. Mayr, M. Kofler, and L. Saltuari. ARMOR: elektromechanischer roboter fr das bewegungstraining der oberen extremitt nach schlaganfall. prospektive randomisierte kontrollierte pilotstudie. *Handchirurgie Mikrochirurgie Plastische Chirurgie*, 40(1):66–73, Feb. 2008. [cited on pp. 26, 29]
- [117] T. Merdler, D. G. Liebermann, M. F. Levin, and S. Berman. Arm-plane representation of shoulder compensation during pointing movements in patients with stroke. *Journal of Electromyography & Kinesiology*, 23(4):938–47, 2013. [cited on pp. 14]
- [118] R. Miall, D. Weir, D. M. Wolpert, and J. Stein. Is the cerebellum a smith predictor? *Journal of Motor Behavior*, 25(3):203–216, 1993. [cited on pp. 12]
- [119] L. M. Miller and J. Rosen. Comparison of multi-sensor admittance control in joint space and task space for a seven degree of freedom upper limb exoskeleton. In *IEEE/RAS-EMBS International Conference on Biomedical Robotics and Biomechatronics, BioRob*, pages 70–75. IEEE, 2010. [cited on pp. 30]
- [120] M.-H. Milot, S. J. Spencer, V. Chan, J. P. Allington, J. Klein, C. Chou, J. E. Bobrow, S. C. Cramer, and D. J. Reinkensmeyer. A crossover pilot study evaluating the functional outcomes of two different types of robotic movement training in chronic stroke survivors using the arm exoskeleton BONES. *Journal of Neuroengineering and Rehabilitation*, 10(1):112, Dec. 2013. [cited on pp. 26, 31, 35, 36, 38]
- [121] M. Mistry, P. Mohajerian, and S. Schaal. Arm movement experiments with joint space force fields using an exoskeleton robot. In *International Conference on Rehabilitation Robotics, ICORR*, pages 408–413. IEEE, 2005. [cited on pp. 57, 74]
- [122] R. Morales, F. J. Badesa, N. Garca-Aracil, J. M. Sabater, and C. Prez-Vidal. Pneumatic robotic systems for upper limb rehabilitation. *Medical & Biological Engineering & Computing*, 49(10):1145–1156, Aug. 2011. [cited on pp. 24, 26]
- [123] S. Moubarak, M. T. Pham, R. Moreau, and T. Redarce. Gravity compensation of an upper extremity exoskeleton. In *IEEE International Conference on Engineering in Medicine and Biology Society, EMBC*, pages 4489–4493. IEEE, 2010. [cited on pp. 28]
- [124] S. Moubarak, M. T. Pham, T. Pajdla, and T. Redarce. Design and modeling of an upper extremity exoskeleton. In O. Dssel and W. C. Schlegel, editors, *World Congress on Medical Physics and Biomedical Engineering, September 7 - 12, 2009, Munich, Germany*, pages 476–479. Springer Berlin Heidelberg, Jan. 2009. [cited on pp. 26]
- [125] T. Nef, M. Mihelj, and R. Riener. ARMin: a robot for patient-cooperative arm therapy. *Medical & Biological Engineering & Computing*, 45(9):887–900, Sept. 2007. [cited on pp. 28]
- [126] K. C. Nishikawa, S. T. Murray, and M. Flanders. Do arm postures vary with the speed of reaching? *Journal of Neurophysiology*, 81(5):2582–2586, 1999. [cited on pp. 11]
- [127] N. Nordin, S. Q. Xie, and B. Wünsche. Assessment of movement quality in robot-assisted upper limb rehabilitation after stroke: a review. *Journal of Neuroengineering and Rehabilitation*, 11(1):137, 2014. [cited on pp. 34, 35, 36, 52]
- [128] R. J. Nudo, B. M. Wise, F. SiFuentes, and G. W. Milliken. Neural substrates for the effects of rehabilitative training on motor recovery after ischemic infarct. *Science*, 272(5269):1791–1794, 1996. [cited on pp. 16]
- [129] A. Otten, A. H. A. Stienen, E. van Asseldonk, R. Aarts, and H. van der Kooij. LIMPACT: a hydraulically powered self-aligning upper limb exoskeleton. In *IEEE/ASME transactions on mechatronics*, 2013. [cited on pp. 26, 28]

- [130] J. L. Patton and F. A. Mussa-Ivaldi. Robot-assisted adaptive training: custom force fields for teaching movement patterns. *IEEE Transactions on Biomedical Engineering*, 51(4):636–646, 2004. [cited on pp. 30]
- [131] J. L. Patton and F. A. Mussa-Ivaldi. Robot-assisted adaptive training: custom force fields for teaching movement patterns. *IEEE Transactions on Biomedical Engineering*, 51(4):636–646, 2004. [cited on pp. 57, 76]
- [132] J. L. Patton, M. E. Stoykov, M. Kovic, and F. A. Mussa-Ivaldi. Evaluation of robotic training forces that either enhance or reduce error in chronic hemiparetic stroke survivors. *Experimental Brain Research*, 168(3):368–383, 2006. [cited on pp. 57]
- [133] A. Pehlivan, D. Losey, and M. OMalley. Minimal assist-as-needed controller for upper limb robotic rehabilitation. *IEEE Transactions on Robotics*, 32(1):113–124, Feb 2016. [cited on pp. 31, 39]
- [134] A. Pennycott, D. Wyss, H. Vallery, V. Klamroth-Marganska, and R. Riener. Towards more effective robotic gait training for stroke rehabilitation: a review. *Journal of Neuroengineering and Rehabilitation*, 9(1):1, 2012. [cited on pp. 37]
- [135] R. Pérez-Rodríguez, C. Rodríguez, Ú. Costa, C. Cáceres, J. M. Tormos, J. Medina, and E. J. Gómez. Anticipatory assistance-as-needed control algorithm for a multijoint upper limb robotic orthosis in physical neurorehabilitation. *Expert Systems with Applications*, 41(8):3922–3934, 2014. [cited on pp. 32, 35]
- [136] J. C. Perry and J. Rosen. Design of a 7 degree-of-freedom upper-limb powered exoskeleton. In *IEEE/RAS-EMBS International Conference on Biomedical Robotics and Biomechatronics, BioRob*, pages 805–810. IEEE, 2006. [cited on pp. 26]
- [137] L. Pignolo, G. Dolce, G. Basta, L. Lucca, S. Serra, and W. Sannita. Upper limb rehabilitation after stroke: Aramis a robo-mechatronic innovative approach and prototype. In *IEEE RAS & EMBS International Conference on Biomedical Robotics and Biomechatronics, BioRob*, pages 1410–1414. IEEE, 2012. [cited on pp. 26, 28, 29, 36]
- [138] E. Pirondini, M. Coscia, S. Marcheschi, G. Roas, F. Salsedo, A. Frisoli, M. Bergamasco, and S. Micera. Evaluation of a new exoskeleton for upper limb post-stroke neuro-rehabilitation: Preliminary results. In *Replace, Repair, Restore, Relieve—Bridging Clinical and Engineering Solutions in Neurorehabilitation*, pages 637–645. Springer, 2014. [cited on pp. 26]
- [139] T. Proietti, V. Crocher, A. Roby-Brami, and N. Jarrass. Upper-limb robotic exoskeletons for neurorehabilitation: a review on control strategies. *IEEE Reviews in Biomedical Engineering*, 9:4–14, 2016. [cited on pp. 24]
- [140] T. Proietti, N. Jarrasse, A. Roby-Brami, and G. Morel. Adaptive control of a robotic exoskeleton for neurorehabilitation. In *IEEE EMBS Conference on Neural Engineering, NER*, 2015. [cited on pp. 31]
- [141] M. Rahman, T. Ouimet, M. Saad, J. Kenne, and P. Archambault. Development and control of a wearable robot for rehabilitation of elbow and shoulder joint movements. In *IECON 2010-36th Annual Conference on IEEE Industrial Electronics Society*, pages 1506–1511. IEEE, 2010. [cited on pp. 26, 28]
- [142] M. H. Rahman, C. Ochoa-Luna, M. Saad, and P. Archambault. EMG based control of a robotic exoskeleton for shoulder and elbow motion assist. *Journal of Automation and Control Engineering*, 3(4), 2015. [cited on pp. 28]
- [143] D. J. Reinkensmeyer, E. Burdet, M. Casadio, J. W. Krakauer, G. Kwakkel, C. E. Lang, S. P. Swinnen, N. S. Ward, and N. Schweighofer. Computational neurorehabilitation: modeling plasticity and learning to predict recovery. *Journal of Neuroengineering and Rehabilitation*, 13(1):1, 2016. [cited on pp. 16]

- [144] D. J. Reinkensmeyer, J. L. Emken, and S. C. Cramer. Robotics, motor learning, and neurologic recovery. *Annual Review of Biomedical Engineering*, 6:497–525, 2004. [cited on pp. 18]
- [145] D. J. Reinkensmeyer, L. E. Kahn, M. Averbuch, A. McKenna-Cole, et al. Understanding and treating arm movement impairment after chronic brain injury: progress with the ARM guide. *Journal of Rehabilitation Research and Development*, 37(6):653, 2000. [cited on pp. 17]
- [146] D. J. Reinkensmeyer, E. T. Wolbrecht, V. Chan, C. Chou, S. C. Cramer, and J. E. Bobrow. Comparison of three-dimensional, assist-as-needed robotic arm/hand movement training provided with pneu-wrex to conventional tabletop therapy after chronic stroke. *American Journal of Physical Medicine & Rehabilitation*, 91(11 Suppl 3):S232–41, 2012. [cited on pp. 26, 31, 35, 36, 38]
- [147] D. S. Reisman and J. P. Scholz. Aspects of joint coordination are preserved during pointing in persons with post-stroke hemiparesis. *Brain*, 126:2510–2527, 2003. [cited on pp. 15]
- [148] D. S. Reisman and J. P. Scholz. Workspace location influences joint coordination during reaching in post-stroke hemiparesis. *Experimental Brain Research*, 170(2):265–76, 2006. [cited on pp. 15]
- [149] Y. Ren, S. H. Kang, H.-S. Park, Y.-N. Wu, and L.-Q. Zhang. Developing a multi-joint upper limb exoskeleton robot for diagnosis, therapy, and outcome evaluation in neurorehabilitation. *IEEE Transactions on Neural Systems and Rehabilitation Engineering*, 21(3):490–499, May 2013. [cited on pp. 26, 29, 33, 35, 36]
- [150] C. Richards, F. Malouin, and S. Nadeau. Chapter 13 - stroke rehabilitation: clinical picture, assessment, and therapeutic challenge. In S. N. Numa Dancause and S. Rossignol, editors, *Sensorimotor RehabilitationAt the Crossroads of Basic and Clinical Sciences*, volume 218 of *Progress in Brain Research*, pages 253 – 280. Elsevier, 2015. [cited on pp. 36]
- [151] R. Riener, M. Guidali, U. Keller, A. Duschau-Wicke, V. Klamroth, and T. Nef. Transferring armin to the clinics and industry. *Topics in Spinal Cord Injury Rehabilitation*, 17(1):54–59, May 2011. [cited on pp. 18, 24, 26]
- [152] A. Roby-Brami, A. Feydy, M. Combeaud, E. Biryukova, B. Bussel, and M. Levin. Motor compensation and recovery for reaching in stroke patients. *Acta neurologica scandinavica*, 107(5):369–381, 2003. [cited on pp. 42, 51]
- [153] A. Roby-Brami, A. Feydy, M. Combeaud, E. V. Biryukova, B. Bussel, and M. F. Levin. Motor compensation and recovery for reaching in stroke patients. *Acta Neurologica Scandinavica*, 107(5):369–81, 2003. [cited on pp. 14]
- [154] A. Roby-Brami, S. Jacobs, N. Bennis, and M. F. Levin. Hand orientation for grasping and arm joint rotation patterns in healthy subjects and hemiparetic stroke patients. *Brain Research*, 969(1-2):217–29, 2003. [cited on pp. 14]
- [155] G. Rosati, P. Gallina, S. Masiero, and A. Rossi. Design of a new 5-DOF wire-based robot for rehabilitation. In *International Conference on Rehabilitation Robotics, ICORR*, pages 430–433. IEEE, 2005. [cited on pp. 24, 26]
- [156] T. Sakurada, T. Kawase, K. Takano, T. Komatsu, and K. Kansaku. A BMI-based occupational therapy assist suit: asynchronous control by ssvep. *Frontiers in Neuroscience*, 7, 2013. [cited on pp. 26, 28, 29, 34, 36]
- [157] Y. Sankai. Leading edge of cybernics: robot suit HAL. In *SICE-ICASE International Joint Conference*, pages P–1. IEEE, 2006. [cited on pp. 19]

- [158] R. A. Scheidt, D. J. Reinkensmeyer, M. A. Conditt, W. Z. Rymer, and F. A. Mussa-Ivaldi. Persistence of motor adaptation during constrained, multi-joint, arm movements. *Journal of Neurophysiology*, 84(2):853–862, 2000. [cited on pp. 56]
- [159] J. P. Scholz, G. Schöner, and M. L. Latash. Identifying the control structure of multijoint coordination during pistol shooting. *Experimental Brain Research*, 135(3):382–404, 2000. [cited on pp. 11, 82]
- [160] N. Schweighofer, Y. Choi, C. Weinstein, and J. Gordon. Task-oriented rehabilitation robotics. *American Journal of Physical Medicine & Rehabilitation*, 91(11):S270–S279, 2012. [cited on pp. 17]
- [161] R. Shadmehr and F. A. Mussa-Ivaldi. Adaptive representation of dynamics during learning of a motor task. *The Journal of Neuroscience*, 14(5):3208–3224, 1994. [cited on pp. 12, 25, 56, 57, 74]
- [162] R. Shadmehr, M. A. Smith, and J. W. Krakauer. Error correction, sensory prediction, and adaptation in motor control. *Annual Review of Neuroscience*, 33:89–108, 2010. [cited on pp. 12]
- [163] M. Simkins, H. Kim, G. Abrams, N. Byl, and J. Rosen. Robotic unilateral and bilateral upper-limb movement training for stroke survivors afflicted by chronic hemiparesis. In *IEEE International Conference on Rehabilitation Robotics, ICORR*, pages 1–6. IEEE, 2013. [cited on pp. 24, 26, 36]
- [164] R. Smith and T. Lee. Motor control and learning: a behavioural emphasis. *Champaign: Human Kinetics*, 1998. [cited on pp. 12]
- [165] Z. Song, S. Guo, M. Pang, S. Zhang, N. Xiao, B. Gao, and L. Shi. Implementation of resistance training using an upper-limb exoskeleton rehabilitation device for elbow joint. *Journal of Medical and Biological Engineering*, 34(2), 2014. [cited on pp. 26, 30]
- [166] P. Staubli, T. Nef, V. Klamroth-Marganska, and R. Riener. Effects of intensive arm training with the rehabilitation robot ARMin ii in chronic stroke patients: four single-cases. *Journal of Neuroengineering and Rehabilitation*, 6:46, 2009. [cited on pp. 28, 30]
- [167] A. Sterr, T. Elbert, I. Berthold, S. Kölbel, B. Rockstroh, and E. Taub. Longer versus shorter daily constraint-induced movement therapy of chronic hemiparesis: an exploratory study. *Archives of Physical Medicine and Rehabilitation*, 83(10):1374–1377, 2002. [cited on pp. 16]
- [168] C. Stinear, S. Ackerley, and W. Byblow. Rehabilitation is initiated early after stroke, but most motor rehabilitation trials are not a systematic review. *Stroke*, 44(7):2039–2045, 2013. [cited on pp. 16]
- [169] T. M. Sukal, M. D. Ellis, and J. P. Dewald. Shoulder abduction-induced reductions in reaching work area following hemiparetic stroke: neuroscientific implications. *Experimental Brain Research*, 183(2):215–23, 2007. [cited on pp. 15]
- [170] E. Taub, G. Uswatte, V. Mark, and D. Morris. The learned nonuse phenomenon: implications for rehabilitation. *Europa Medicophysica*, 42:241–55, 2006. [cited on pp. 15]
- [171] E. Taub, G. Uswatte, V. W. Mark, and D. M. Morris. The learned nonuse phenomenon: implications for rehabilitation. *Europa Medicophysica*, 42(3):241–56, 2006. [cited on pp. 56]
- [172] L. H. Ting. Dimensional reduction in sensorimotor systems: a framework for understanding muscle coordination of posture. *Progress in Brain Research*, 165:299–321, 2007. [cited on pp. 11]
- [173] A. Toth, G. Fazekas, G. Arz, M. Jurak, and M. Horvath. Passive robotic movement therapy of the spastic hemiparetic arm with REHAROB: report of the first clinical test and the follow-up system improvement. In *International Conference on Rehabilitation Robotics, ICORR*, pages 127–130. IEEE, 2005. [cited on pp. 24, 26, 28]

- [174] B.-C. Tsai, W. W. Wang, L.-C. Hsu, L. C. Fu, and J. Lai. An articulated rehabilitation robot for upper limb physiotherapy and training. In *IEEE/RSJ International Conference on Intelligent Robots and Systems, IROS*, pages 1470–1475, Oct. 2010. [cited on pp. 30]
- [175] J. van Kordelaar, E. E. van Wegen, and G. Kwakkel. Unraveling the interaction between pathological upper limb synergies and compensatory trunk movements during reach-to-grasp after stroke: a cross-sectional study. *Experimental Brain Research*, 221(3):251–62, 2012. [cited on pp. 15]
- [176] R. Vertechy, A. Frisoli, A. Dettori, M. Solazzi, and M. Bergamasco. Development of a new exoskeleton for upper limb rehabilitation. In *IEEE International Conference on Rehabilitation Robotics, ICORR*, pages 188–193. IEEE, 2009. [cited on pp. 26, 28]
- [177] R. Vertechy, A. Frisoli, M. Solazzi, D. Pellegrinetti, and M. Bergamasco. An interaction-torque controller for robotic exoskeletons with flexible joints: Preliminary experimental results. In *IEEE/RSJ International Conference on Intelligent Robots and Systems, IROS*, pages 335–340. IEEE, 2012. [cited on pp. 34]
- [178] C. Vincent, I. Deaudelin, L. Robichaud, J. Rousseau, C. Viscogliosi, L. R. Talbot, and J. Desrosiers. Rehabilitation needs for older adults with stroke living at home: perceptions of four populations. *BMC Geriatrics*, 7(1):1, 2007. [cited on pp. 16]
- [179] B. Volpe, H. Krebs, N. Hogan, L. Edelsteinn, C. Diels, and M. Aisen. Robot training enhanced motor outcome in patients with stroke maintained over 3 years. *Neurology*, 53(8):1874–1874, 1999. [cited on pp. 18]
- [180] D. Wade, R. Langton-Hewer, V. Wood, C. Skilbeck, and H. Ismail. The hemiplegic arm after stroke: measurement and recovery. *Journal of Neurology, Neurosurgery & Psychiatry*, 46(6):521–524, 1983. [cited on pp. 16]
- [181] C. J. Walsh, K. Endo, and H. Herr. A quasi-passive leg exoskeleton for load-carrying augmentation. *International Journal of Humanoid Robotics*, 4(03):487–506, 2007. [cited on pp. 19]
- [182] R. Wei, S. Balasubramanian, L. Xu, and J. He. Adaptive iterative learning control design for RUPERT iv. In *IEEE RAS/EMBS International Conference on Biomedical Robotics and Biomechatronics, BioRob*, pages 647–652. IEEE, 2008. [cited on pp. 28, 39]
- [183] Y. Wei, P. Bajaj, R. Scheidt, and J. Patton. Visual error augmentation for enhancing motor learning and rehabilitative relearning. In *International Conference on Rehabilitation Robotics, ICORR*, pages 505–510. IEEE, 2005. [cited on pp. 25]
- [184] A. M. Wing, S. Lough, A. Turton, C. Fraser, and J. R. Jenner. Recovery of elbow function in voluntary positioning of the hand following hemiplegia due to stroke. *Journal of Neurology, Neurosurgery & Psychiatry*, 53(2):126–134, 1990. [cited on pp. 15]
- [185] C. J. Weinstein and D. B. Kay. Translating the science into practice: shaping rehabilitation practice to enhance recovery after brain damage. *Progress in Brain Research*, 218:331–360, 2015. [cited on pp. 15, 17, 30, 36, 90]
- [186] C. J. Weinstein, J. Stein, R. Arena, B. Bates, L. R. Cherney, S. C. Cramer, F. Deruyter, J. J. Eng, B. Fisher, R. L. Harvey, et al. Guidelines for adult stroke rehabilitation and recovery a guideline for healthcare professionals from the american heart association/american stroke association. *Stroke*, 47(6):e98–e169, 2016. [cited on pp. 17]
- [187] E. Wolbrecht, V. Chan, D. Reinkensmeyer, and J. Bobrow. Optimizing compliant, model-based robotic assistance to promote neurorehabilitation. *IEEE Transactions on Neural Systems and Rehabilitation Engineering*, 16(3):286–297, June 2008. [cited on pp. 27, 28, 30, 31, 36, 38, 39]

- [188] E. T. Wolbrecht, D. J. Reinkensmeyer, and J. E. Bobrow. Pneumatic control of robots for rehabilitation. *The International Journal of Robotics Research*, 29(1):23–38, May 2009. [cited on pp. 26]
- [189] D. M. Wolpert. Computational approaches to motor control. *Trends in Cognitive Sciences*, 1(6):209–216, 1997. [cited on pp. 12]
- [190] D. M. Wolpert, J. Diedrichsen, and J. R. Flanagan. Principles of sensorimotor learning. *Nature Reviews Neuroscience*, 12(12):739–751, 2011. [cited on pp. 12]
- [191] G. Wu, S. Siegler, P. Allard, C. Kirtley, A. Leardini, D. Rosenbaum, M. Whittle, D. D DLima, L. Cristofolini, H. Witte, et al. Isb recommendation on definitions of joint coordinate system of various joints for the reporting of human joint motionpart i: ankle, hip, and spine. *Journal of Biomechanics*, 35(4):543–548, 2002. [cited on pp. 42]
- [192] C. Yang, G. Ganesh, S. Haddadin, S. Parusel, A. Albu-Schaeffer, and E. Burdet. Human-like adaptation of force and impedance in stable and unstable interactions. *IEEE Transactions on Robotics*, 27(5):918–930, 2011. [cited on pp. 41]
- [193] W. Yu and J. Rosen. Neural PID control of robot manipulators with application to an upper limb exoskeleton. *IEEE Transactions on Cybernetics*, 43(2):673–684, 2013. [cited on pp. 27]
- [194] W. Yu, J. Rosen, and X. Li. PID admittance control for an upper limb exoskeleton. In *American Control Conference, ACC*, pages 1124–1129. IEEE, 2011. [cited on pp. 30]
- [195] H. Zhang, H. Austin, S. Buchanan, R. Herman, J. Koeneman, and J. He. Feasibility study of robot-assisted stroke rehabilitation at home using RUPERT. In *IEEE/ICME International Conference on Complex Medical Engineering, CME*, pages 604–609. IEEE, 2011. [cited on pp. 31, 36]
- [196] S.-H. Zhou, J. Fong, V. Crocher, Y. Tan, D. Oetomo, and I. Mareels. Learning control in robot-assisted rehabilitation of motor skills a review. *Journal of Control and Decision*, 3(1):19–43, 2016. [cited on pp. 56]

List of Figures

1.1	An example of upper-limb redundancy while grasping an object	11
1.2	Stroke causes and effects	13
1.3	Example of a pathological reaching movement in a patient with a right brain lesion.	14
1.4	Hypothetical pattern of recovery after stroke in humans	16
1.5	Overview of upper-limb rehabilitation robotics timeline	17
1.6	Comparison between manipulandum and exoskeleton	18
1.7	The 4-DOF ABLE exoskeletons	20
2.1	Examples of available exoskeletons for rehabilitation	24
2.2	General neurorehabilitation timeline	25
2.3	The three global strategies for robotic-mediated rehabilitation	27
2.4	General control scheme for exoskeletons for neurorehabilitation	27
2.5	Existing discrete mapping between patient recovery and control strategies	37
3.1	Example of typical trial-by-trial offline adaptation of feedforward control based on former trial feedback values, in the human CNS	39
3.2	Desired behaviour for our adaptive controller	40
3.3	EMG sensors position on the five selected muscles	43
3.4	Robot adaptation to the different performance of the subject	44
3.5	Trials details	45
3.6	Advanced robot adaptation to the human performance	46
3.7	Comparison of proportional gain values by changing the learning factor β and keeping fixed the decay factor γ	47
3.8	Experimental setup and ABLE close-up	48
3.9	An example of <i>self-motion</i>	49
3.10	Mean evolution of the proportional gains	50
3.11	Average error indexes	51
3.12	Joint trajectories for the three strategies	52
4.1	The four typical consecutive phases of human motor adaptation and after-effects on 2D experiments	56
4.2	KSC experimental setup	59
4.3	Example of goal-directed pointing task (GDM)	60
4.4	Example of path-constrained tracking task (PCT)	60
4.5	WAM positions	61
4.6	Phases of the KSC experiment	61
4.7	Two illustrative cases of KSC perturbation effects	65
4.8	Inter-individual differences on the effect of the KSC exposition	66
4.9	Mean joint final displacement on movement towards ET 3	67
4.10	Mean motion duration, mean peak velocity, and mean smoothness (ET)	68

4.11 Mean trajectory curvature (ET)	69
4.12 PCs distance from PRE, on ET pointing task, for the two tasks GDM and PCT	70
4.13 PCs distance from constraining vector, on ET pointing task, for the two tasks GDM and PCT . .	70
4.14 Mean joint final displacement on movement towards GT 3	71
4.15 Mean motion duration, mean peak velocity, and mean smoothness (GT)	72
4.16 Mean trajectory curvature (GT)	72
4.17 PCs distance from PRE, on GT pointing task, for the two tasks GDM and PCT	73
4.18 PCs distance from constraining vector, on GT pointing task, for the two tasks GDM and PCT .	74
4.19 Transferring outside of the exoskeleton - setup	77
4.20 Transferring outside of the exoskeleton - pattern of phases	77
4.21 Transferring outside of the exoskeleton - 3D view of the movements, marker 3	78
4.22 Transferring outside of the exoskeleton - 2D views, marker 3	79
4.23 Transferring outside of the exoskeleton - marker 1-4	80
4.24 Transferring outside of the exoskeleton - mean elevation	80
4.25 Transferring outside of the exoskeleton - PCA analysis	81
4.26 Control scheme of the adaptive KSC	82
A.1 Principal bones of the human arm	85
A.2 Shoulder girdle degrees of freedom	86
A.3 Shoulder joint and arm movements	86
A.4 Wrist movements and arm muscles	87

List of Tables

1.1	ABLE exoskeleton main specifications	20
2.1	Exoskeletons for upper limb rehabilitation	26
2.2	Control strategies tested on stroke survivors with robotic exoskeletons	36
3.1	Pattern of requested muscular activity for the advanced test of the adaptive controller	46
3.2	The characteristics of the three different adaptive paradigms	53

Abstract

While many robotic exoskeletons have been developed for stroke rehabilitation in recent years, there were not yet improvements to the traditional therapy. A key to unleash the potentiality of robotics is to adapt the assistance provided by the robot in order to maximize the subject engagement and effort, by having the robotic therapy evolving with the patient recovery. For this reason, we aim at better understanding the process of reciprocal adaptation in a context of physical Human-Robot Interaction (pHRI). We first developed a new adaptive controller, which assists the subject "as-needed", by regulating its interaction to maximize the human involvement. We further compared different signals driving this adaptation, to better following the functional recovery level of the patients. While the control is performed by the robot, the subject is also adapting his movements, and this adaptation has not yet been studied when dealing with 3D movements and exoskeletons. Therefore, we exposed human motions to distributed force fields, generated by the exoskeleton at the joint level, to produce specific inter-joint coordination and to analyse the effects of this exposition. With healthy participants, we observed important inter-individual difference, with adaptation to the fields in 21% of the participants, but post-effects and persisting retention of these in time in 85% of the subjects, together with spatial generalization, and, preliminarily, transfer of the effects outside of the exoskeleton context. This work towards understanding pHRI could provide insights on innovative ways to develop new controllers for improving stroke motor recovery with exoskeletons.

Keywords: Rehabilitation Robotics, Upper-limb Robotic Exoskeletons, Adaptive Control, Motor Coordination Learning.

Résumé

Alors que de nombreux exosquelettes destinés à la rééducation neuromotrice ont été développés ces dernières années, ces dispositifs n'ont pas encore permis de vrai progrès dans la prise en charge des patients cérébro-lésés. Une des clés pour améliorer les faibles résultats thérapeutiques obtenus serait de constamment adapter la thérapie robotisée en fonction de l'évolution du patient et de sa récupération, en adaptant l'assistance fournie par le robot pour maximiser l'engagement du patient. L'objectif de cette thèse est donc de comprendre les processus d'adaptations réciproques dans un contexte d'interaction physique Homme-Exosquelette. Dans un premier temps nous avons donc développé un nouveau type de contrôleur adaptatif qui assiste le sujet "au besoin", en modulant l'assistance fournie; et évalué différents signaux pour piloter cette adaptation afin de suivre au mieux la récupération du patient. Dans un deuxième temps, nous avons étudié l'adaptation de sujets sains à l'application de champs de forces distribués par un exosquelette sur leur bras durant la réalisation de mouvements dans l'espace. En effet, lors d'une interaction physique homme-robot, le sujet adapte aussi son comportement aux contraintes exercées par le robot. D'importantes différences inter-individuelles ont été observées, avec une adaptation à la contrainte imposée chez seulement 21% des sujets, mais avec des effets à-posteriori persistants mesurés chez 85% d'entre eux; ainsi qu'une généralisation dans l'espace de ces effets et un transfert à des contextes différents (hors du robot). Ces premiers résultats devraient permettre à terme d'améliorer la rééducation neuromotrice robotisée.

Mots clés: Robotique de rééducation, Exosquelettes de membre supérieur, Contrôle adaptatif, Apprentissage de coordinations motrices.
